

2

USAFSAM-TR-86-36-PT-4

RESEARCH AND DEVELOPMENT OF ANTI-G LIFE SUPPORT SYSTEMS:

Part 4. Engineering Test and Evaluation of Six Anti-G Valves

Larry J. Meeker, B.S. (USAFSAM/VNS)
Arnold G. Krueger
Paul E. Love
Emily M. Gause, M.S.
Robert W. Krutz, Ph.D.

AD-A206 996

Life Sciences Division
Technology Incorporated
San Antonio, TX 78216

August 1988

Final Report for Period 1 April 1981 - 31 July 1985

DTIC
ELECTE
APR 21 1989
S H D

Approved for public release; distribution is unlimited.

089 4 21 011

Prepared for
USAF SCHOOL OF AEROSPACE MEDICINE
Human Systems Division (AFSC)
Brooks Air Force Base, TX 78235-5301




NOTICES

This final report was submitted by the Life Sciences Division, Technology Incorporated, 406 Breesport, San Antonio, TX 78216, under contract F33615-81-C-0600, job order 7930-14-42, with the USAF School of Aerospace Medicine, Human Systems Division, AFSC, Brooks Air Force Base, Texas. Larry J. Meeker (USAFSAM/VNS) was the Laboratory Project Scientist-in-Charge.


When Government drawings, specifications, or other data are used for any purpose other than in connection with a definitely Government-related procurement, the United States Government incurs no responsibility nor any obligation whatsoever. The fact that the Government may have formulated or in any way supplied the said drawings, specifications, or other data, is not to be regarded by implication, or otherwise in any manner construed, as licensing the holder, or any other person or corporation; or as conveying any rights or permission to manufacture, use, or sell any patented invention that may in any way be related thereto.

The Office of Public Affairs has reviewed this report, and it is releasable to the National Technical Information Service, where it will be available to the general public, including foreign nationals.

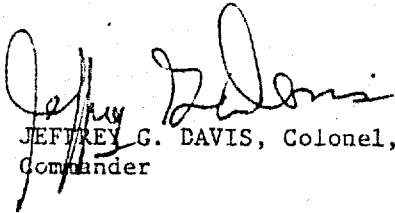
This report has been reviewed and is approved for publication.



LARRY J. MEEKER
Project Scientist



W. C. ALEXANDER, Ph.D.
Supervisor



JEFFREY G. DAVIS, Colonel, USAF, MC
Commander

UNCLASSIFIED

SECURITY CLASSIFICATION OF THIS PAGE

REPORT DOCUMENTATION PAGE

Form Approved
OMB No. 0704-0188

1a. REPORT SECURITY CLASSIFICATION Unclassified			1b. RESTRICTIVE MARKINGS		
2a. SECURITY CLASSIFICATION AUTHORITY			3. DISTRIBUTION / AVAILABILITY OF REPORT Approved for public release; distribution is unlimited.		
2b. DECLASSIFICATION / DOWNGRADING SCHEDULE			4. PERFORMING ORGANIZATION REPORT NUMBER(S)		
4. PERFORMING ORGANIZATION REPORT NUMBER(S)			5. MONITORING ORGANIZATION REPORT NUMBER(S) USAFSAM-TR-86-36-PT-4		
6a. NAME OF PERFORMING ORGANIZATION Technology Incorporated Life Sciences Division		6b. OFFICE SYMBOL (If applicable)	7a. NAME OF MONITORING ORGANIZATION USAF School of Aerospace Medicine (VNS)		
6c. ADDRESS (City, State, and ZIP Code) 406 Breesport San Antonio, TX 78216		7b. ADDRESS (City, State, and ZIP Code) Human Systems Division (AFSC) Brooks Air Force Base, TX 78235-5301			
8a. NAME OF FUNDING / SPONSORING ORGANIZATION		8b. OFFICE SYMBOL (If applicable)	9. PROCUREMENT INSTRUMENT IDENTIFICATION NUMBER F33615-81-C-0600		
8c. ADDRESS (City, State, and ZIP Code)		10. SOURCE OF FUNDING NUMBERS			
		PROGRAM ELEMENT NO. 62202F	PROJECT NO. 7930	TASK NO. 14	WORK UNIT ACCESSION NO. 42
11. TITLE (Include Security Classification) RESEARCH AND DEVELOPMENT OF ANTI-G LIFE SUPPORT SYSTEMS: Part 4 Engineering Test and Evaluation of Six Anti-G Valves					
12. PERSONAL AUTHOR(S) Meeker, Larry J. (USAFSAM/VNS); Krueger, Arnold G.; Love, Paul E.; Gause, Emily M.; Krutz, Robert W.					
13a. TYPE OF REPORT Final		13b. TIME COVERED FROM 81/04/01 TO 85/07/31		14. DATE OF REPORT (Year, Month, Day) 1988, August	15. PAGE COUNT 119
16. SUPPLEMENTARY NOTATION					
17. COSATI CODES			18. SUBJECT TERMS (Continue on reverse if necessary and identify by block number)		
FIELD	GROUP	SUB-GROUP	Life-Support Equipment, Anti-G Valve Performance, Anti-G Valve Testing, Anti-G Suits		
23	05				
13	11				
19. ABSTRACT (Continue on reverse if necessary and identify by block number) Six anti-G valves (i.e., valves designed to rapidly deliver output pressures proportional to +Gz forces acting upon valve control elements) were evaluated for performance under conditions simulating the spectrum of Gz-onset conditions likely to be encountered by pilots of current U.S. Air Force high-performance aircraft. This Engineering Test and Evaluation Task was conducted on-site at Brooks Air Force Base, Texas, using the School of Aerospace Medicine (USAFSAM) human centrifuge facility. One objective was validation of uniform testing procedures for evaluation of anti-G valves under controlled conditions of: acceleration, source pressure, valve angles, and simulated anti-G suit volumes. A second objective was measurement of actual dynamic performance of the standard ALAR 8400A anti-G valve and five new experimental valves. The experimental valves evaluated were: ALAR High-flow Ready-pressure; ALAR High-flow; Garrett Electronic/Pneumatic; Hymatic VAG-110-022; and AAMRL Electropneumatic (Bang Bang). The battery of test conditions employed was divided into three phases: Phase I - Maximum Flow Capacity Testing; Phase II - Dynamic Response Testing; and Phase III - Complex Dynamic Response Testing. Results of testing under all conditions are presented for each valve and the performance characteristics of all six valves are compared. (AW)					
20. DISTRIBUTION / AVAILABILITY OF ABSTRACT <input checked="" type="checkbox"/> UNCLASSIFIED/UNLIMITED <input type="checkbox"/> SAME AS RPT <input type="checkbox"/> OTIC USERS			21. ABSTRACT SECURITY CLASSIFICATION Unclassified		
22a. NAME OF RESPONSIBLE INDIVIDUAL Larry J. Meeker			22b. TELEPHONE (Include Area Code) (512) 536-3811	22c. OFFICE SYMBOL USAFSAM/VNS	

CONTENTS

	<u>Page</u>
1. INTRODUCTION	1
2. OBJECTIVES.....	2
3. TESTING EQUIPMENT AND PROCEDURES.....	3
3.1 Testing Equipment.....	3
3.1.1 General Test Configurations.....	3
3.1.2 Test Configuration Elements	5
3.1.2.1 Source Pressure (P_s).....	5
3.1.2.2 Valve Output Pressure (P_o).....	5
3.1.2.3 Air Flow (F_v)	5
3.1.2.4 Simulated Suit Volume Pressure (P_v)	5
3.1.2.5 Acceleration (+ G_z)	6
3.1.2.6 Valve Angle.....	6
3.1.2.7 Pressure Transducers.....	6
3.1.2.8 Flow Meter.....	6
3.1.2.9 Control Console Signal Conditioners.....	6
3.1.2.10 Strip-Chart Recorders.....	6
3.2 Testing Procedures	7
3.2.1 Phase I - Maximum Flow Capacity Testing.....	7
3.2.2 Phase II - Dynamic Response Testing.....	7
3.2.3 Phase III - Complex Dynamic Response Testing.....	8
3.2.4 Simulated Suit Volume Estimation.....	10
3.2.5 Data Acquisition.....	10
3.2.6 Data Analysis.....	11
4. RESULTS AND DISCUSSION	12
4.1 ALAR 8400A Anti-G Valve.....	13
4.1.1 Description.....	13
4.1.2 Phase I - Determination of Maximum Flow Capacity	13
4.1.3 Phase II - Determination of Dynamic Response Capability....	15
4.1.3.1 Low G_z -Onset-Rate Conditions.....	15
4.1.3.2 High G_z -Onset-Rate Conditions.....	19
4.1.4 Phase III - Determination of Complex Dynamic Response Capability	23



	For
	<input checked="" type="checkbox"/>
	<input type="checkbox"/>
	<input type="checkbox"/>
	ion
	on/
	ity Codes
	and/or
	ial

A-1

	<u>Page</u>
4.2 ALAR High-Flow Ready-Pressure Anti-G Valve.....	28
4.2.1 Description.....	28
4.2.2 Phase I - Determination of Maximum Flow Capacity	28
4.2.3 Phase II - Determination of Dynamic Response Capability....	31
4.2.3.1 Low G _z -Onset-Rate Conditions.....	31
4.2.3.2 High G _z -Onset-Rate Conditions.....	34
4.2.4 Phase III - Determination of Complex Dynamic Response Capability	37
4.3 ALAR High-Flow Anti-G Valve.....	41
4.3.1 Description.....	41
4.3.2 Phase I - Determination of Maximum Flow Capacity	41
4.3.3 Phase II - Determination of Dynamic Response Capability....	43
4.3.3.1 Low G _z -Onset-Rate Conditions.....	43
4.3.3.2 High G _z -Onset-Rate Conditions.....	47
4.3.4 Phase III - Determination of Complex Dynamic Response Capability	50
4.4 Garrett Electronic/Pneumatic Anti-G Valve	54
4.4.1 Description.....	54
4.4.2 Phase I - Determination of Maximum Flow Capacity	54
4.4.3 Phase II - Determination of Dynamic Response Capability....	56
4.4.3.1 Low G _z -Onset-Rate Conditions.....	56
4.4.3.2 High G _z -Onset-Rate Conditions.....	59
4.4.4 Phase III - Determination of Complex Dynamic Response Capability	64
4.5 Hymatic VAG-110-022 Anti-G Valve	69
4.5.1 Description.....	69
4.5.2 Phase I - Determination of Maximum Flow Capacity	71
4.5.3 Phase II - Determination of Dynamic Response Capability....	71
4.5.3.1 Low G _z -Onset-Rate Conditions.....	71
4.5.3.2 High G _z -Onset-Rate Conditions.....	75
4.5.4 Phase III - Determination of Complex Dynamic Response Capability	78

	<u>Page</u>
4.6 AAMRL Anti-G Valve	83
4.6.1 Description.....	83
4.6.2 Phase I - Determination of Maximum Flow Capacity	83
4.6.3 Phase II - Determination of Dynamic Response Capability	86
4.6.3.1 Low G_z -Onset-Rate Conditions.....	86
4.6.3.2 High G_z -Onset-Rate Conditions.....	89
4.6.4 Phase III - Determination of Complex Dynamic Response Capability	93
5. DISCUSSION AND CONCLUSIONS.....	96
6. REFERENCES	102
ABBREVIATIONS, ACRONYMS, AND SYMBOLS.....	103
APPENDIXES.....	105
APPENDIX A: ALAR 8400A Anti-G Valve Experimental Data	
APPENDIX B: ALAR High-Flow Ready-Pressure Anti-G Valve Experi- mental Data	
APPENDIX C: ALAR High-Flow Anti-G Valve Experimental Data	
APPENDIX D: Garrett Servo-Controlled Rapid-Response Anti-G Valve Experimental Data	
APPENDIX E: Hymatic VAG-110-022 Anti-G Valve Experimental Data	
APPENDIX F: AAMRL ("Bang Bang") Anti-G Valve Experimental Data	

List of Figures

Fig. No.

3.1 Testing Equipment

3.1-1 Phase I Open-Flow Capability Test Configuration.....	3
3.1-2 Phase II Dynamic Test Configuration	4

3.2 Testing Procedures

3.2-1 Conditions of the Three Phase-II "Trapezoid" Centrifuge Performance Evaluation Tests Performed at All Three Source Pressures, with Valve Angle Held at 0°	9
3.2-2 Conditions of Phase-III SACM Testing of Anti-G Valves.....	9

	<u>Page</u>
<u>4.1 ALAR 8400A Anti-G Valve</u>	
4.1-1 ALAR 8400A Anti-G Valve	14
4.1-2 Maximum flow through ALAR 8400A anti-G valve	16
4.1-3 "Suit" pressures produced during acceleration/deceleration by ALAR 8400A anti-G valve under conditions of: 150-psig source pressure; low G onset; 10-liter volume; 0° angle.....	16
4.1-4 "Suit" pressures produced during acceleration/deceleration by ALAR 8400A anti-G valve under conditions of: 150-psig source pressure; low G onset; 10-liter volume; 15° angle	17
4.1-5 "Suit" pressures produced during acceleration/deceleration by ALAR 8400A anti-G valve under conditions of: 150-psig source pressure; low G onset; 10-liter volume; 30° angle	18
4.1-6 "Suit" pressures produced during acceleration/deceleration by ALAR 8400A anti-G valve under conditions of: 30-psig source pressure; low G onset; 10-liter volume; 0° angle.....	18
4.1-7 "Suit" pressures produced during acceleration/deceleration by ALAR 8400A anti-G valve under conditions of: 300-psig source pressure; low G onset; 10-liter volume; 0° angle.....	19
4.1-8 "Suit" pressures produced during acceleration/deceleration by ALAR 8400A anti-G valve under conditions of: 150-psig source pressure; high G onset; 10-liter volume; 0° angle.....	20
4.1-9 "Suit" pressures produced during acceleration/deceleration by ALAR 8400A anti-G valve under conditions of: 150-psig source pressure; high G onset; 10-liter volume; 15° angle.....	21
4.1-10 "Suit" pressures produced during acceleration/deceleration by ALAR 8400A anti-G valve under conditions of: 150-psig source pressure; high G onset; 10-liter volume; 30° angle.....	22
4.1-11 "Suit" pressures produced during acceleration/deceleration by ALAR 8400A anti-G valve under conditions of: 30-psig source pressure; high G onset; 10-liter volume; 0° angle.....	22
4.1-12 "Suit" pressures produced during acceleration/deceleration by ALAR 8400A anti-G valve under conditions of: 300-psig source pressure; high G onset; 10-liter volume; 0° angle.....	23
4.1-13 "Suit" pressures produced during SACM by ALAR 8400A anti-G valve under conditions of: 150-psig source pressure; 10-liter volume; 0° angle	24
4.1-14 "Suit" pressures produced during SACM by ALAR 8400A anti-G valve under conditions of: 150-psig source pressure; 10-liter volume; 15° angle	26
4.1-15 "Suit" pressures produced during SACM by ALAR 8400A anti-G valve under conditions of: 150-psig source pressure; 10-liter volume; 30° angle.....	26
4.1-16 "Suit" pressures produced during SACM by ALAR 8400A anti-G valve under conditions of: 30-psig source pressure; 14-liter volume; 0° angle	27
4.1-17 "Suit" pressures produced during SACM by ALAR 8400A anti-G valve under conditions of: 300-psig source pressure; 6-liter volume; 0° angle.....	27

		<u>Page</u>
<u>4.2 ALAR High-Flow Ready-Pressure Anti-G Valve</u>		
4.2-1	ALAR High-Flow Ready-Pressure Anti-G Valve	29
4.2-2	Maximum flow through ALAR HFRP anti-G valve with pressure off.....	30
4.2.3	Maximum flow through ALAR HFRP anti-G valve with pressure on.....	30
4.2-4	"Suit" pressures produced during acceleration/deceleration by ALAR HFRP anti-G valve under conditions of: 150-psig source pressure; low G onset; 10-liter volume; 0° angle.....	32
4.2-5	"Suit" pressures produced during acceleration/deceleration by ALAR HFRP anti-G valve under conditions of: 150-psig source pressure; low G onset; 10-liter volume; 15° angle	32
4.2-6	"Suit" pressures produced during acceleration/deceleration by ALAR HFRP anti-G valve under conditions of: 150-psig source pressure; low G onset; 10-liter volume; 30° angle	33
4.2-7	"Suit" pressures produced during acceleration/deceleration by ALAR HFRP anti-G valve under conditions of: 30-psig source pressure; low G onset; 10-liter volume; 0° angle.....	33
4.2-8	"Suit" pressures produced during acceleration/deceleration by ALAR HFRP anti-G valve under conditions of: 300-psig source pressure; low G onset; 10-liter volume; 0° angle.....	35
4.2-9	"Suit" pressures produced during acceleration/deceleration by ALAR HFRP anti-G valve under conditions of: 150-psig source pressure; high G onset; 10-liter volume; 0° angle.....	35
4.2-10	"Suit" pressures produced during acceleration/deceleration by ALAR HFRP anti-G valve under conditions of: 150-psig source pressure; high G onset; 10-liter volume; 15° angle.....	36
4.2-11	"Suit" pressures produced during acceleration/deceleration by ALAR HFRP anti-G valve under conditions of: 150-psig source pressure; high G onset; 10-liter volume; 30° angle.....	36
4.2-12	"Suit" pressures produced during acceleration/deceleration by ALAR HFRP anti-G valve under conditions of: 30-psig source pressure; high G onset; 10-liter volume; 0° angle.....	38
4.2-13	"Suit" pressures produced during acceleration/deceleration by ALAR HFRP anti-G valve under conditions of: 300-psig source pressure; high G onset; 10-liter volume; 0° angle.....	38
4.2-14	"Suit" pressures produced during SACM by ALAR HFRP anti-G valve under conditions of: 150-psig source pressure; 10-liter volume; 0° angle	39
4.2-15	"Suit" pressures produced during SACM by ALAR HFRP anti-G valve under conditions of: 150-psig source pressure; 10-liter volume; 30° angle	39
4.2-16	"Suit" pressures produced during SACM by ALAR HFRP anti-G valve under conditions of: 30-psig source pressure; 14-liter volume; 0° angle	40
4.2-17	"Suit" pressures produced during SACM by ALAR HFRP anti-G valve under conditions of: 300-psig source pressure; 6-liter volume; 0° angle.....	41

	<u>Page</u>
4.3 ALAR High-Flow Anti-G Valve	
4.3-1 ALAR High-flow Anti-G Valve	42
4.3-2 Maximum flow through ALAR High-flow anti-G valve	44
4.3-3 "Suit" pressures produced during acceleration/deceleration by ALAR High-flow anti-G valve under conditions of: 150-psig source pressure; low G onset; 10-liter volume; 0° angle.....	44
4.3-4 "Suit" pressures produced during acceleration/deceleration by ALAR High-flow anti-G valve under conditions of: 150-psig source pressure; low G onset; 10-liter volume; 15° angle	45
4.3-5 "Suit" pressures produced during acceleration/deceleration by ALAR High-flow anti-G valve under conditions of: 150-psig source pressure; low G onset; 10-liter volume; 30° angle	45
4.3-6 "Suit" pressures produced during acceleration/deceleration by ALAR High-flow anti-G valve under conditions of: 30-psig source pressure; low G onset; 10-liter volume; 0° angle.....	46
4.3-7 "Suit" pressures produced during acceleration/deceleration by ALAR High-flow anti-G valve under conditions of: 300-psig source pressure; low G onset; 10-liter volume; 0° angle.....	46
4.3-8 "Suit" pressures produced during acceleration/deceleration by ALAR High-flow anti-G valve under conditions of: 150-psig source pressure; high G onset; 10-liter volume; 0° angle	48
4.3-9 "Suit" pressures produced during acceleration/deceleration by ALAR High-flow anti-G valve under conditions of: 150-psig source pressure; high G onset; 10-liter volume; 15° angle.....	48
4.3-10 "Suit" pressures produced during acceleration/deceleration by ALAR High-flow anti-G valve under conditions of: 150-psig source pressure; high G onset; 10-liter volume; 30° angle.....	49
4.3-11 "Suit" pressures produced during acceleration/deceleration by ALAR High-flow anti-G valve under conditions of: 30-psig source pressure; high G onset; 10-liter volume; 0° angle	49
4.3-12 "Suit" pressures produced during acceleration/deceleration by ALAR High-flow anti-G valve under conditions of: 300-psig source pressure; high G onset; 10-liter volume; 0° angle.....	51
4.3-13 "Suit" pressures produced during SACM by ALAR High-flow anti-G valve under conditions of: 150-psig source pressure; 10-liter volume; 0° angle	51
4.3-14 "Suit" pressures produced during SACM by ALAR High-flow anti-G valve under conditions of: 150-psig source pressure; 10-liter volume; 15° angle	52
4.3-15 "Suit" pressures produced during SACM by ALAR High-flow anti-G valve under conditions of: 150-psig source pressure; 10-liter volume; 30° angle	52
4.3-16 "Suit" pressures produced during SACM by ALAR High-flow anti-G valve under conditions of: 30-psig source pressure; 14-liter volume; 0° angle	53
4.3-17 "Suit" pressures produced during SACM by ALAR High-flow anti-G valve under conditions of: 300-psig source pressure; 6-liter volume; 0° angle.....	53

	<u>Page</u>
<u>4.4 Garrett Electronic/Pneumatic Anti-G Valve</u>	
4.4-1 Garrett Electronic/Pneumatic Anti-G Valve	55
4.4-2 Maximum flow through Garrett Electronic/Pneumatic anti-G valve	57
4.4-3 "Suit" pressures produced during acceleration/deceleration by Garrett Electronic/Pneumatic anti-G valve under conditions of: 150-psig source pressure; low G onset; 10-liter volume; 0° angle	57
4.4-4 "Suit" pressures produced during acceleration/deceleration by Garrett Electronic/Pneumatic anti-G valve under conditions of: 150-psig source pressure; low G onset; 10-liter volume; 15° angle	58
4.4-5 "Suit" pressures produced during acceleration/deceleration by Garrett Electronic/Pneumatic anti-G valve under conditions of: 150-psig source pressure; low G onset; 10-liter volume; 30° angle	59
4.4-6 "Suit" pressures produced during acceleration/deceleration by Garrett Electronic/Pneumatic anti-G valve under conditions of: 30-psig source pressure; low G onset; 10-liter volume; 0° angle	60
4.4-7 "Suit" pressures produced during acceleration/deceleration by Garrett Electronic/Pneumatic anti-G valve under conditions of: 300-psig source pressure; low G onset; 10-liter volume; 0° angle	60
4.4-8 "Suit" pressures produced during acceleration/deceleration by Garrett Electronic/Pneumatic anti-G valve under conditions of: 150-psig source pressure; high G onset; 10-liter volume; 0° angle	61
4.4-9 "Suit" pressures produced during acceleration/deceleration by Garrett Electronic/Pneumatic anti-G valve under conditions of: 150-psig source pressure; high G onset; 10-liter volume; 15° angle	61
4.4-10 "Suit" pressures produced during acceleration/deceleration by Garrett Electronic/Pneumatic anti-G valve under conditions of: 150-psig source pressure; high G onset; 10-liter volume; 30° angle	63
4.4-11 "Suit" pressures produced during acceleration/deceleration by Garrett Electronic/Pneumatic anti-G valve under conditions of: 30-psig source pressure; high G onset; 10-liter volume; 0° angle	63
4.4-12 "Suit" pressures produced during acceleration/deceleration by Garrett Electronic/Pneumatic anti-G valve under conditions of: 300-psig source pressure; high G onset; 10-liter volume; 0° angle	65
4.4-13 "Suit" pressures produced during SACM by Garrett Electronic/Pneumatic anti-G valve under conditions of: 150-psig source pressure; 10-liter volume; 0° angle	65

	<u>Page</u>
4.4-14 "Suit" pressures produced during SACM by Garrett Electronic/Pneumatic anti-G valve under conditions of: 150-psig source pressure; 10-liter volume; 15° angle.....	67
4.4-15 "Suit" pressures produced during SACM by Garrett Electronic/Pneumatic anti-G valve under conditions of: 150-psig source pressure; 10-liter volume; 30° angle.....	67
4.4-16 "Suit" pressures produced during SACM by Garrett Electronic/Pneumatic anti-G valve under conditions of: 30-psig source pressure; 14-liter volume; 0° angle	68
4.4-17 "Suit" pressures produced during SACM by Garrett Electronic/Pneumatic anti-G valve under conditions of: 300-psig source pressure; 6-liter volume; 0° angle	68
 <u>4.5 Hymatic VAG-110-022 Anti-G Valve</u>	
4.5-1 Hymatic VAG-110-022 Anti-G Valve.....	70
4.5-2 Maximum flow through Hymatic VAG-110-022 anti-G valve.....	73
4.5-3 "Suit" pressures produced during acceleration/deceleration by Hymatic VAG-110-022 anti-G valve under conditions of: 60-psig source pressure; low G onset; 10-liter volume; 0° angle	73
4.5-4 "Suit" pressures produced during acceleration/deceleration by Hymatic VAG-110-022 anti-G valve under conditions of: 60-psig source pressure; low G onset; 10-liter volume; 15° angle.....	74
4.5-5 "Suit" pressures produced during acceleration/deceleration by Hymatic VAG-110-022 anti-G valve under conditions of: 60-psig source pressure; low G onset; 10-liter volume; 30° angle.....	74
4.5-6 "Suit" pressures produced during acceleration/deceleration by Hymatic VAG-110-022 anti-G valve under conditions of: 30-psig source pressure; low G onset; 10-liter volume; 0° angle	76
4.5-7 "Suit" pressures produced during acceleration/deceleration by Hymatic VAG-110-022 anti-G valve under conditions of: 120-psig source pressure; low G onset; 10-liter volume; 0° angle	76
4.5-8 "Suit" pressures produced during acceleration/deceleration by Hymatic VAG-110-022 anti-G valve under conditions of: 60-psig source pressure; high G onset; 10-liter volume; 0° angle	77
4.5-9 "Suit" pressures produced during acceleration/deceleration by Hymatic VAG-110-022 anti-G valve under conditions of: 60-psig source pressure; high G onset; 10-liter volume; 15° angle.....	77
4.5-10 "Suit" pressures produced during acceleration/deceleration by Hymatic VAG-110-022 anti-G valve under conditions of: 60-psig source pressure; high G onset; 10-liter volume; 30° angle.....	79

	<u>Page</u>
4.5-11 "Suit" pressures produced during acceleration/deceleration by Hymatic VAG-110-022 anti-G valve under conditions of: 30-psig source pressure; high G onset; 10-liter volume; 0° angle	79
4.5-12 "Suit" pressures produced during acceleration/deceleration by Hymatic VAG-110-022 anti-G valve under conditions of: 120-psig source pressure; high G onset; 10-liter volume; 0° angle	80
4.5-13 "Suit" pressures produced during SACM by Hymatic VAG-110-022 anti-G valve under conditions of: 60-psig source pressure; 10-liter volume; 0° angle	80
4.5-14 "Suit" pressures produced during SACM by Hymatic VAG-110-022 anti-G valve under conditions of: 60-psig source pressure; 10-liter volume; 15° angle	81
4.5-15 "Suit" pressures produced during SACM by Hymatic VAG-110-022 anti-G valve under conditions of: 60-psig source pressure; 10-liter volume; 30° angle	82
4.5-16 "Suit" pressures produced during SACM by Hymatic VAG-110-022 anti-G valve under conditions of: 30-psig source pressure; 14-liter volume; 0° angle	82
4.5-17 "Suit" pressures produced during SACM by Hymatic VAG-110-022 anti-G valve under conditions of: 120-psig source pressure; 6-liter volume; 0° angle	83
 <u>4.6 AAMRL Anti-G Valve</u>	
4.6-1 AAMRL Anti-G Valve ("Bang Bang")	84
4.6-2 Maximum flow through AAMRL anti-G valve with pressure off.....	85
4.6-3 Maximum flow through AAMRL anti-G valve with pressure on.....	85
4.6-4 "Suit" pressures produced during acceleration/deceleration by AAMRL anti-G valve under conditions of: 150-psig source pressure; low G onset; 10-liter volume; 0° angle.....	87
4.6-5 "Suit" pressures produced during acceleration/deceleration by AAMRL anti-G valve under conditions of: 150-psig source pressure; low G onset; 10-liter volume; 15° angle	87
4.6-6 "Suit" pressures produced during acceleration/deceleration by AAMRL anti-G valve under conditions of: 150-psig source pressure; low G onset; 10-liter volume; 30° angle	88
4.6-7 "Suit" pressures produced during acceleration/deceleration by AAMRL anti-G valve under conditions of: 30-psig source pressure; low G onset; 10-liter volume; 0° angle.....	88
4.6-8 "Suit" pressures produced during acceleration/deceleration by AAMRL anti-G valve under conditions of: 300-psig source pressure; low G onset; 10-liter volume; 0° angle.....	90
4.6-9 "Suit" pressures produced during acceleration/deceleration by AAMRL anti-G valve under conditions of: 150-psig source pressure; high G onset; 10-liter volume; 0° angle	90

	<u>Page</u>
4.6-10 "Suit" pressures produced during acceleration/deceleration by AAMRL anti-G valve under conditions of: 150-psig source pressure; high G onset; 10-liter volume; 15° angle.....	91
4.6-11 "Suit" pressures produced during acceleration/deceleration by AAMRL anti-G valve under conditions of: 150-psig source pressure; high G onset; 10-liter volume; 30° angle.....	91
4.6-12 "Suit" pressures produced during acceleration/deceleration by AAMRL anti-G valve under conditions of: 30-psig source pressure; high G onset; 10-liter volume; 0° angle.....	92
4.6-13 "Suit" pressures produced during acceleration/deceleration by AAMRL anti-G valve under conditions of: 300-psig source pressure; high G onset; 10-liter volume; 0° angle.....	92
4.6-14 "Suit" pressures produced during SACM by AAMRL anti-G valve under conditions of: 150-psig source pressure; 10-liter volume; 0° angle	94
4.6-15 "Suit" pressures produced during SACM by AAMRL anti-G valve under conditions of: 150-psig source pressure; 10-liter volume; 15° angle.....	94
4.6-16 "Suit" pressures produced during SACM by AAMRL anti-G valve under conditions of: 150-psig source pressure; 10-liter volume; 30° angle.....	95
4.6-17 "Suit" pressures produced during SACM by AAMRL anti-G valve under conditions of: 30-psig source pressure; 14-liter volume; 0° angle	95
4.6-18 "Suit" pressures produced during SACM by AAMRL anti-G valve under conditions of: 300-psig source pressure; 6-liter volume; 0° angle.....	96

List of Tables

Table No.

3. TESTING EQUIPMENT AND PROCEDURES

3.2-1 Summary of Conditions Employed for Testing Anti-G Valves.....	8
---	---

4. RESULTS AND DISCUSSION

4.0-1 Anti-G Suit Design Requirements	13
---	----

5. DISCUSSION AND CONCLUSIONS

5.0-1 Maximum Airflow Capacity (SCFM) as a Function of Acceleration (G_z) for all Anti-G Valves.....	97
5.0-2 Seconds Required to Attain Various Suit Volume Pressures Under High-Onset Conditions.....	99
5.0-3 Suit Volume Pressure (PSIG) Produced Under Low-Onset Conditions as Function of Acceleration (G_z).....	100

	<u>Page</u>
5.0-4 Suit Volume Pressure (PSIG) Produced Under High-Onset Conditions as Function of Acceleration (G_z).....	101

RESEARCH AND DEVELOPMENT OF ANTI-G LIFE SUPPORT SYSTEMS:

Part 4. Engineering Test and Evaluation of Six Anti-G Valves

1. INTRODUCTION

Many U.S. Air Force (USAF) aerial combat maneuvers (ACMs) can result in severe physiological stress and hazardous performance deficits for aircrew members due to the high-onset $+G_z$ acceleration encountered. Anti-G life-support equipment (LSE) helps to enable aircrew to manage physiological stress and maintain performance.

Among the possible methods to improve tolerance to high-onset $+G_z$ acceleration are state-of-the-art anti-G suits and anti-G valves, which together comprise the total anti-G LSE available to pilots of today's high-performance aircraft. Results of research and development by Technology Incorporated on multiple-capstan and reticulated-foam anti-G suits were presented in Part 1 of this report. This volume (Part 4) describes characterization of current and prototype anti-G valves.

The anti-G valve (or G valve) is a special type of pressure regulator that delivers an output pressure proportional to the $+G_z$ forces acting upon its control elements at a given instant. The standard type of anti-G valve uses a movable mass as the acceleration-sensing element. This movable mass is aligned so that it applies force proportional to $+G_z$ forces to the pressure-regulating elements, which are usually a spring-loaded diaphragm and valve arrangement. At some designated $+G_z$ threshold (usually around $+2 G_z$), the force exerted by the mass supplies the necessary force to open the inlet valve. The inlet valve allows air to flow into the anti-G suit; as suit pressure increases, the back-force exerted on the diaphragm increases and tends to counteract the force applied by the movable mass. When the suit pressure reaches a level that causes the mass and diaphragm forces to cancel, flow ceases. A relief valve arrangement is also incorporated into the anti-G valve. This relief valve functions to limit the maximum suit pressure, usually to within 8 to 11 psig.

Some anti-G valves incorporate an electronic, or servo, control mechanism whereby a linear force motor controls the valve as a function of a G-related electrical signal. Such an electronic valve offers a possibility of improved control of anti-G suit pressurization characteristics.

High sustained $+G_z$ conditions are defined as exposure to $+6 G_z$ and greater for periods longer than 15 s. Newer high-performance aircraft, such as the F-15 and F-16 are capable of producing $+G_z$ conditions which approach or even exceed man's tolerance.

The inflation rates and schedules of anti-G valves have remained essentially unchanged since the 1940s; i.e., the valve is activated at $+2 G_z$ and increases anti-G suit pressure at a rate of 1.5 psi per G to a maximum pressure of 10.5 psi. Until recently, this inflation schedule has been adequate (when used with an efficient straining maneuver) to provide the increase in G-tolerance required in operational

aircraft. With the advent of more maneuverable fighter aircraft, however, it has been found that the inflation schedule of the anti-G suit does not provide maximal acceleration protection, indicating a need for further research and development of anti-G valves.

The ability to screen prototype anti-G valves for performance characteristics is essential to the research, development, test, and evaluation (RDT&E) processes. This report describes methods for testing anti-G valves for performance under simulated high-onset and high-sustained G conditions; it also details performance characteristics measured for current operational anti-G valves and several new prototype anti-G valves.

The term "High" G onset used in this text represents G_z -onset rates between 4 and 6 $G_z s^{-1}$. The actual G_z -onset performance of the USAF School of Aerospace Medicine (USAFSAM) centrifuge is varied depending upon test requirements, and no attempt was made to standardize "High G Onset" beyond these limits.

2. OBJECTIVES

Results of work performed under Task 7, "Engineering Test and Evaluation of Six Anti-G Valves," Contract F33615-81-C-0600, are described here. This test and evaluation (T&E) effort was conducted on-site at Brooks Air Force Base using the USAFSAM Centrifuge Facility, and monitored by USAFSAM/VNS.

One objective of Task 7 was to provide uniform testing procedures for evaluating performance characteristics of the anti-G valves included in this study. Performance characteristics of interest were the dynamic responses of the anti-G valves under closely controlled conditions of: acceleration, source pressure, valve angles and simulated suit volumes. Evaluation of parameters such as physical dimensions, material specifications, environmental suitability or static performance characteristics was not within the scope of this task.

Another objective of this task was to measure and document actual dynamic performance characteristics of the ALAR 8400A valve and 5 new or experimental valves. The 5 experimental valves evaluated were:

- (1) ALAR High-Flow Ready-Pressure;
- (2) ALAR High-Flow;
- (3) Garrett Electronic/Pneumatic Rapid-Response;
- (4) Hymatic VAG-110-022; and
- (5) AAMRL ("Bang Bang").

3. TESTING EQUIPMENT AND PROCEDURES

The testing equipment and procedures employed here are similar, but not identical, to those described in SAM-TR-79-30 (1). Similarity to this previous Technical Report (TR) was desired in order to allow for comparisons with an existing data base. The acceleration profiles used during the tests described in this report, however, differed from those employed in the previous work because much higher onset rates became attainable after completion of recent modifications to the USAFSAM centrifuge. The onset rate is now approximately 6 G s^{-1} measured from baseline G_z ($+1.4 \text{ G}_z$) to $+13 \text{ G}_z$, whereas the maximum onset rate used in the previous measurements was 1.5 G s^{-1} .

3.1 Testing Equipment

3.1.1 General Test Configurations

Two basic test configurations were employed for evaluating anti-G valves. One configuration was used for open-flow tests; i.e., tests in which no resistance to flow--such as would be provided by an anti-G suit--was encountered. A schematic of this configuration is shown in Figure 3.1-1. The second configuration was identical to the first except that a simulated anti-G suit volume and pressure transducer were included downstream from the flow transducer as shown in Figure 3.1-2.

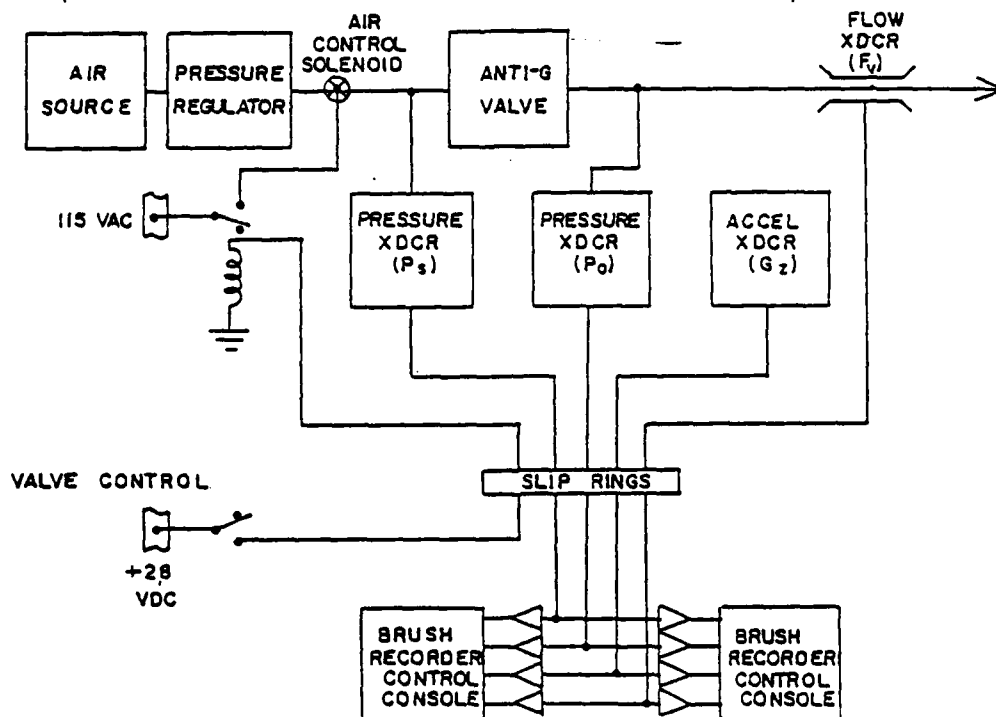


Figure 3.1-1. Phase I Open-flow Capability Test Configuration. F_v = airflow; P_s = source pressure; P_o = valve outlet pressure; G_z = acceleration; XDCR = transducer; VDC = volts direct current; VAC = volts alternating current.

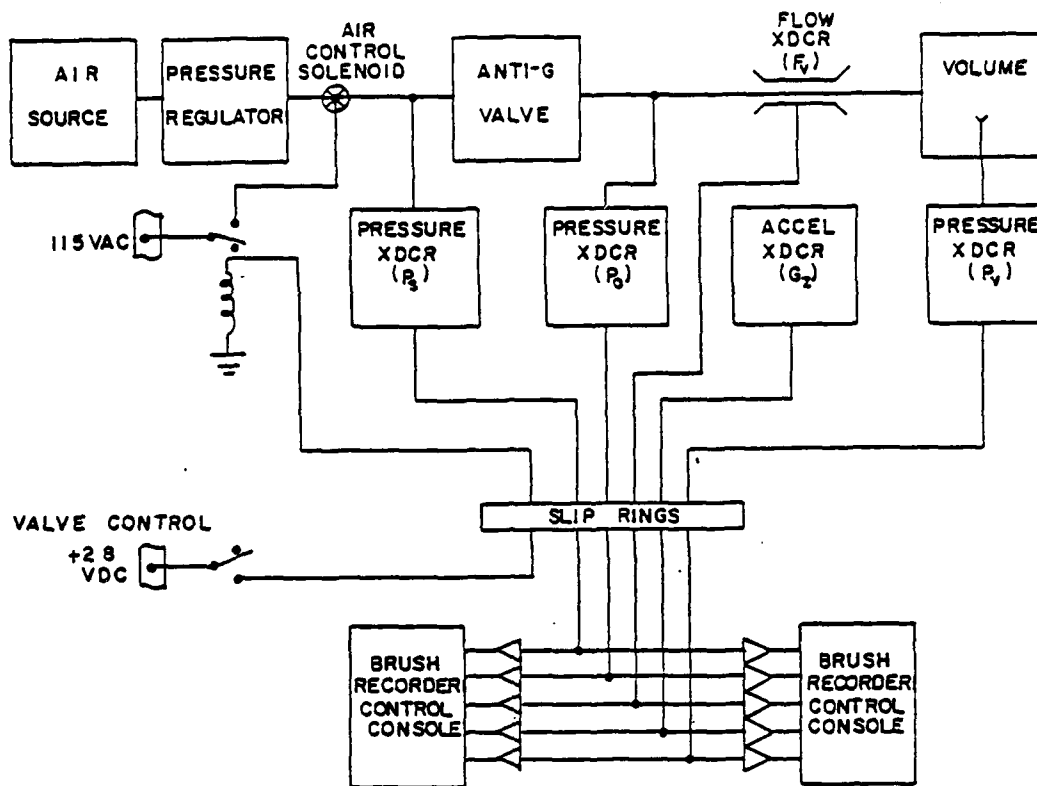


Figure 3.1-2. Phase II Dynamic Test Configuration. F_v = airflow; P_s = source pressure; P_o = valve outlet pressure; G_z = acceleration; P_v = volume pressure; XDCR = transducer; VDC = volts direct current; VAC = volts alternating current.

For both test configurations, the pressure (air) source consisted of a standard "K bottle" containing 222 SCF water-pumped breathing air at 2200 psig which was installed in the gondola of the USAFSAM centrifuge. A high-flow regulator mounted directly on the air bottle was used to maintain the desired source pressure at the inlet of the valve under test. This regulator was manually adjusted to maintain the desired inlet pressure under flow conditions.

A remotely controlled solenoid valve was placed in the air line between the regulator output port and the inlet port of the anti-G valve. This solenoid valve was controlled by a relay that was activated by a 28 VDC signal sent through the slip rings from a switch located at the control console.

The anti-G valve to be tested was mounted on a plate which was indexed in degrees and could be locked in place at any angular position; however, for these tests, only the 0°, 15°, and 30° positions were used. The plate was mounted on a special test stand which aligned the center of the anti-G valve with the gondola accelerometer.

The simulated anti-G suit volume or "sink volume" used to terminate the flow through a valve under test consisted of a rubber bladder sewn between two layers of low-stretch canvas material. This "flexible volume" was adjusted and optimized to represent the incompressible volume required to fill a suit at 5 psig. The inherent stretch of the flexible volume was limited to an increase of 10% when the pressure was increased from 5 psig to 15 psig. To measure the internal pressure of the "sink volume," a small flexible catheter was inserted at the neck of the inlet hose and extended into the volume with the opening placed near the geometric center of the volume.

3.1.2 Test Configuration Elements

3.1.2.1 Source Pressure (P_s)

The pressure-transducer port was located downstream from the solenoid valve and just upstream of the inlet port of the anti-G valve under test. This port was mounted on a section of smooth-bore copper tubing to minimize venturi effects and to provide the necessary rigidity to prevent kinking of the high-pressure hose used to plumb the test stand. Each valve was tested at three different source pressures; high, low, and median pressures which were consistent with the design specifications of each individual valve were used.

3.1.2.2 Valve Output Pressure (P_o)

The valve output pressure transducer port was located immediately downstream from the outlet port of the anti-G valve under test. This port was also on a section of smooth-bore copper tubing to minimize Venturi effects.

3.1.2.3 Air Flow (F_v)

The flow transducer, which was located downstream from the valve-output transducer port, was of the hot-wire type with a fast response to fluctuations in flow. The transducer was also temperature-compensated, and linear over the range of 1.0 - 40.0 standard cubic feet per minute (SCFM). The transducer was plumbed into the system with pipe of dimensions recommended by the manufacturer to assure optimal performance.

3.1.2.4 Simulated Suit Volume Pressure (P_v)

The port for accessing the simulated suit volume pressure was a small catheter extending from the neck of the inlet hose down into the center of the volume. This apparatus necessitated the use of a low-compliance, low-internal-volume type of pressure transducer. The total volume of the catheter and the pressure transducer combination was insignificant when compared to the simulated suit volume. Suit volumes of 6, 10, and 14 liters were used.

3.1.2.5 Acceleration (+G_z)

Acceleration was measured in the +Z axis only--i.e., perpendicular to the floor of the gondola. Measuring acceleration along other axes was not included within the scope of this task.

3.1.2.6 Valve Angle

The valve under test was attached to a circular plate which was indexed in degrees, such that the centerline of the valve and the centerline of the plate were superimposed. The geometric center of the circular plate was the single attaching point between the indexed plate and the special test stand. The zero-degree index mark on the test stand was a line running perpendicular to the floor of the gondola. The valve could be rotated to, and firmly fixed at, any desired angle. The mounting plate was aligned as nearly as possible to the accelerometer in the gondola. For these tests only 0°, 15°, and 30° valve angles were used.

3.1.2.7 Pressure Transducers

The strain-gauge type pressure transducers were used for measuring pressures. A Taber Teledyne type 176 transducer, which had a range of 0-500 psid, was used to measure source pressures. A Gould/Statham type PL131TC-50-350 transducer with a range of 0-50 psid, permanently mounted in the gondola, was used to measure valve output pressure. The simulated anti-G suit volume pressure was measured with a Statham type P6TC-20D-400 pressure transducer with a range of ± 20 psid.

3.1.2.8 Flow Meter

A Technology Incorporated linear flow meter, model LFC-20 with a range of 0-40 SCFM, was used to measure airflow. The maximum error of this system was $\pm 2\%$ of reading or $\pm 0.5\%$ full scale, whichever was greater; repeatability was within 0.1% of flow rate measured. Response time for the sensor was < 0.07 s, and the system had a linear output of 0-5 VDC (0 to full-scale) available for recording.

3.1.2.9 Control Console Signal Conditioners

A Gould universal amplifier, model 13-4615-555604, was used to condition each transducer output measured during testing. These amplifiers had built-in offset nulling and signal filtering. The direct current (DC) measurement range was 500 mV full-scale to 25 V full-scale. Attenuator inaccuracy was $\pm 0.5\%$ of calibrated step, and the nonlinearity was $\pm 0.1\%$ of full-scale.

3.1.2.10 Strip-Chart Recorders

Two Gould model 2800S recorders were used to record all data collected during these tests. The nonlinearity of these recorders was $\pm 0.35\%$ of full-scale; gain instability was $\pm 0.1\%$ of reading for 24 h and zero-line drift was $\pm 0.1\%$ of full-scale range for 24 h. The rise time (10% to 90% full-scale with less than 1% overshoot) was 5 ms.

3.2 Testing Procedures

The performance evaluation tests for the anti-G valves were conducted in three phases, which are described later. All testing on the USAFSAM centrifuge was performed in the automated mode, using computer programs specifically written and tailored for these anti-G valve testing procedures. Automated operation provided greater reproducibility than that attainable in the manual mode.

A test centrifuge run in which G levels were increased from baseline G (1.4 G) to 11 G, held 5 s at 11 G, and then decreased back to baseline G, was defined as a "trapezoid run." This terminology arises from the shape of the actual $+G_z$ profile traced on a strip-chart recorder when time was recorded as one axis, which approximates a trapezoid.

3.2.1 Phase I--Maximum Flow Capacity Testing

Phase I testing was designed to determine the maximum flow capability of the anti-G valve under test. The source pressure employed was the median value for the specific valve under test. Three trapezoidal runs were made using 0.5 G s^{-1} onset and offset rates. Flow was the parameter of primary interest during these tests; however, the source pressure and valve output pressure were also closely monitored. The source pressure regulator was set empirically such that the pressure at the inlet of the valve under test remained within $\pm 10\%$ of the desired value. The valve output pressure was monitored to determine if there was any excessive restriction of airflow downstream from the outlet port of the anti-G valve under test. The valve angle for these tests was 0° . Test conditions for each of the three phases are summarized in Table 3.2-1.

3.2.2 Phase II--Dynamic Response Testing

Phase II testing was undertaken to determine the dynamic response capability of an anti-G valve. All measurements were obtained with the anti-G valve terminated in a flexible "sink volume" of 10 liters. Three 0.1-G s^{-1} trapezoids were run at each source pressure (i.e., minimum, median, and maximum source pressure) with the valve angle held at 0° . The two additional valve angles required three 0.1 G s^{-1} trapezoids at each angle (i.e., 15° and 30°), while the source pressure was held at the median value (Table 3.2-1). As used here, the term "output pressure" refers to pressure within the suit volume, unless otherwise noted.

Three trapezoids (4.42 G s^{-1}) were also run at each source pressure with the valve angle held at 0° (Fig. 3.2-1). The two additional valve angles required three trapezoids at each angle (i.e., 15° and 30°), while the source pressure was held at the median value (Table 3.2-1).

3.2.3 Phase III--Complex Dynamic Response Testing

Phase III testing was designed to provide a measure of the relative capability of an anti-G valve to function under Simulated Aerial Combat Maneuver (SACM) conditions. The G profile used is shown in Figure 3.2-2. This SACM G profile was repeated for each source pressure (minimum, median, and maximum), while the valve angle was held at 0°. The runs at minimum source pressure used the maximum suit volume (14 liters); the runs at maximum source pressure used the minimum suit volume (6 liters); and the runs at median source pressure used the median suit volume (10 liters). In addition, valves were tested under SACM conditions at valve angles of 15° and 30° with median source and suit pressures.

TABLE 3.2-1. SUMMARY OF CONDITIONS EMPLOYED FOR TESTING ANTI-G VALVES

G _z -onset rate (G _z s ⁻¹)	Source pressure (psig)	Suit volume (liters)	Valve angle (°)	Other parameters	Valves
<u>Phase I - Maximum flow (trapezoidal G profile)</u>					
0.5	Med	—	0	—	all
0.5	Med	—	0	Elec "Off" ^a	AAMRL
0.5	Med	—	0	RP "Off" ^b	ALAR HFRP
<u>Phase II - Dynamic response (trapezoidal G profile)</u>					
0.1	Min	Med	0	—	all
High	Min	Med	0	—	all
0.1	Med	Med	0	—	all
0.1	Med	Med	15	—	all
0.1	Med	Med	30	—	all
High	Med	Med	0	—	all
High	Med	Med	15	—	all
High	Med	Med	30	—	all
0.1	Max	Med	0	—	all
High	Max	Med	0	—	all
<u>Phase III - SACM G profile</u>					
—	Min	Max	0	—	all
—	Med	Med	0	—	all
—	Med	Med	15	—	all
—	Med	Med	30	—	all
—	Max	Min	0	—	all

^a AAMRL valve normal operation/testing = electronics "On."

^b ALAR HFRP valve normal operation/testing = ready pressure "On."

SACM = simulated aerial combat maneuver;

Min, Med, Max = minimum, median, maximum values, respectively.

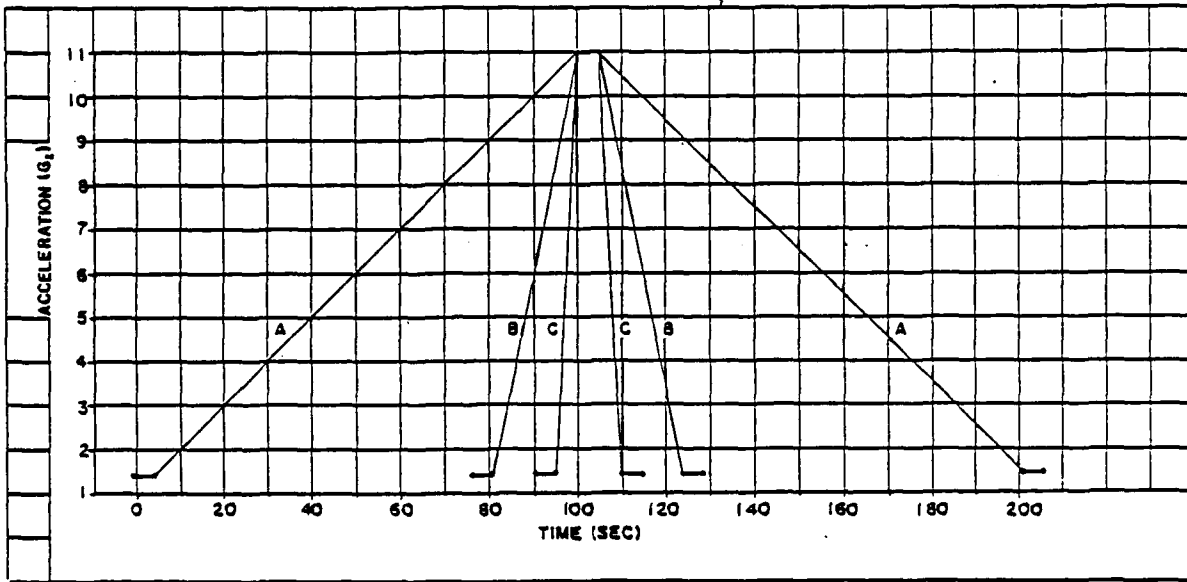


Figure 3.2-1. Conditions of the three Phase-II "trapezoid" centrifuge performance evaluation tests performed at all three source pressures, with valve angle held at 0°.

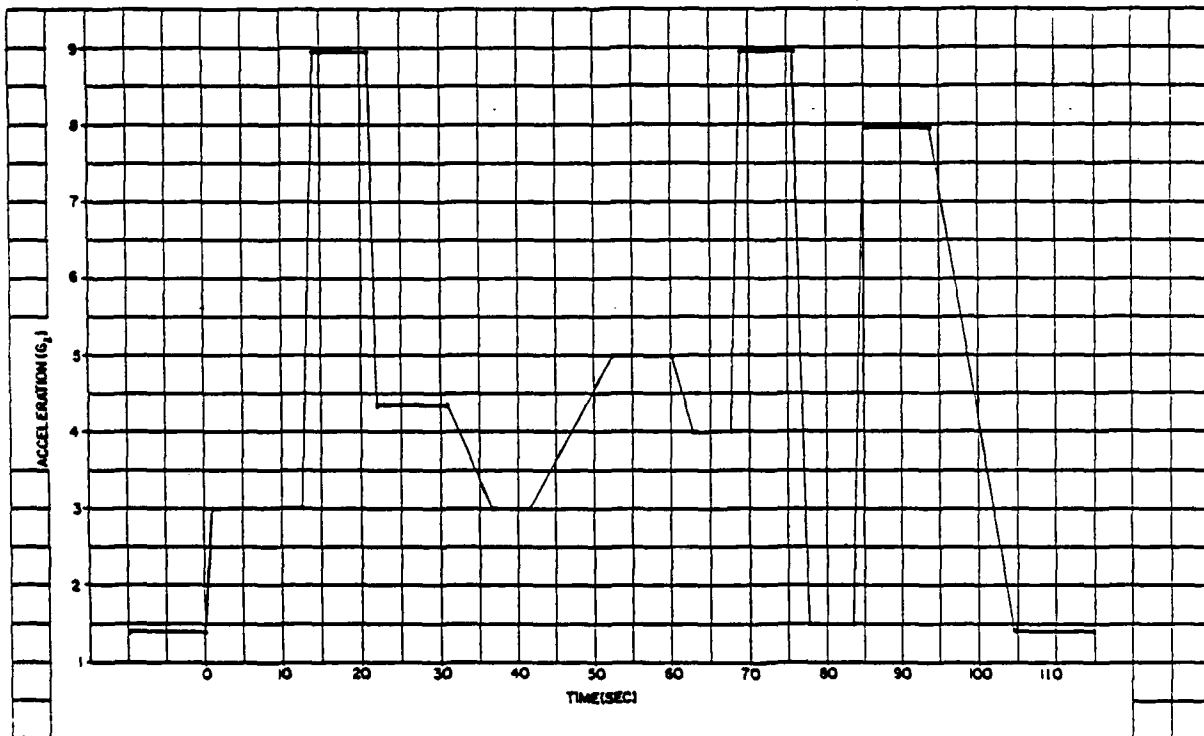


Figure 3.2-2. Conditions of Phase-III SACM Testing of Anti-G valves. The G-profile was run at minimum (30 psi), median (150 psi), and maximum (300 psi) source pressures.

3.2.4 Simulated Suit Volume Measurement

Estimation of the simulated anti-G suit volume (the "sink volume") which was incorporated into test configuration two (Fig. 3.1-1) was performed by evacuating the sink components of the system under mild vacuum, and pressurizing to 5 psig by equilibration with a defined volume at determined initial and final pressures. The volume of the sink was then calculated from the pressure drop in the source volume according to the following relationship:

$$\frac{(P_o - P_r)(V_o)}{P_i - P_s} = V_s$$

when P_o = initial pressure of known volume in psig;
 P_r = final pressure of known volume in psig;
 P_s = final suit pressure in psig;
 P_i = initial suit pressure in psig;
 V_o = known volume in in.³ (or liters); and
 V_s = unknown suit volume in in.³ (or liters).

This relationship assumes that the temperature of the air does not change. The V_s and V_o are the "incompressible volumes," or volumes of water required to fill the space as opposed to the "standard air volume" or volume of air at standard temperature and pressure which would be required to fill the volume at the subject pressure.

3.2.5 Data Acquisition

When the electronic equipment, test stand, and control devices were secured in the Centrifuge gondola, all required signal outputs were connected through slip rings to the control-console patch panel. Each signal pair coming from the gondola was input in parallel to two preamplifiers, each preamplifier occupying the same channel slot in separate but identical strip-chart recorders. The signal pairs from the gondola and brush recorder channels were standardized, in that they were assigned the same parameters for all anti-G valves tested. A preprogrammable patch board for routing the signals and control voltage was made up for the control-console patch panel so that the configuration was standardized for all tests.

The signal conditioners used were all of the same type and model. Signal conditioner gain was matched to the transducer output so that both were in the middle of the measurement range for the parameters monitored.

After all patching was completed, the coarse gain on all preamplifiers was set appropriately and all instrumentation was turned on (in stand-by position) for a warm-up period of at least 10 min. When the instrumentation had stabilized, all channels were calibrated, using the strip-chart recorders as the readout. The usual calibration points were "minimum" (almost always zero) and "maximum" (generally full-scale). The zero points were always calibrated first and any small offset in the transducer

output was nulled out by using the zero-suppression controls incorporated into the preamplifier. All pressure transducers were calibrated using the Datametrics digital-pressure calibration system installed in the gondola.

The flowmeter was calibrated by sending a DC calibration voltage through the slip rings to the preamplifier at the control console. The magnitude of the calibration voltage was determined from the calibration chart for the flow transducer. The calibration voltage was generated by a regulated DC power supply and monitored at the gondola by a calibrated digital voltmeter.

The acceleration channels were calibrated by using the accelerometer calibrator which is permanently installed in the control console. The minimum calibration point was 1 G and the maximum was 10 G. The 1 G baseline corresponded to zero baseline on the strip-chart recorder, thereby affording a full-scale value of 11 G.

The end products of the data-acquisition process were two identical strip-chart recordings, each consisting of five channels of test data. Chart speeds for the strip-chart recorders were selected to afford the proper resolution, with respect to elapsed time, for manual extraction of the required data points. One set of recorded data was kept as backup. The second set of recorded data was manually extracted from the strip-chart recorder trace and transcribed onto standardized tabular forms for data analysis. The data from the strip-chart recordings were presented in final form either as X-Y plots or tabulated.

Access to the signal lines from the gondola to the control console was available through a patch board on the back panel of the gondola interior. The signal lines were American wire gauge (AWG) #20 single-conductor shielded wire. These signal lines were not continuous runs, but were divided into sections terminating or beginning at the slip rings while interconnecting at terminal boards between the slip rings and the control console. The average DC resistance of the signal lines was 4 ohms.

3.2.6 Data Analysis

Three iterations of each type of test run were performed. The dependent variable during these measurements was either the open-flow capability of the anti-G valve, or the pressure developed by the anti-G valve interfacing with a simulated suit volume. Independent variables were acceleration, source pressure, and simulated suit volumes. A special, but useful, independent variable was time (in seconds) which is a function of the acceleration profile. The response times of the valves could be accurately determined since acceleration profiles were standardized and runs were computer controlled.

For the trapezoidal runs, both ascending and descending portions were handled identically for the purposes of extraction of data-point values. Values of open flows (F_v) and simulated suit volume pressures (P_v) were extracted from the strip-chart recordings at intervals of 0.5 G unless there was a stepwise response, or other nonlinear response, to the smooth acceleration rate of the centrifuge. In regions of nonlinear responses, data points were taken at sufficiently close G intervals to furnish enough resolution to accurately display the results on the final graphs. After the run was holding steady at 11 G, data points were taken at 1.5-s intervals; unless there

were fluctuations in the defined parameters. If there were fluctuations, data points were extracted at sufficiently close time intervals to allow graphing.

For the SACM runs, procedures for extracting data-point values were the same as just described for the trapezoidal runs. Acceleration profiles for these runs were more complex; therefore, smaller time intervals were required for sampling.

The strip-chart recordings were grouped into sets, each set consisting of three iterations of the same run conditions. Each iteration was inspected and compared within its set to ensure that the data had been precisely recorded. Numerical values for F_v and P_v for all iterations were transcribed onto a form designed for this operation*. Arithmetical means for each data point were obtained. Working graphs were made on rectilinear graph paper, plotting mean F_v and P_v vs. G; and graphs and numerical data were cross-checked to verify that graphical values were accurate.

Data obtained from all anti-G valves are compared in summary tables (Tables 5.0-1 - 5.0-4). These tables compare means of values obtained from each valve for a specified parameter under varying G conditions. Table 5.0-1 summarizes means for airflow vs. acceleration; Table 5.0-2 shows means for time vs. volume pressure; Table 5.0-3 compares means for volume pressure vs. acceleration low onset; and Table 5.0-4 compares means for volume pressure vs. acceleration high onset.

For graphical presentation, both the ascending (increasing G_z) and descending (decreasing G_z) portions of the trapezoidal runs for each anti-G valve are presented on one graph. The independent variables, acceleration (G_z) and time (s), are represented along the x-axis. In the ascending regions, F_v and P_v were taken at intervals of 0.5 G from baseline G (1.4 G) to 11 G; when acceleration had plateaued at 11 G, data points were taken at intervals of 1.5 s during the plateau phase. In the descending regions, F_v and P_v were taken at intervals of 0.5 G from 11 G to baseline G, beginning at the instant that deceleration started and ending when baseline G was reached. For the purposes of time evaluation, "zero" time corresponded to the instant that deceleration began, and the end point was defined as 1.5 s after baseline G was reached.

4. RESULTS AND DISCUSSION

The anti-G suit design requires that the suit be linearly pressurized, and contain between 0.1 psig and 1.2 psig at 2 G_z and between 8.7 and 11.0 psig at 10 G_z . Performance characteristics of all acceptable anti-G valves must be consistent with the design requirements, which are restated in tabular form in Table 4.0-1.

* Copies of these forms which show all experimental data recorded for each iteration, for all valves, are available as Appendixes A-F.

TABLE 4.0-1. ANTI-G SUIT DESIGN REQUIREMENTS

G _z	Suit pressure* (psig)
2	0.1 - 1.2
10	8.7 - 11.0

* Suit must be linearly pressurized.

4.1 ALAR 8400A Anti-G Valve

4.1.1 Description

The ALAR 8400A anti-G valve (Fig. 4.1-1) is manufactured by ALAR Products, Inc., Macedonia, Ohio. This valve employs a mass/spring system for sensing acceleration and regulating anti-G suit pressure. Source pressure (30 to 300 psig) connects to an inlet fitting on the left side of the valve; the outlet to the anti-G suit is on the right side.

As G_z force is encountered, the mass at the top of the ALAR 8400A valve is forced down against the spring, pushing against a diaphragm regulator assembly and valve stem which opens a flow path to the suit outlet at the right of the valve. As pressure builds up in the suit, back pressure against the diaphragm reduces flow until the G_z force and the suit pressure are balanced, at which time the valve is closed. As G_z force is reduced, the spring moves the mass assembly and diaphragm upward opening the exhaust valve and relieving the suit pressure until G_z force and pressure are again matched. When the valve is returned to conditions of 1 G_z, the valve vents the suit back to ambient pressure.

The ALAR 8400A is designed to actuate (i.e., begin to apply suit pressure) between 1.5 G_z and 2 G_z. The valve is fitted with a spring-loaded relief valve with sufficient flow capacity to limit the suit pressure to 11 psig with 300-psig source pressure. The relief valve is designed to open between 8.7 psig and 11.0 psig. An exposed button located at the top of the 8400A valve assembly allows the G-sensing mass to be depressed manually to provide a functional test feature (i.e., "press-to-test").

4.1.2 Phase I - Determination of Maximum Flow Capacity

To determine maximum flow capacity of the valve, open-flow conditions were established by omitting the terminating ("suit") volume, while leaving the normal hose attached to the output port of the flow transducer. The hose is terminated by the female quick-disconnect fitting used for attaching the simulated anti-G suit volume. The source pressure used for these tests was 150 psig, the selected median pressure.

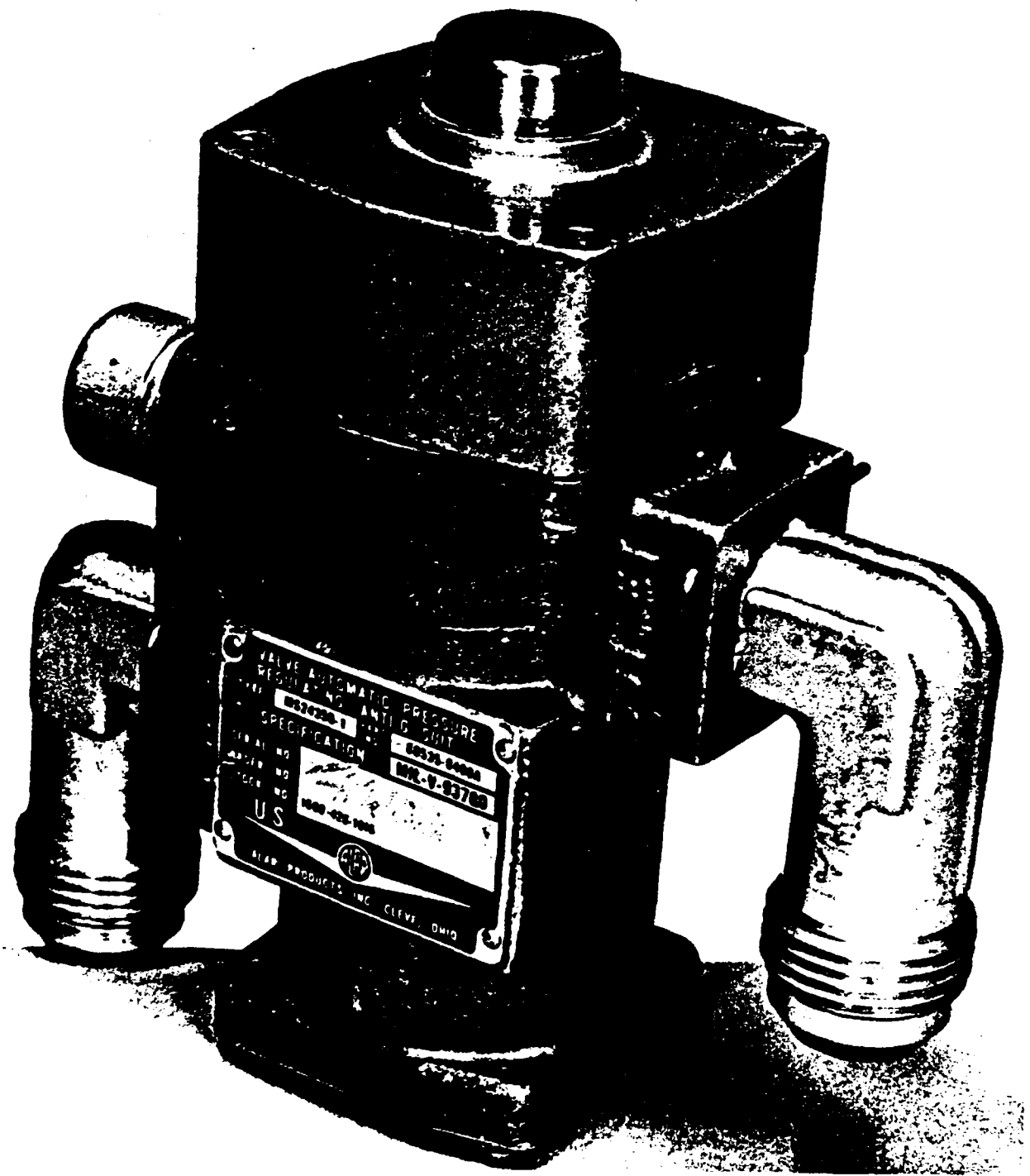


Figure 4.1-1. ALAR 8400A anti-G valve.

Open-flow characteristics of the ALAR 8400A valve are shown in Figure 4.1-2. Flow began at approximately 1.85 G and increased rapidly and almost linearly to a value of 7.6 SCFM at 4.3 G; a small shoulder occurred at this point with flow steady at 7.6 SCFM between 4.3 G and 4.6 G. Flow rapidly increased again, curvilinearly, to a maximum value of 11.1 SCFM at 7.5 G; flow then remained steady at 11.1 SCFM from 7.5 G through the duration at 11 G. Formation of the shoulder is consistent between runs; it is therefore presumed to be an inherent characteristic of this ALAR 8400A valve.

4.1.3 Phase II - Determination of Dynamic Response Capability

The dynamic response capability of the ALAR anti-G valve was determined as described in Testing Procedures, section 3.2.2. Pressure delivered by the valve was measured at the output port and inside the simulated anti-G suit volume. As used here, the term "output pressure" refers to the pressure within the suit volume, unless otherwise noted.

4.1.3.1 Low G_z -Onset-Rate Conditions

The simulated suit volume used for all low G_z -onset measurements was 10 liters, and the G profile was the 0.1 G s⁻¹ trapezoidal profile. The pressure delivered by the valve was measured inside the simulated anti-G suit volume. "Output pressure" as used here refers to the pressure within the suit volume, unless otherwise stated.

When tested under conditions of 150-psig source pressure, 10-liter volume, and a valve angle of 0°, the ALAR 8400A responded in an almost linear fashion between the points where it opened and where its maximum output pressure was reached (Fig. 4.1-3). The valve opened at 2.3 G and delivered a maximum pressure of 7.1 psig at a level of 8 G. The relief valve was actuated at 7.5 G and rapidly began limiting the maximum pressure delivered into the suit volume. The average ALAR 8400A pressurization rate was 1.4 psig G⁻¹ over its useful range.

Angle-dependent measurements employed valve angles of 15° and 30° while the source pressure and simulated anti-G suit volume were held at 150 psig and 10 liters, respectively. At an angle of 15°, the valve opened at 2.5 G and then responded almost linearly from 3 to 8 G (Fig. 4.1-4). At 8 G, the delivered pressure was 6.7 psig, and the relief valve actuated to effect a slowing of the pressurization rate. The pressure increased slightly and curvilinearly from 8 G to 9.5 G, corresponding to a maximum value of 7.0 psig.

At an angle of 30°, opening of the valve was delayed until 3 G was reached, but normal response was not attained until 3.5 G (Fig. 4.1-5). From 3.5 G to 9.5 G, the response was essentially linear except for small deviations (approximately 0.2 psig). At 9.5 G the valve delivered 6.5 psig and then began limiting the pressurization rate. There was some slight wandering of the pressure while "on top" at 11 G, but the pressure essentially continued to increase slowly and reached a maximum of 7.2 psig only after deceleration had begun and progressed to 8.5 G.

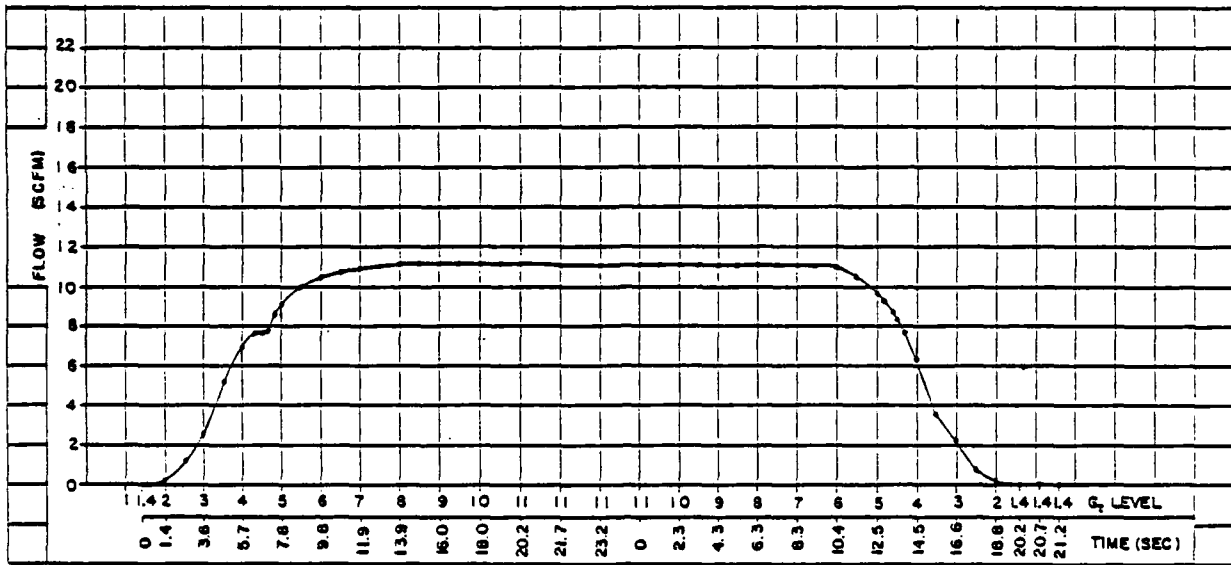


Figure 4.1-2. Maximum flow through ALAR 8400A anti-G valve.

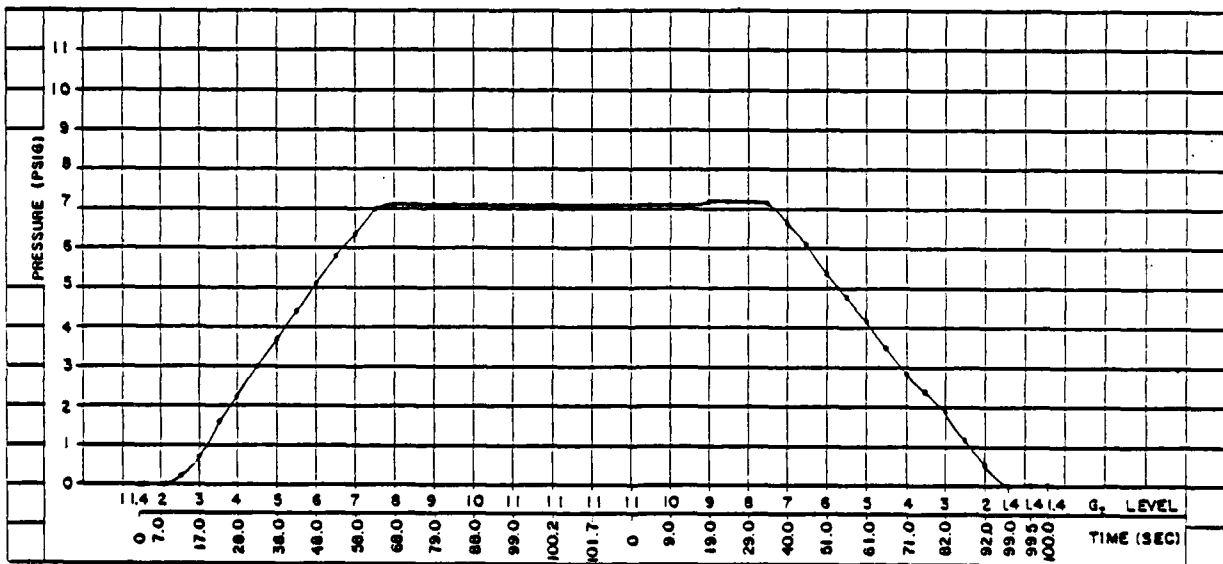


Figure 4.1-3. "Suit" pressures produced during acceleration/deceleration by ALAR 8400A anti-G valve under conditions of: 150-psig source pressure; low G onset; 10-liter volume; 0° angle.

Two other source pressure-dependent measurements were obtained with a valve angle of 0° and suit volume of 10 liters. Minimum (30 psig) and maximum (300 psig) source pressures were investigated. For 30-psig source pressure (Fig. 4.1-6), the valve opened at 2.2 G but normal operation appeared to begin at 2.5 G. The output pressure increased almost linearly from 2.5 G to 7.7 G, where the valve began limiting the pressure to 6.5 psig. A slight drop in pressure (0.1 psig) occurred while "on top" at 11 G. The specified operating threshold of the relief valve apparently was not reached during this study.

At a source pressure of 300 psig (Fig. 4.1-7), the valve again opened at 2.2 G and began a slow increase in output pressure until 2.5 G was reached, at which point normal operation began. Linear operation began at 2.5 G and continued until 7.6 G was reached. At 7.6 G, the valve rapidly began to limit the output pressure to 7.0 psig. Under these source pressure conditions (300 psig), opening of the relief valve appeared to have little effect on the output pressure of this valve.

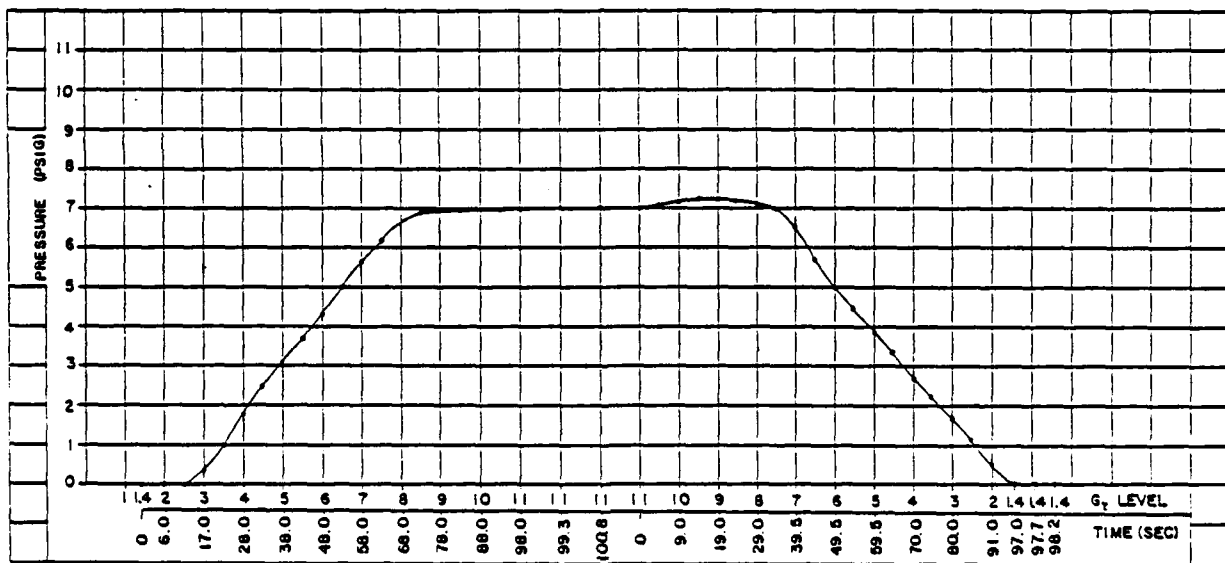


Figure 4.1-4. "Suit" pressures produced during acceleration/deceleration by ALAR 8400A anti-G valve under conditions of: 150-psig source pressure; low G onset; 10-liter volume; 15° angle.

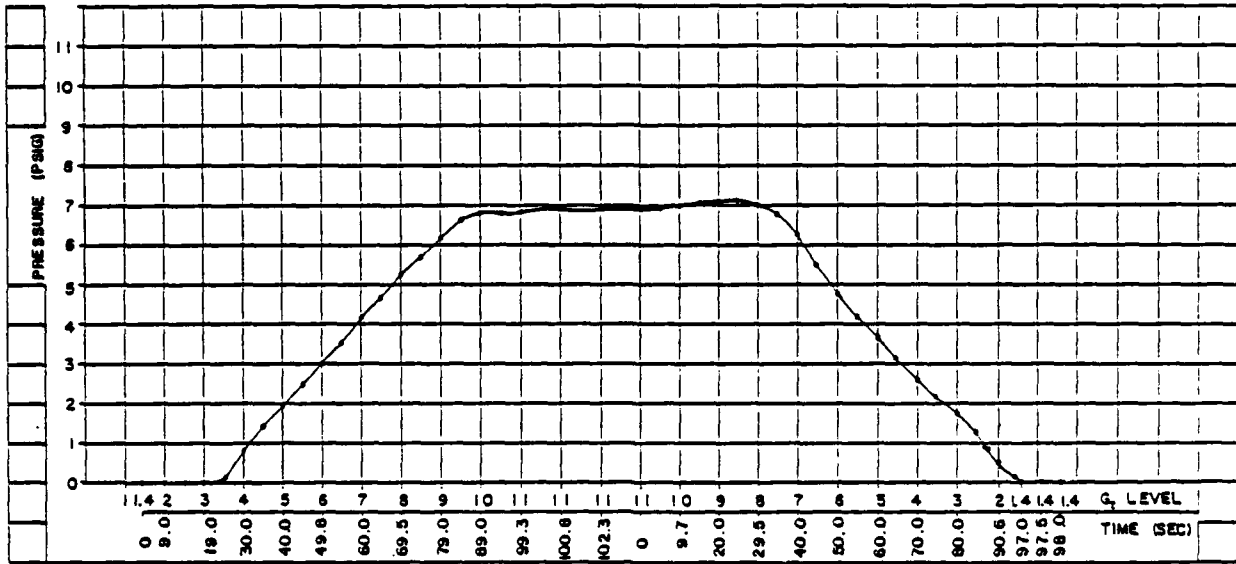


Figure 4.1-5. "Suit" pressures produced during acceleration/deceleration by ALAR 8400A anti-G valve under conditions of: 150-psig source pressure; low G onset; 10-liter volume; 30° angle.

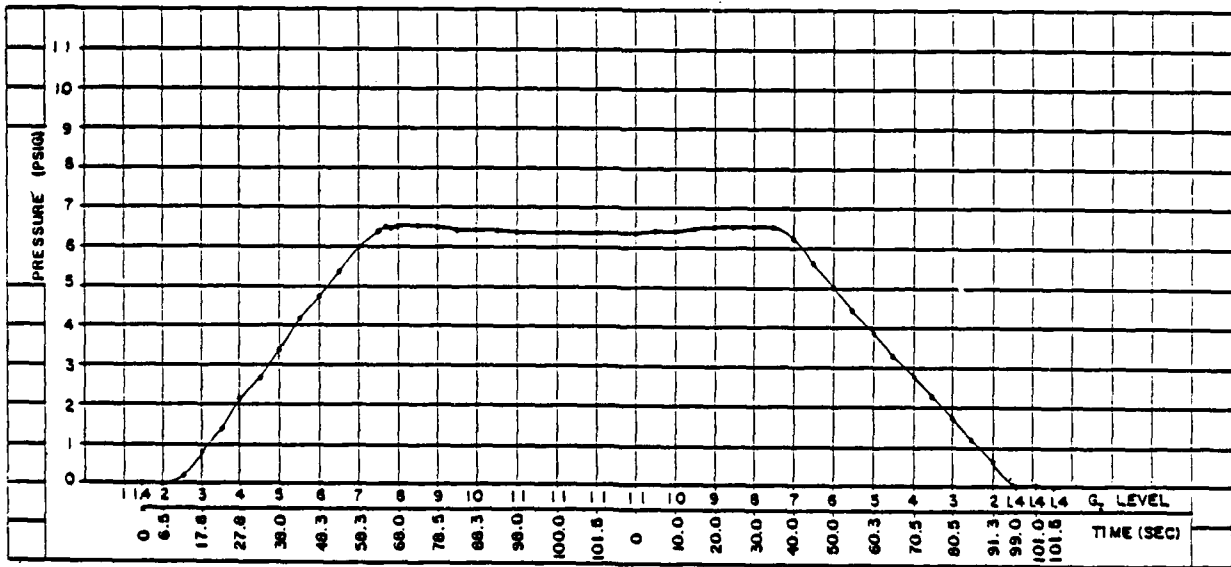


Figure 4.1-6. "Suit" pressures produced during acceleration/deceleration by ALAR 8400A anti-G valve under conditions of: 30-psig source pressure; low G onset; 10-liter volume; 0° angle.

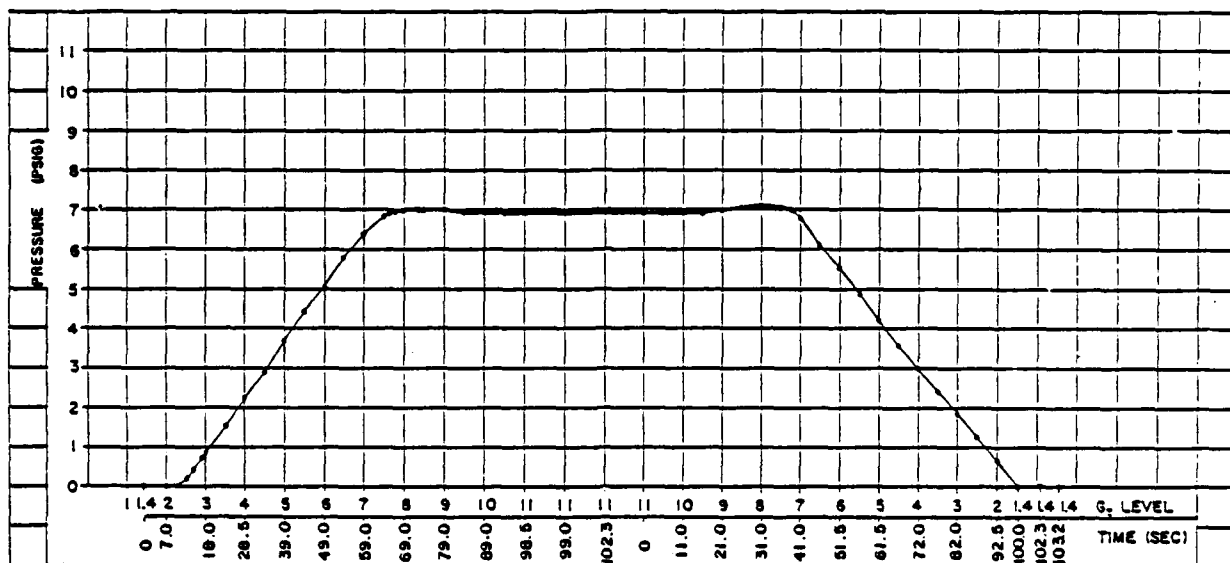


Figure 4.1-7. "Suit" pressures produced during acceleration/deceleration by ALAR 8400A anti-G valve under conditions of: 300-psig source pressure; low G onset; 10-liter volume; 0° angle.

4.1.3.2 High G_z-Onset-Rate Conditions

The simulated anti-G suit volume used in all high-onset tests was 10 liters. The G profile for all tests was the 6 G s⁻¹ trapezoidal profile. The pressure delivered by the valve was measured inside the simulated anti-G suit volume. References to output pressure indicate pressure within the suit volume, unless otherwise defined.

When a source pressure of 150 psig and valve angle of 0° were employed (Fig. 4.1-8), the pressurization schedule (psig G⁻¹) significantly lagged that observed during low G_z-onset testing, seen in Figure 4.1-3. The ALAR 8400A valve initially began pressurization at 2.7 G, but oscillation was observed at the valve outlet port beginning at 1.4 G. The valve oscillated over the interval from 1.4 G to 3 G at an amplitude of 0.7 psig peak-to-peak (p-p). During acceleration from 2.7 G to 11 G, pressurization occurred at a less-than-linear rate; at the instant that 11 G was reached, suit pressure was 6.0 psig. During the time that acceleration was plateaued at 11 G, output pressure rapidly increased to 9.6 psig.

At the instant of deceleration, the valve began oscillating at a low frequency at an amplitude of 0.2 psig; and continued to oscillate until 6 G was reached. Output pressure remained at 9.6 psig until deceleration had reached the 10-G level and then began to decrease almost linearly until it reached 2.7 psig at 2 G. The valve closed at approximately 2 G and the pressure vented rapidly through the exhaust until baseline G was reached at 1.4 G.

The angle-dependent studies of the ALAR 8400A during Phase II high-G_z onset testing used valve angles of 15° and 30° while the source pressure and simulated anti-G suit volume were kept at their median values of 150 psig and 10 liters. At a valve angle of 15° (Fig. 4.1-9), the valve began pressurization at 2.5 G; however, a low-frequency oscillation at an amplitude of 0.3 psig p-p was observed at 1.5 G. This low-level oscillation occurred during the interval from 1.5 G to 3 G; the valve began to operate normally after the oscillation ceased at 3 G and 0.2 psig pressure had developed within the suit volume. The pressurization rate was linear from 0.2 psig at the 3-G level up to 10 G, although the slope of the line decreased somewhat from 6 G to 10 G (4.7 psig); at 10 G the slope began to increase, reaching 5.9 psig at the instant that 11 G was attained. After 1 s "on top" at 11 G, the pressure increased sharply to 8.8 psig, then slowly climbed to the maximum pressure of 9.3 psig by the end of the 5-s interval at 11 G.

At the instant that deceleration began, a 0.2 psig p-p oscillation was detected at the valve outlet port. This oscillation continued until the 6-G level was reached. The pressure decreased slowly from 9.3 psig to 8.8 psig during the interval from 11 G to 9 G, the rate of decrease then became essentially linear from this point down to 2 G (2.5 psig). Since the valve had closed and only the exhaust function was enabled, the pressure decreased rapidly to essentially zero at baseline G.

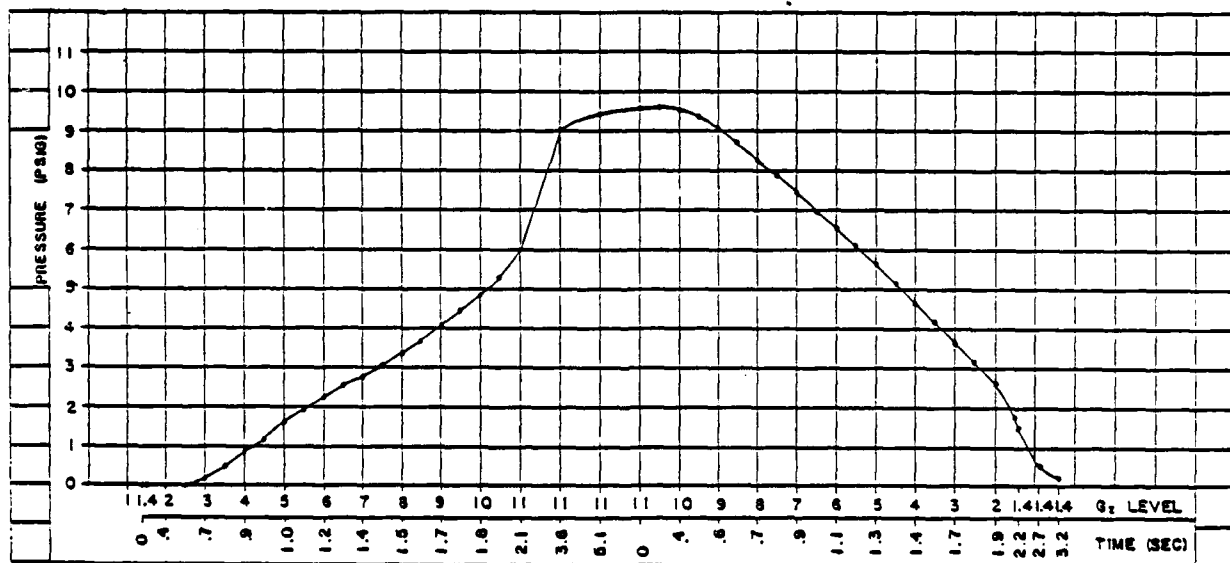


Figure 4.1-8. "Suit" pressures produced during acceleration/deceleration by ALAR 8400A anti-G valve under conditions of: 150-psig source pressure; high G onset; 10-liter volume; 0° angle.

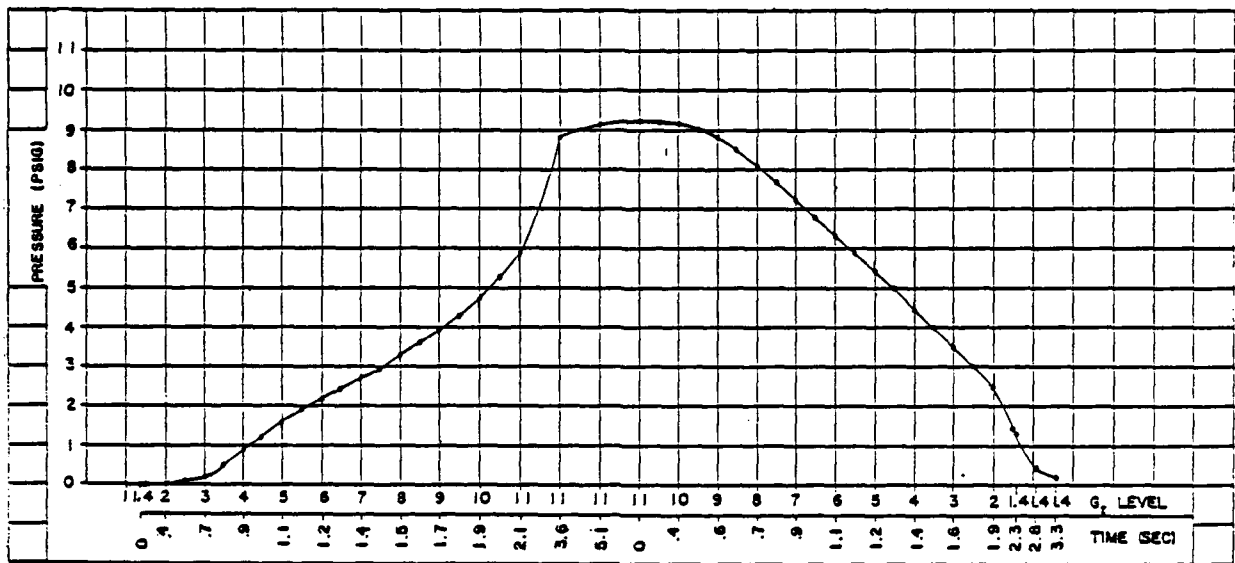


Figure 4.1-9. "Suit" pressures produced during acceleration/deceleration by ALAR 8400A anti-G valve under conditions of: 150-psig source pressure; high G onset; 10-liter volume; 15° angle.

At a valve angle of 30° (Fig. 4.1-10), the valve opened at 3.3 G; the pressurization rate was much slower than that observed during the 0° valve angle testing (Fig. 4.1-8). When acceleration reached 11 G, pressure was 4.9 psig. During 1.5 s at 11 G, pressure rapidly increased to 8.4 psig, then slowly increased to a maximum value of 9.0 psig near the end of the 5-s interval.

At the instant that deceleration began, an oscillation of 0.2 psig p-p was observed at the outlet of the valve; this oscillation continued until 7 G was reached. The pressure remained at 9.0 psig until the G level had decreased to 10 G; it decreased linearly from 8.5 psig to 2.3 psig over the interval from 9 G to 2 G, where the valve closed and the exhaust function allowed the pressure to rapidly decrease to essentially zero at baseline G.

Two source pressure-dependent studies of the ALAR 8400A were conducted: one at 30 psig and the other at 300 psig. Both studies used the 0° valve angle. The 30-psig source pressure study (Fig. 4.1-11) revealed that a low-level oscillation of 0.2 psig p-p occurred over the interval from 1.4 G to 3 G. Pressure began to increase at 2.8 G and at the instant that 11 G was reached, the suit pressure had reached only 4.5 psig; pressure increased rapidly over the next 15 s to a level of 7.8 psig. The maximum pressure developed was 8.3 psig, which occurred at the end of the time at 11 G. The pressure remained at 8.3 psig until the G level had decreased to 9 G, at which time a low-amplitude oscillation and a decrease in pressure occurred simultaneously. The oscillation persisted over the interval from 9 G to 6 G. Pressure decreased at a nearly linear rate over the interval from 8.0 G to 2.0 G; however, as soon as the valve closed, the pressure dropped rapidly to essentially zero at baseline G.

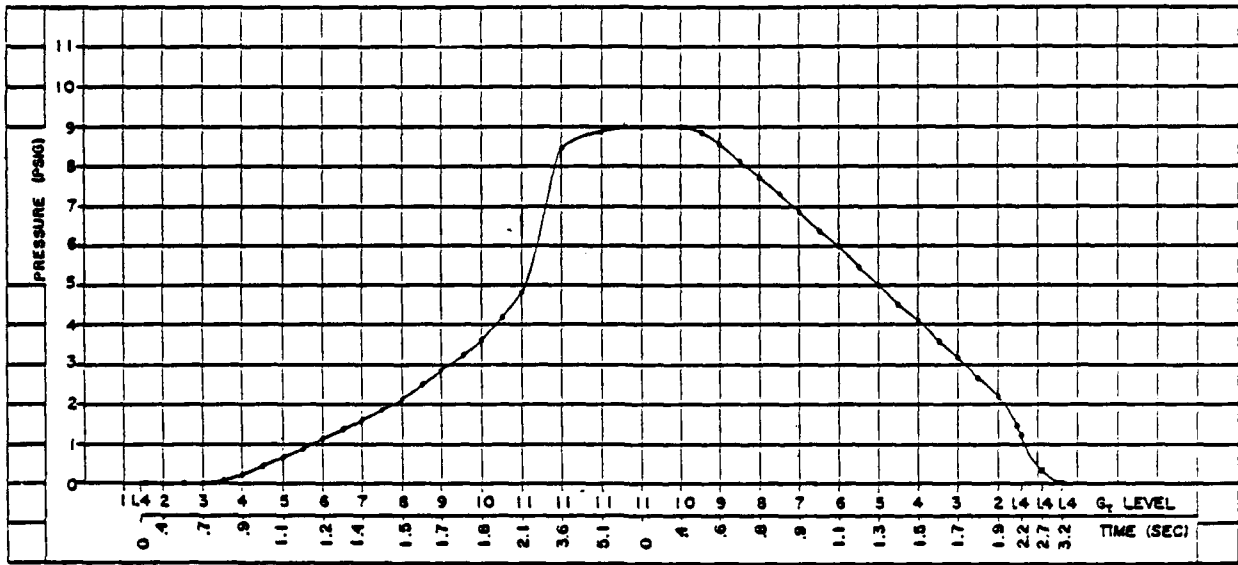


Figure 4.1-10. "Suit" pressures produced during acceleration/ deceleration by ALAR 8400A anti-G valve under conditions of: 150-psig source pressure; high G onset; 10-liter volume; 30° angle.

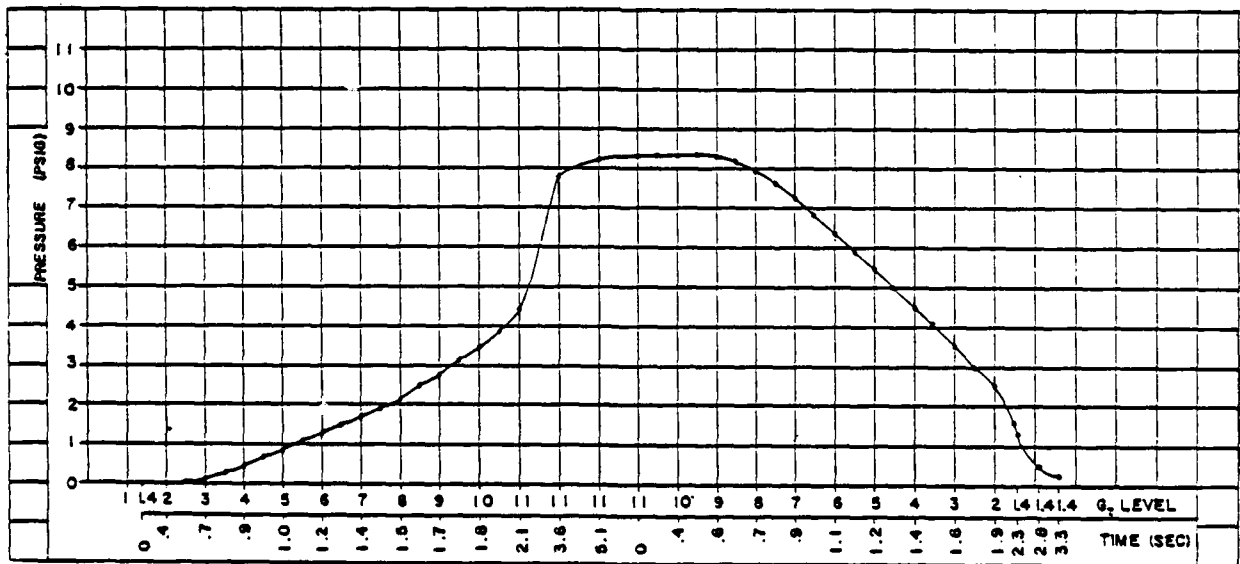


Figure 4.1-11. "Suit" pressures produced during acceleration/deceleration by ALAR 8400A anti-G valve under conditions of: 30-psig source pressure; high G onset; 10-liter volume; 0° angle.

The 300-psig source pressure testing (Fig. 4.1-12) did not reveal the oscillations that were previously seen during the increasing-acceleration portions of the G profile. The valve opened at 2.5 G and the pressurization rate was almost linear over the interval from 3 G to 11 G. The pressure was 5.9 psig at the instant 11 G was reached, but after 2 s "on top," the pressure had rapidly increased to 7.6 psig and stabilized.

During the deceleration portions of the G profile, the pressure showed no decrease until 8.5 G was reached. A low-amplitude oscillation began at 8 G and persisted until 6 G was reached. The pressure decreased from 7 psig (7 G) to 2.5 psig (2 G) at a nearly linear rate. After the valve had closed, the pressure rapidly decreased to essentially zero at baseline G.

4.1.4 Phase III - Determination of Complex Dynamic Response Capability

For testing of the ALAR 8400A anti-G valve under SACM conditions, a valve angle of 0° was used for both minimum and maximum source-pressure testing.

Testing the valve under SACM conditions with a source pressure of 150 psig and valve angle of 0° showed a considerable lag between the valve and G profile (Fig. 4.1-13). On the first high-onset run to 9 G, the "suit" pressure was 8.2 psig and slowly climbed to a maximum of 8.4 psig, which was higher than the maximum pressure on any other run during the testing of this valve. The valve had a low oscillation (0.4 psig p-p) between 3 G and 5 G and again on deceleration between 9 G and 6 G. This oscillation was seen only in the valve outlet pressure and not in the suit

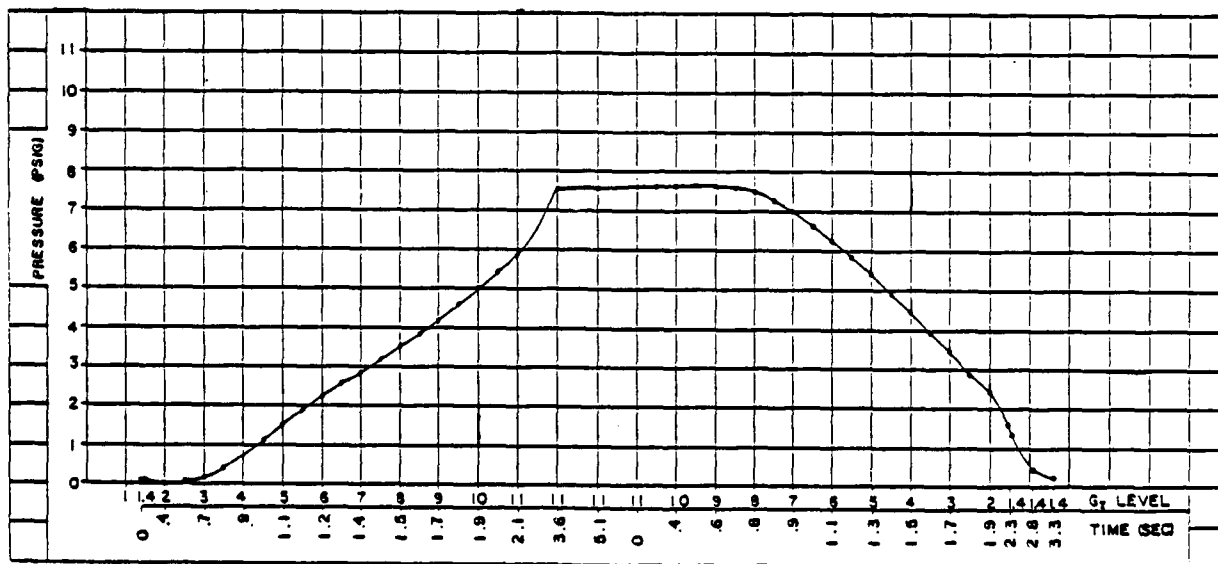


Figure 4.1-12. "Suit" pressures produced during acceleration/deceleration by ALAR 8400A anti-G valve under conditions of: 300-psig source pressure; high G onset; 10-liter volume; 0° angle.

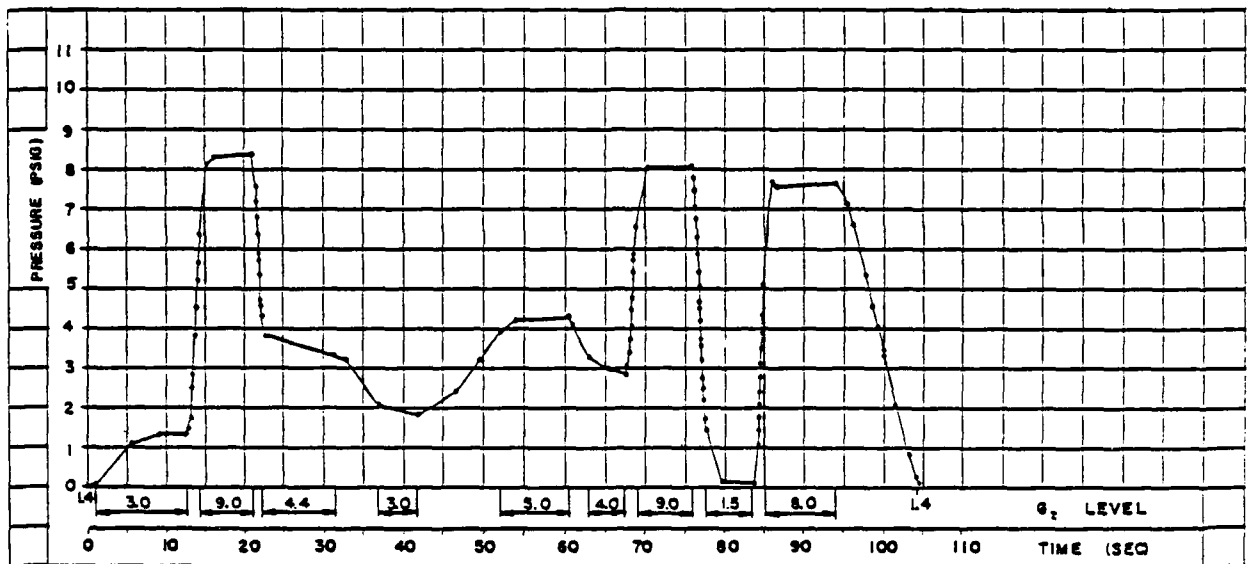


Figure 4.1-13. "Suit" pressures produced during SACM by ALAR 8400A anti-G valve under conditions of: 150-psig source pressure; 10-liter volume; 0° angle.

pressure. At 4.4 G the pressure was 4.3 psig and after about 9.5 s the suit pressure dropped to 3.4 psig and again oscillated between 5 G and 4.4 G. At 3 G the suit pressure was 2.1 psig, dropping off after about 5 s to 1.8 psig. Accelerating again to 5 G, the pressure was 4.0 psig and leveled off at 4.3 psig after about 8.5 s. Decelerating to 4 G produced a pressure of 3.3 psig, which after about 4.5 s leveled off to 2.9 psig. High-onset acceleration again to 9 G produced a suit pressure of 6.6 psig, which after 1.5 s leveled off to 8.1 psig. A high-offset rate to 1.5 G caused a pressure of 1.6 psig which slowly dropped to 0.2 psig. A subsequent rapid-onset acceleration to 8 G produced a pressure of 4.4 psig at 8 G, and a leveling off at 7.7 psig after about 1.5 s. Decelerating from 8 G to 1.4 G caused the suit pressure to drop rapidly to 0.2 psig, which after about 1 s went to zero.

Angle-dependent studies of the ALAR 8400A under SACM conditions used valve angles of 15° and 30°, source pressure of 150 psig, and simulated anti-G suit volume of 10 liters. At a valve angle of 15° (Fig. 4.1-14), the valve began pressurization at 3 G; a low-level oscillation (0.4 psig p-p) was observed between 1.5 and 3 G. The valve began to operate normally after the oscillation stopped, and the "suit" pressure rose to 1 psig at 3 G. A high-onset acceleration to 9 G caused the pressure to rise rapidly to 5.5 psig, and after about 1.5 s "on top" at 9 G, the "suit" pressure leveled off at 8 psig.

With a rapid-offset rate from 9 G to 4.4 G, the suit pressure decreased rapidly to 4 psig, and after about 9.5 s the pressure slowly decreased to, and leveled off at, 3.1 psig (Fig. 4.1-14). Low-level oscillation (0.2 psig p-p) was observed again between 9 G and 5.5 G. Decelerating from 4.4 G to 3 G at a slow descent rate, the pressure dropped to 2 psig and then slowly to 1.6 psig at the end of the 3-G interval.

Accelerating back up to 5 G, the pressure slowly climbed to 2 psig at 4 G and then quickly rose to 3.5 psig. After 2.5 s into the 5-G plateau, the pressure steadily

increased to, and leveled off at, 4 psig. At 4 G the pressure decreased to 2.5 psig. With a rapid-onset acceleration to 9 G and some low oscillation (0.3 psig p-p, from 4 G to 5.5 G), the pressure climbed rapidly to 6.1 psig and then steadily increased to 7.9 psig over the remaining 9-G interval.

Leaving 9 G with a high-offset rate down to 1.5 G, the pressure dropped to 1.4 psig at 1.5 G, and after about 5 s, decreased essentially to zero. Low-level oscillation (0.2 psig p-p) was again observed between 9 G and 6 G.

With another high-onset-rate acceleration from 1.5 G to 8 G, the suit pressure increased rapidly and linearly to 4.2 psig at 8 G and low oscillation occurred between 1.5 G and 3.5 G. After about 1.5 s, the pressure increased to 7.8 psig.

Returning to baseline G (1.5 G) with a high-offset rate, the pressure decreased linearly to zero with low oscillation occurring between 4.5 G and 1.5 G. The pressurization rate under these conditions (15° angle) was a little slower (0.2 psi G⁻¹) than for the 0°-angle conditions.

When a valve angle of 30° was employed (Fig. 4.1-15), test results exhibited the same characteristics as those from the 15°-angle tests, except that the pressurization rate was still slower. The rate for the 30° angle was 0.6 psi G⁻¹ slower than that for 15° angle, and 0.8 psi G⁻¹ slower than the 0° angle testing.

Two source pressure-dependent experiments were conducted on the ALAR 8400A valve while the valve angle was held at 0°. One experiment used a source pressure of 30 psig (the design minimum source pressure) with a 14-liter simulated suit volume (Fig. 4.1-16). The other experiment used the design maximum source pressure of 300 psig and a 6-liter simulated suit volume (Fig. 4.1-17).

For minimum source pressure conditions (i.e., 30-psig source pressure and a suit volume of 14 liters (Fig. 4.1-16)), the valve started to pressurize at 3 G with a suit pressure of 0.05 psig. A low oscillation was observed between 1.5 G and 3 G. With a high-onset acceleration from 3 G to 9 G, the pressure increased to 3.7 psig with a low oscillation of 0.3 psig p-p at 3.5 G. After 7 s at 9 G the suit pressure increased to 8.2 psig. Upon decreasing from 9 G to 4.4 G, the pressure dropped to 4.8 psig; a low-level oscillation occurred from 9 G to 6 G (0.3 psig p-p). After 9.5 s at 4.4 G, the suit pressure decreased to 3.5 psig with a low-level oscillation from 4.4 G (0.4 psig p-p). The G level was then decreased to 3 G, yielding a suit pressure of 2.3 psig which dropped to 2.0 psig within about 7 s. At a low-onset rate to the 5-G level, suit pressure climbed gradually to 3.8 psig then leveled off at 4.3 psig. As G level decreased to 4 G, suit pressure dropped to 3.2 psig, then 3.0 psig. Upon rapid-onset acceleration to 9 G, suit pressure rose to 4 psig, then to 7.8 psig within 7 s; a low oscillation of 0.3 psig p-p was observed at 4.5 G. Rapid-offset deceleration from 9 to 1.5 G resulted in the suit pressure dropping to 2.6 psig; after 5.5 s at 1.5 G, suit pressure dropped to 0.2 psig. An oscillation (0.2 psig p-p) occurred between 9 G and 6 G. A subsequent high-onset acceleration to 8 G produced a suit pressure of 2.4 psig which then increased to 8 psig after 9 s; this was accompanied by an oscillation of 0.2 psig p-p between 1.5 G and 3 G. A high-offset deceleration down to 1.4 G resulted in a decrease in suit pressure to 0.2 psig, with an oscillation (0.3 psig p-p) between 3.5 G and 1.5 G.

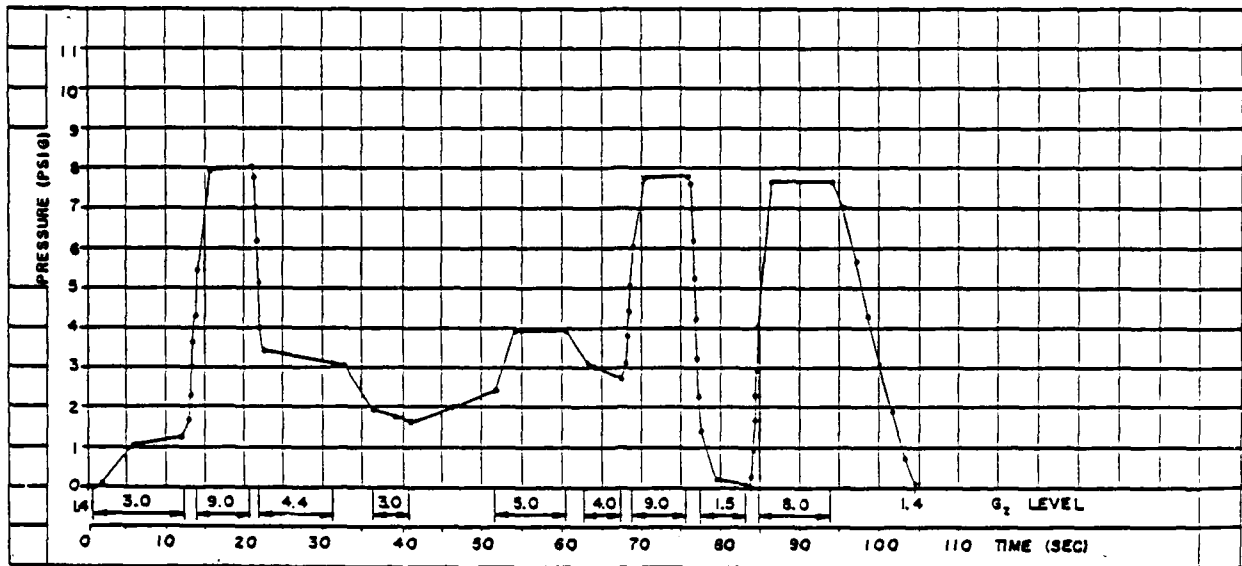


Figure 4.1-14. "Suit" pressures produced during SACM by ALAR 8400A anti-G valve under conditions of: 150-psig source pressure; 10-liter volume; 15° angle.

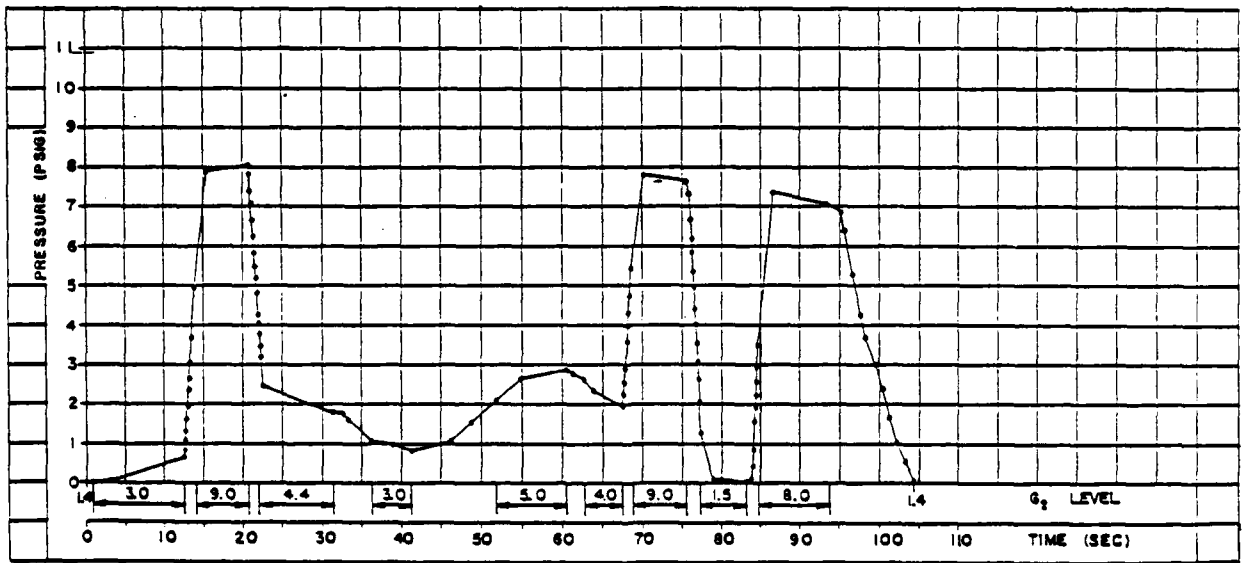


Figure 4.1-15. "Suit" pressures produced during SACM by ALAR 8400A anti-G valve under conditions of: 150-psig source pressure; 10-liter volume; 30° angle.

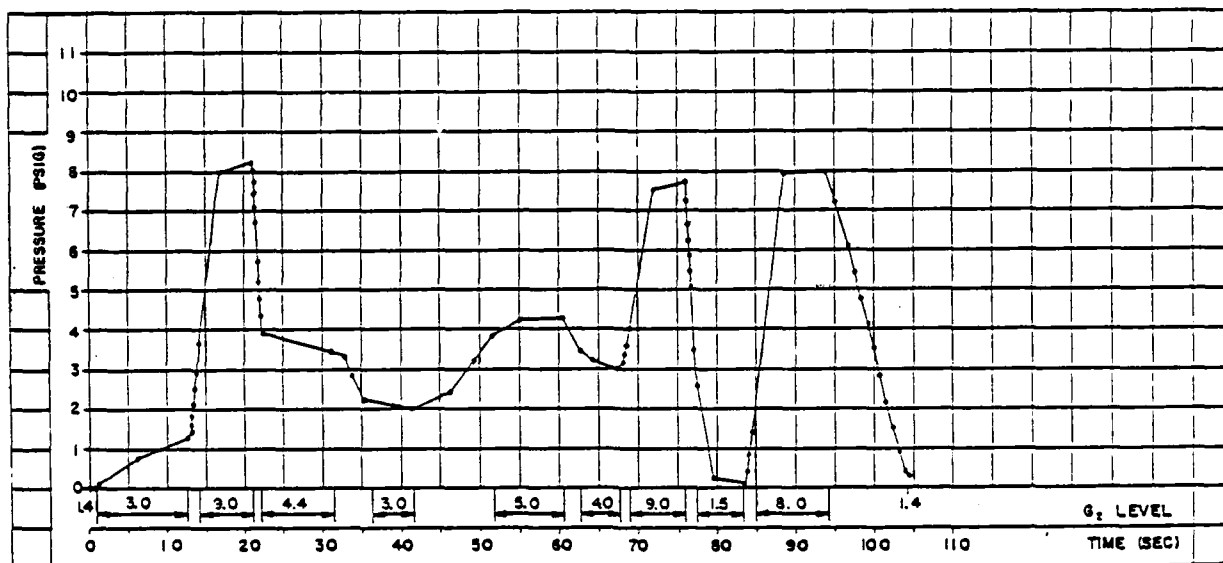


Figure 4.1-16. "Suit" pressures produced during SACM by ALAR 8400A anti-G valve under conditions of: 30-psig source pressure; 14-liter volume; 0° angle.

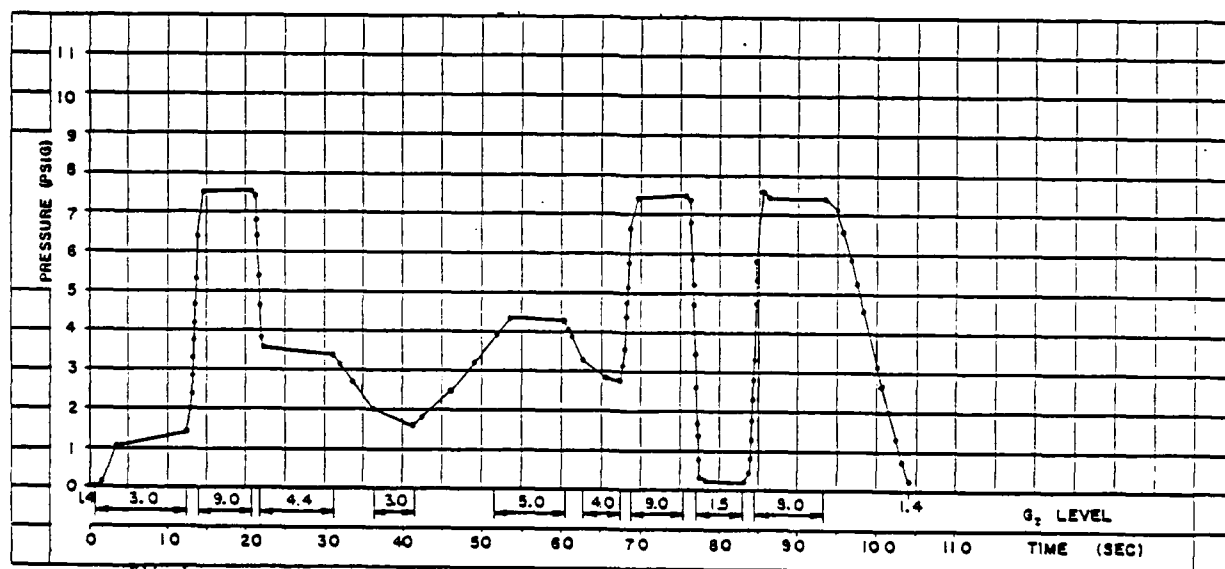


Figure 4.1-17. "Suit" pressures produced during SACM by ALAR 8400A anti-G valve under conditions of: 300-psig source pressure; 6-liter volume; 0° angle.

Under maximum source pressure (300 psig) and a simulated suit volume of 6 liters (Fig. 4.1.-17), the suit started to inflate at 3 G with a suit pressure of 0.1 psig; after 12 s at 3 G suit pressure was 1.4 psig; a low-level oscillation occurred between 1.5 G and 3 G. A rapid-onset acceleration to 9 G resulted in a suit pressure of 6.4 psig at 9 G, which increased to 7.6 psig within 7 s at the 9-G level; an oscillation of 0.4 psig p-p was observed between 3 G and 5.5 G. During a rapid-offset deceleration to 4.4 G, the valve oscillated between 8.5 G and 6.5 G (0.2 psig p-p) and again between 5 G and 4.4 G (0.2 psig p-p). Suit pressure decreased to 3.6 psig as 4.4 G was reached, and dropped to 3.4 psig within 9 s at this G level. A deceleration to 3 G produced a suit pressure of 2 psig, which decreased to 1.6 psig after 5 s. Acceleration to 5 G yielded a suit pressure of 3.9 psig, while dropping back to 4 G resulted in a suit pressure of 3.3 psig. A rapid-onset acceleration to 9 G gave a suit pressure of 6.7 psig, and a low-level oscillation (0.4 psig p-p) between 4 G and 7 G. Rapid deceleration to 1.5 G caused the suit pressure to fall rapidly to 0.7 psig; after 5.5 s at 1.5 G, the pressure decreased to 0.2 psig. A subsequent high-onset acceleration to 8 G produced a suit pressure of 7.6 psig, which stabilized at 7.5 psig within 1 s. Rapidly decreasing the G level down to 1.4 G caused suit pressure to drop to 0.2 psig, and produced a low-level oscillation (0.2 psig p-p) between 4.5 G and 1.5 G.

4.2 ALAR High-Flow Ready-Pressure Anti-G Valve

4.2.1 Description

The ALAR High-Flow Ready-Pressure (ALAR HFRP) anti-G valve (Fig. 4.2-1) is a modified version of the ALAR 8400A. The 8400A valve was modified to obtain a 50% increase in airflow through enlargement of orifices, and an increase in first stage pressure from 10 psig to 19 psig through adjustments to the first stage regulator internal pressure. Initiation of airflow was at 2 G. In addition, a manual mechanical "Off/On" ready-pressure switch was added. When this switch is actuated (in the "On" position), the ready pressure causes the anti-G suit to inflate to 60% of its air-volume capacity, and to maintain a pressure of approximately 0.2 psig within the suit.

4.2.2 Phase I - Determination of Maximum Flow Capacity

Under open-flow conditions, the ALAR HFRP valve performed as shown in Figures 4.2-2 and 4.2-3. With the ready-pressure switch in the "Off" position, flow started at approximately 2 G (Fig. 4.2-2). At baseline G (1.4 G), the flow was 0.3 SCFM; as G_z increased, flow increased rapidly to 22.7 SCFM at 11 G. A shoulder on the curve was observed in the region of 2.6 G where flow briefly leveled off at 6.3 SCFM, dropped to 6.0 SCFM, and rose again to 6.3 SCFM in approximately 0.5 s.

With the ready-pressure switch "On," flow was initiated at about 2 G (Fig. 4.2-3). At baseline G (1.4 G), flow was 3.3 SCFM; this flow was maintained as G level increased to 2.1 G, when flow increased until 2.7 G before leveling off momentarily at 5.7 SCFM. Flow then increased rapidly to 10 SCFM at 3.6 G before slowing somewhat; it then increased to a maximum of 22.6 SCFM at 9 G. No increase in flow was observed as the G level was raised from 9 G to 11 G.

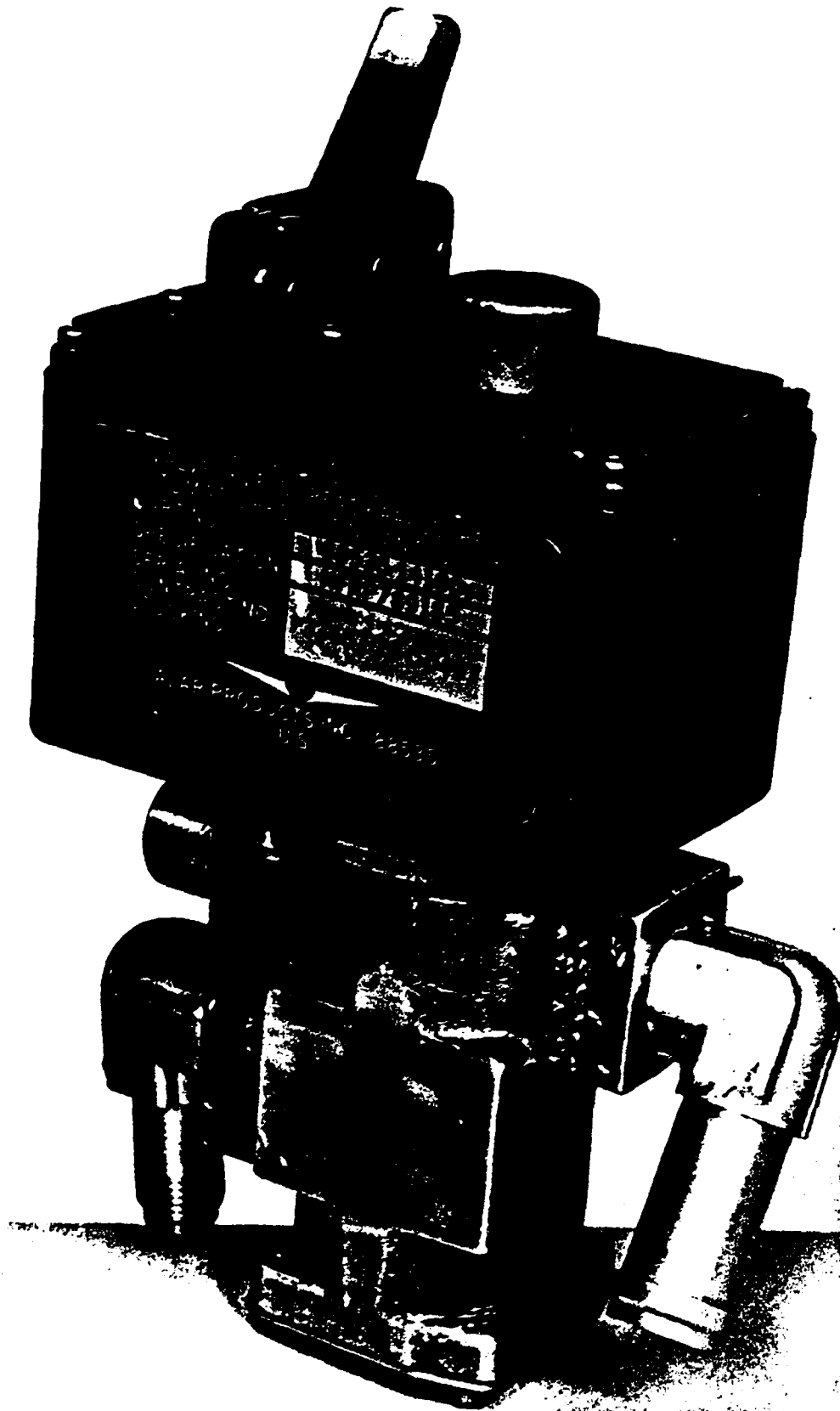


Figure 4.2-1. ALAR High-Flow Ready Pressure anti-G valve.

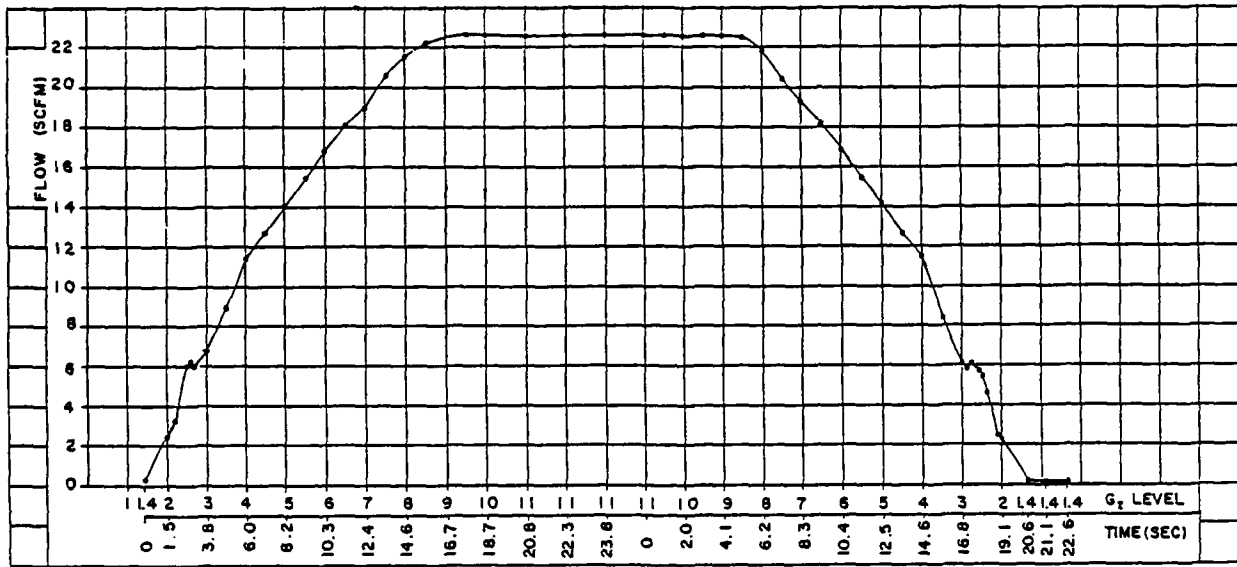


Figure 4.2-2. Maximum flow through ALAR HFRP anti-G valve with pressure off.

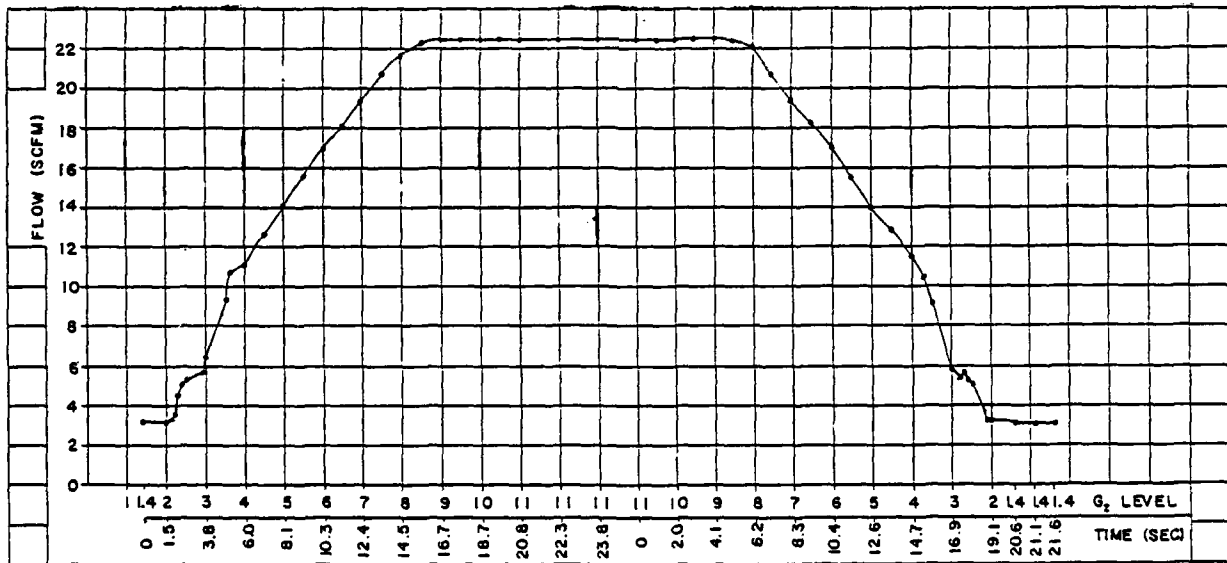


Figure 4.2-3. Maximum flow through ALAR HFRP anti-G valve with pressure on.

4.2.3 Phase II - Determination of Dynamic Response Capability

The dynamic response capability of the ALAR HFRP anti-G valve was determined as described in Testing Procedures, section 3.2.2. Pressure delivered by the valve was measured at the output port and inside the simulated anti-G suit volume.

4.2.3.1 Low G_z -Onset Rate Conditions

The low G_z -onset test conditions employed were: 0.1 $G\ s^{-1}$ trapezoidal profile and simulated suit volume of 10 liters. The pressure delivered by the valve was measured at the output port and from the interior of the simulated anti-G suit volume. All tests for this phase were conducted with the ready pressure switch in the "On" position.

When the ALAR HFRP valve was tested under conditions of 150-psig source pressure, 10-liter volume, and 0° valve angle, the results shown in Figure 4.2-4 were observed. Flow was slow initially with a suit pressure of 0.4 psig at 1.4 G which increased to 0.5 psig at 2 G; as G_z level increased from 2 G to 7.5 G, suit pressure increased to 8.2 psig in an essentially linear fashion. From 7.5 G to 11 G, the pressurization rate slowed due to the relief valve cutting in. The average pressurization rate was 1.3 psig G^{-1} over the useful range of the valve.

For a 15° valve angle (and all other conditions the same), the performance characteristics in Figure 4.2-5 were observed. The valve responded almost linearly from 2 G to 8 G, which corresponded to a suit pressure of 8 psig. The relief valve was activated at this point, resulting in a slowing of pressurization rate such that suit pressure increased to 10.3 psig at 11 G.

When the valve angle was 30°, the valve did not open until 2.4 G was reached (Fig. 4.2-6). From 2.5 G to 8 G, suit pressure increased linearly from 0.5 to 6.8 psig. The relief valve then started to open, slowing the rate of suit pressure increase; a pressure of 9.5 psig was observed when 11 G was attained, but 1 s later it increased to the maximum of 9.6 psig.

The effect of source pressure upon valve performance under low- G_z -onset conditions was explored. Holding the valve angle at 0° and the suit volume at 10 liters, a minimum source pressure (30 psig) and a maximum source pressure (300 psig) were employed. From 2 G to 8 G, suit pressure increased almost linearly to 8 G where the suit pressure was 8.5 psig. From 8 G to 11 G, the pressure increased curvilinearly to a maximum of about 10.3 psig. (See Fig. 4.2-7.)

When a source pressure of 300 psig was employed (Fig. 4.2-8), the valve started to pressurize at 2 G and pressurization rate was linear up to 7.5 G (7.8 psig suit pressure). From 7.5 G to 11 G, the rate slowed somewhat, yielding a suit volume pressure of 10.7 psig at 11 G.

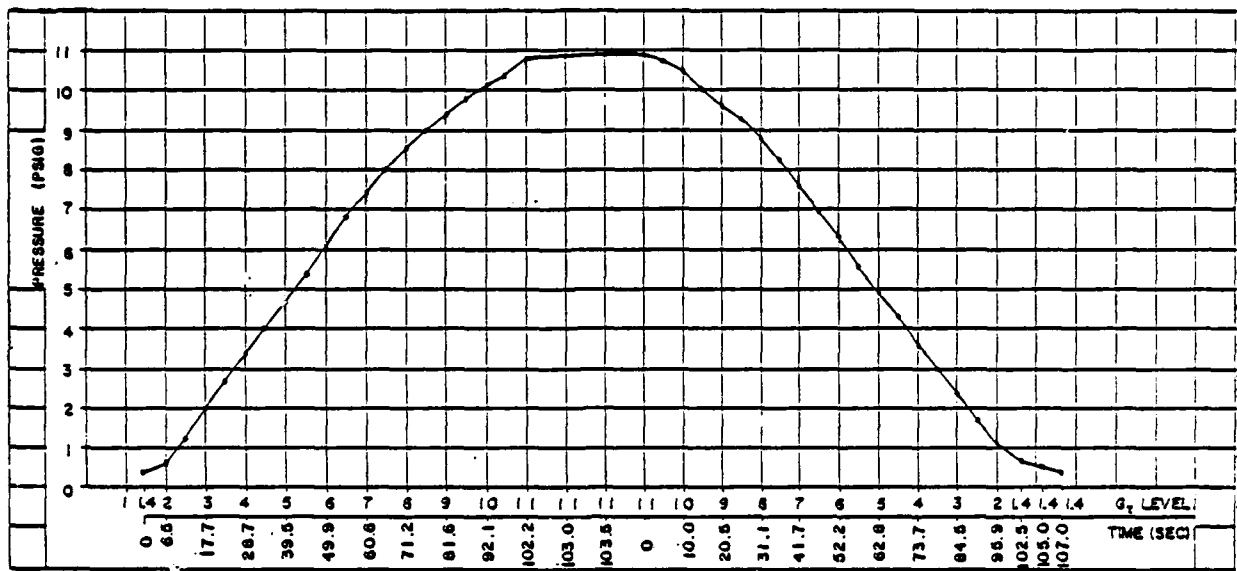


Figure 4.2-4. "Suit" pressures produced during acceleration/deceleration by ALAR HFRP anti-G valve under conditions of: 150-psig source pressure; low G onset; 10-liter volume; 0° angle.

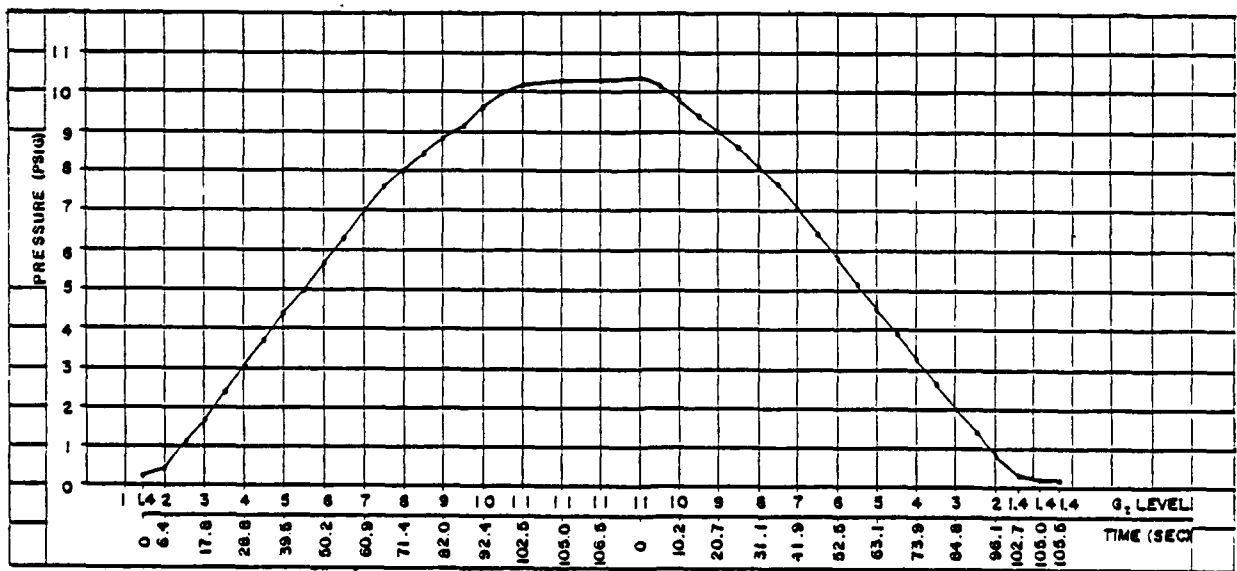


Figure 4.2-5. "Suit" pressures produced during acceleration/deceleration by ALAR HFRP anti-G valve under conditions of: 150-psig source pressure; low G onset; 10-liter volume; 15° angle.

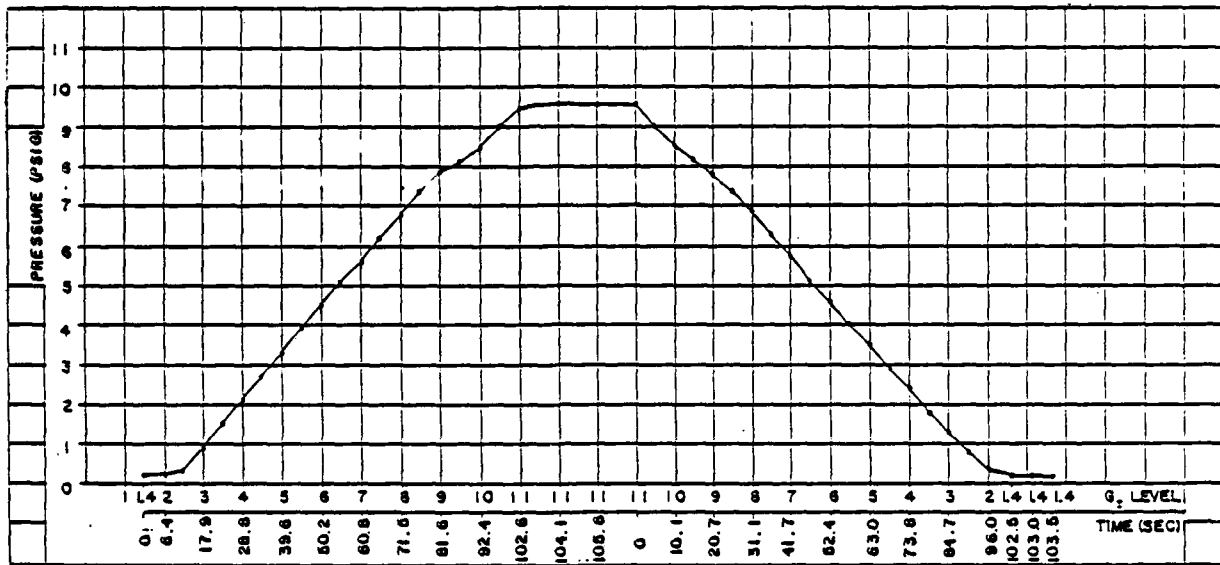


Figure 4.2-6. "Suit" pressures produced during acceleration/deceleration by ALAR HFRP anti-G valve under conditions of: 150-psig source pressure; low G onset; 10-liter volume; 30° angle.

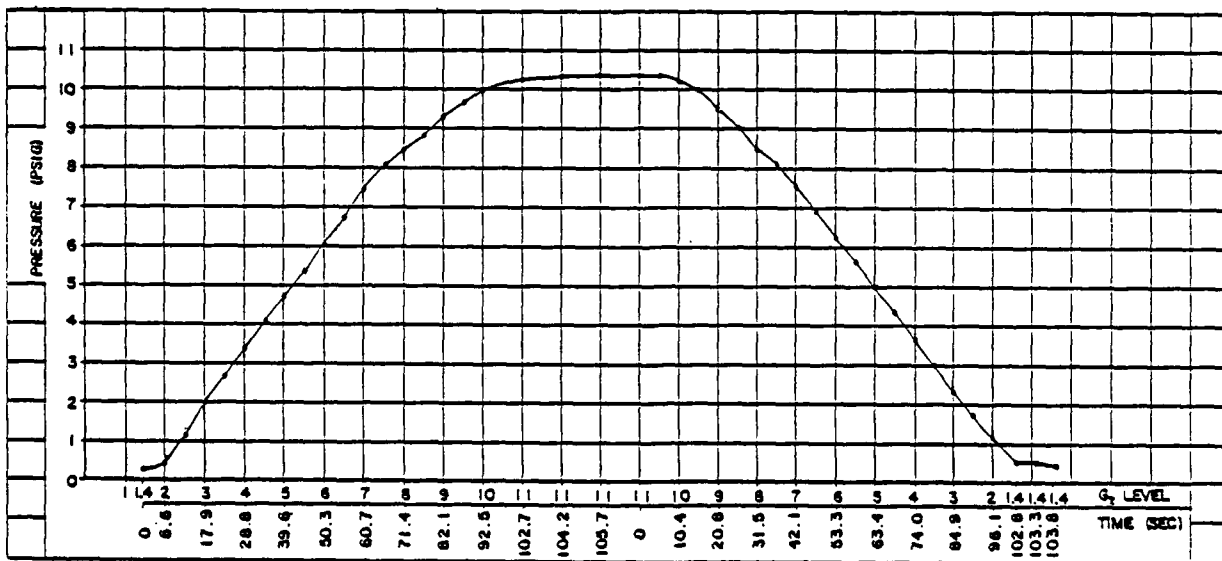


Figure 4.2-7. "Suit" pressures produced during acceleration/deceleration by ALAR HFRP anti-G valve under conditions of: 30-psig source pressure; low G onset; 10-liter volume; 0° angle.

4.2.3.2 High G_z-Onset-Rate Conditions

High G_z-onset-rate testing employed the median simulated anti-G suit volume of 10 liters, and a trapezoidal profile of 6 G s⁻¹. The pressure delivered by the valve was measured at both the output port and inside the simulated G-suit volume; however, only suit-volume pressures are discussed here.

At a source pressure of 150 psig and valve angle of 0°, the pressurization schedule (psig G⁻¹) exhibited a significant lag behind that observed during low G_z-onset testing. Under high G_z-onset conditions (Fig. 4.2-9), the valve initially began pressurization at 2 G, but oscillation was observed at the valve outlet port from 1.4 G. Oscillation of amplitude 0.6 psig p-p continued from 1.4 G to 9 G. From 2 to 11 G, the pressurization rate was linear; the slope of the line was such that the suit pressure was 1.1 psig at 3 G and 7.2 psig at 9 G. From 9 to 11 G the response rate deviated slightly from linearity with a suit pressure of 9.9 psig when 11 G was attained; however, pressure rapidly increased to 11.1 psig during the period at 11 G. Upon initiation of deceleration, the valve exhibited a low-frequency oscillation of 0.5 psig p-p amplitude which continued as deceleration continued down to 5 G.

Effects of valve angle upon ALAR HFRP valve performance under high G_z-onset conditions were observed using valve angles of 15° and 30° and keeping source pressure and suit volume constant at 150 psig and 10 liters, respectively. For a valve angle of 15° (Fig. 4.2-10), a low-frequency oscillation with amplitude 0.3 psig p-p started at 1.5 G and continued until 10 G. The valve began pressurization at 2 G and the rate was generally linear up to 10 G: suit pressure was 0.4 psig at 2 G, 3.9 psig at 6 G, and 8 psig at 10 G. Upon attaining 11 G, suit pressure was 9.3 psig; during the time "on top" at 11 G, pressure increased to 10.7 psig within 1.5 s, and climbed to a maximum of 10.8 psig by 5 s. Upon deceleration under these conditions, an oscillation of 0.2 psig p-p occurred and continued until 5.5 G where suit pressure was 6.1 psig. The depressurization rate was linear down to about 4.1 psig at 3 G, dropping off rapidly to 0.5 psig at 1.4 G.

When the valve angle was 30° (Fig. 4.2-11), the valve opened at about 2.5 G; however, the suit pressurization rate was noticeably slower than when the valve angle was 15°. At the instant the acceleration reached 11 G, the suit volume pressure was only 8 psig; after 1.5 s at 11 G, pressure was at its maximum value of 9.5 psig. As deceleration was initiated, a low-frequency oscillation of 0.3 psig p-p amplitude was observed at the valve outlet port, and this oscillation continued until 5.5 G while suit pressure decreased essentially linearly from 11 G to 1.4 G.

The effects of source pressure upon performance of the ALAR HFRP valve were examined by testing the valve at 30 and 300 psig and 0° valve angle. At 30 psig source pressure (Fig. 4.2-12), a low-frequency oscillation of 0.5 psig p-p in suit volume pressure occurred over the interval of 1.4 G to 8 G. The suit pressure was 5.7 psig at 8 G, and 9.7 psig at the instant that 11 G was attained. A maximum suit pressure of 10.8 psig was measured at the end of the interval "on top" at 11 G. The low-level oscillation (0.6 psig p-p) reoccurred immediately upon deceleration, and continued until the 5-G point; the suit pressure decreased linearly down to 2 G.

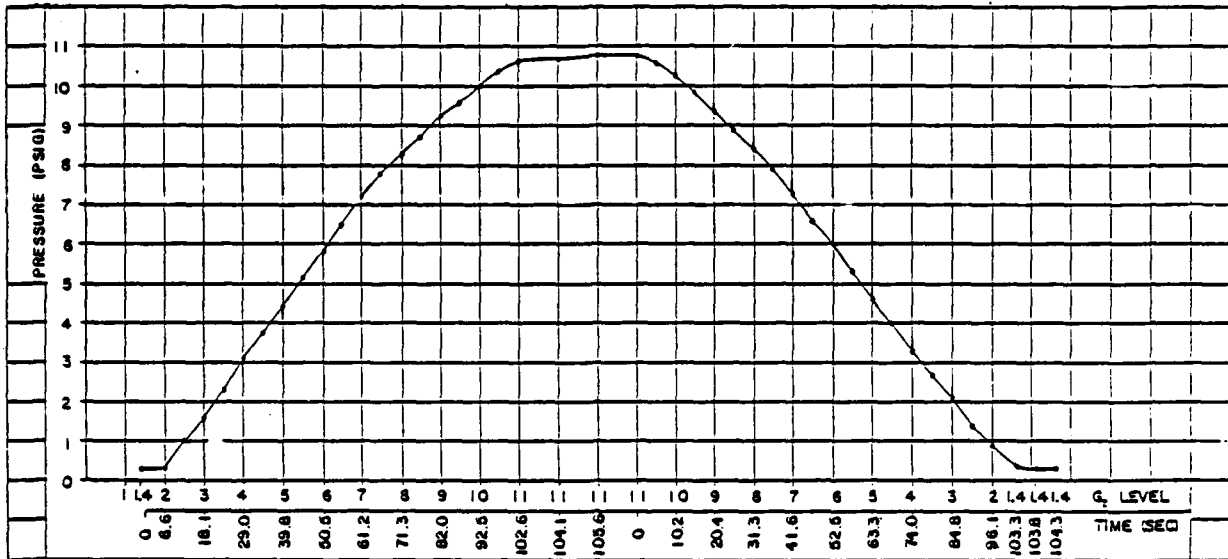


Figure 4.2-8. "Suit" pressures produced during acceleration/deceleration by ALAR HFRP anti-G valve under conditions of: 300-psig source pressure; low G onset; 10-liter volume; 0° angle.

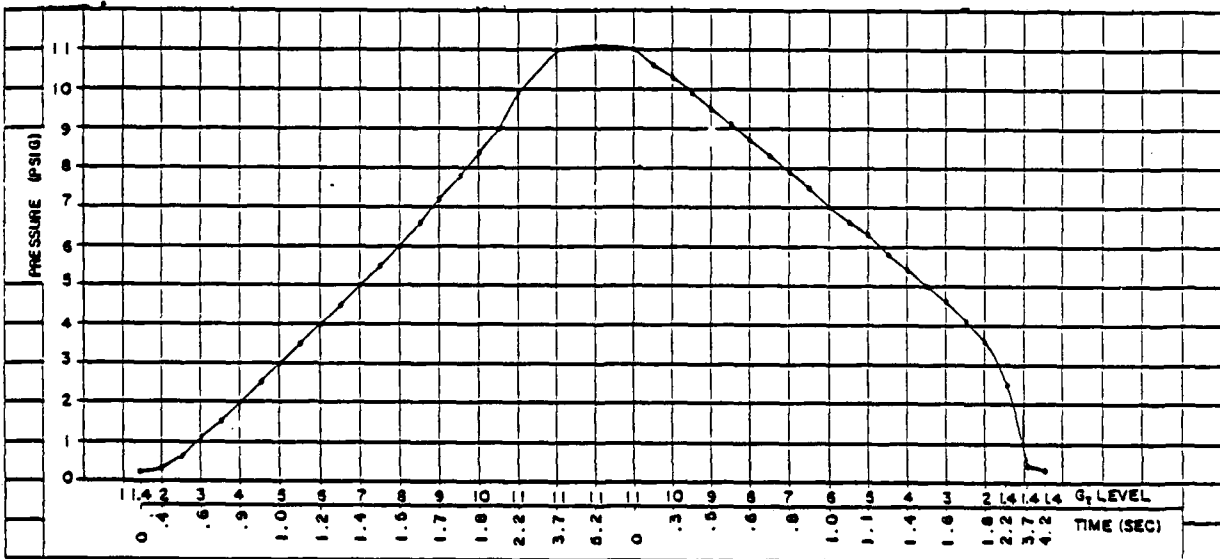


Figure 4.2-9. "Suit" pressures produced during acceleration/deceleration by ALAR HFRP anti-G valve under conditions of: 150-psig source pressure; high G onset; 10-liter volume; 0° angle.

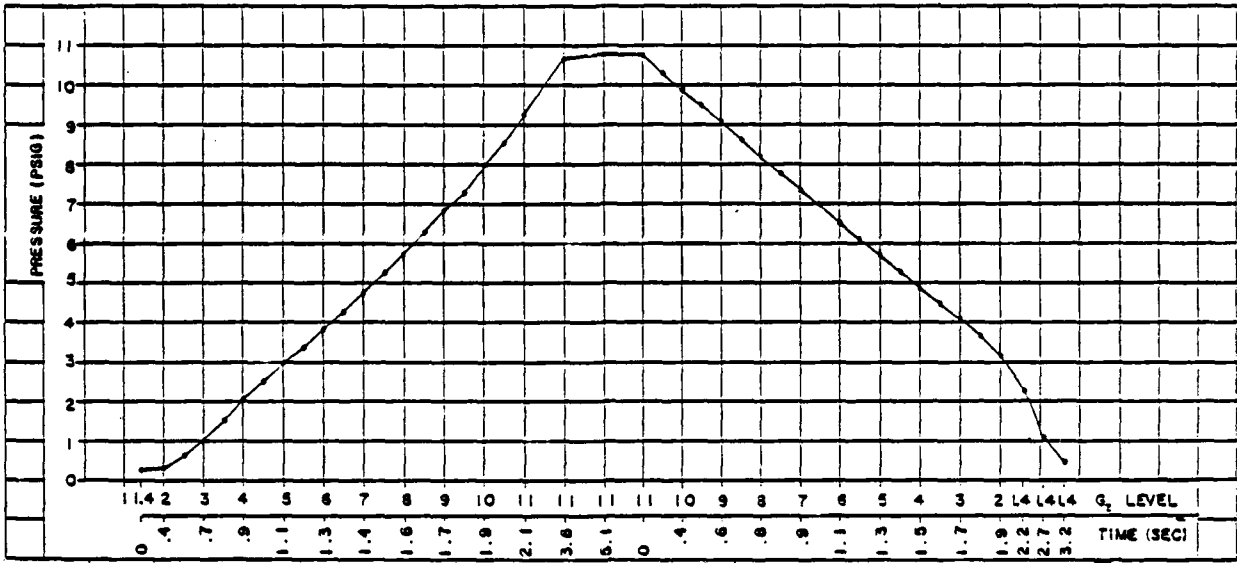


Figure 4.2-10. "Suit" pressures produced during acceleration/deceleration by ALAR HFRP anti-G valve under conditions of: 150-psig source pressure; high G onset; 10-liter volume; 15° angle.

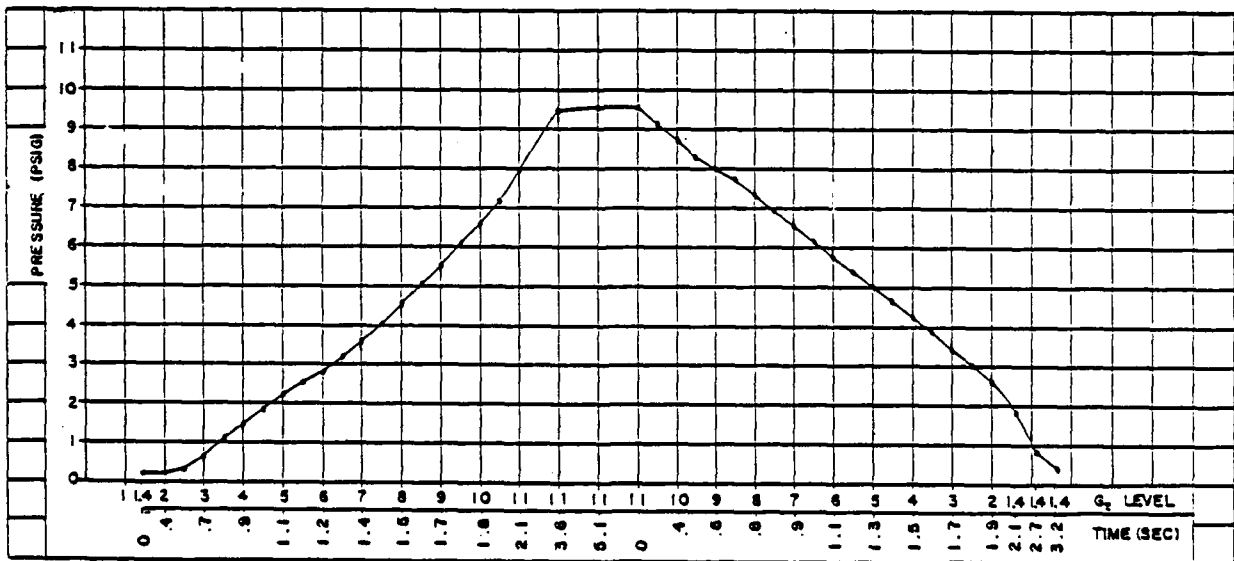


Figure 4.2-11. "Suit" pressures produced during acceleration/deceleration by ALAR HFRP anti-G valve under conditions of: 150-psig source pressure; high G onset; 10-liter volume; 30° angle.

Under 300 psig source pressure (Fig. 4.2-13), the low-frequency oscillation was again observed. Under ascending G conditions, an oscillation of 0.6 psig p-p occurred over the interval of 1.4 G to 10 G. A pressure of 9.7 psig was measured as 11 G was attained, and after 1.5 s the pressure had increased to 11 psig; it then stabilized at 11.1 psig. Immediately upon deceleration, the oscillation (0.5 psig p-p) recurred and persisted until the 5.5-G level.

4.2.4 Phase III - Determination of Complex Dynamic Response Capability

Results of testing the ALAR HFRP anti-G valve under SACM conditions of 150 psig source pressure and 0° valve angle are shown in Figure 4.2-14. On the first high-onset acceleration to 9 G, suit pressure at 9 G was 8.9 psig; after about 2.4 s "on top" the pressure had increased to 9.6 psig and it continued to increase to a maximum of 9.7 psig. A low-frequency oscillation in valve outlet pressure (but not in suit pressure) was observed on acceleration between 3 G and 9 G, and on deceleration from 9 G to 5 G. Under 4.4 G, the suit pressure was 5.1 psig but dropped to 3.8 psig after 9.5 s. Under 3 G, suit pressure was 2.2 psig initially then dropped to 2 psig after about 5 s. Upon accelerating again to 5 G, the suit pressure rose to 4.6 psig and leveled off at 4.7 psig. The next deceleration to 4 G produced a pressure of 3.6 psig which then stabilized at 3.3 psig. During the second high-onset acceleration to 9 G the suit pressure reached 9 psig and leveled off at 9.6 psig after 1.5 s. The subsequent high-offset rate to 1.5 G yielded a suit pressure of 2.6 psig, which slowly fell to 0.4 psig. A rapid-onset acceleration to 8 G then produced a suit pressure of 7.5 psig, which then increased and stabilized at 8.7 psig within about 2 s. Deceleration from 8 G to 1.4 G resulted in a rapid reduction in suit pressure to 0.4 psig, and a low-level (0.2 psig p-p) oscillation.

The effects of valve angle upon performance of the ALAR HFRP valve under SACM conditions were explored by varying the angle (15° and 30°) while holding the source pressure and suit volume at the median values of 150 psig and 10 liters, respectively. However, results of the 15°-angle experiment had to be discarded because of spurious signals from an improperly functioning transducer.

At a valve angle of 30° (Fig. 4.2-15), a low-frequency oscillation of 0.3 psig p-p occurred from 3 G through 9 G. Suit pressures of 1.5 psig at 3 G and 7.9 psig at 9 G were observed; after 6.5 s at 9 G, pressure rose to 8.8 psig. Upon deceleration, the suit pressure decreased rapidly to 4.5 psig, hesitated for 9 s at 4.4 G, and then dropped slowly to 3.2 psig. An oscillation of 0.9 psig p-p occurred from 9 to 5.5 G. At a low-offset rate from 4.4 G to 3 G, pressure dropped to 1.9 psig, then slowly declined to 1.5 psig by the end of the 3-G plateau. Upon subsequent low-onset acceleration to 5 G, the pressure climbed slowly to 3.9 psig then leveled off at 4.5 psig within 1.5 s. Upon deceleration to 4 G, the suit pressure decreased to 3.1 psig. During the next rapid-onset acceleration to 9 G, the suit pressure climbed rapidly to 8.1 psig and leveled off at 8.9 psig; this was accompanied by an oscillation of 0.6 psig p-p. Upon deceleration, an oscillation of 0.5 psig p-p was observed from 9 G to 5 G. At 1.5 G, the initial pressure was 1.9 psig which leveled off at 0.5 psig after 1.5 s. The subsequent acceleration to 8 G produced a suit pressure of 8 psig, and an oscillation of 0.3 psig p-p. Upon rapid deceleration to 1.4 G, suit pressure dropped to 0.5 psig.

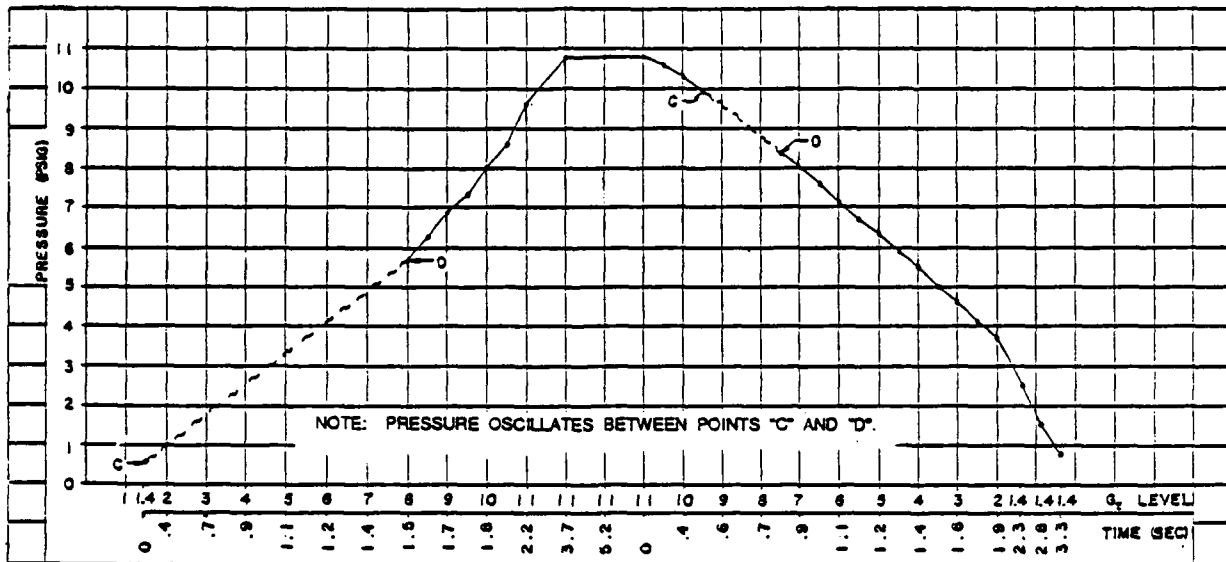


Figure 4.2-12. "Suit" pressures produced during acceleration/deceleration by ALAR HFRP anti-G valve under conditions of: 30-psi source pressure; high G onset; 10-liter volume 0° angle.

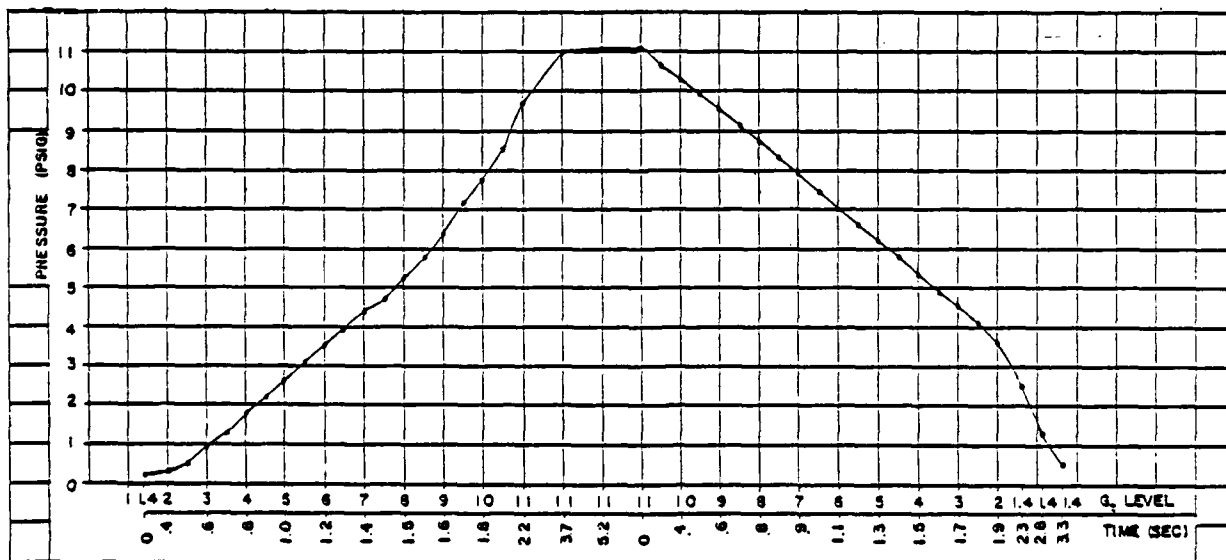


Figure 4.2-13. "Suit" pressures produced during acceleration/deceleration by ALAR HFRP anti-G valve under conditions of: 300-psi source pressure; high G onset; 10-liter volume; 0° angle.

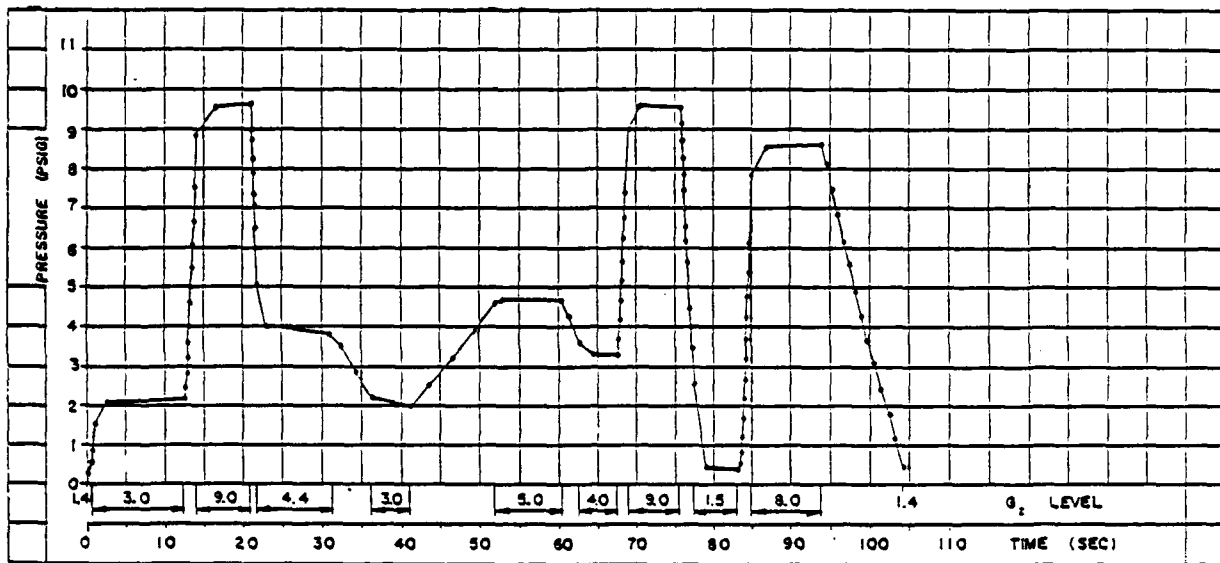


Figure 4.2-14. "Suit" pressures produced during SACM by ALAR HFRP anti-G valve under conditions of: 150-psig source pressure; 10-liter volume; 0° angle.

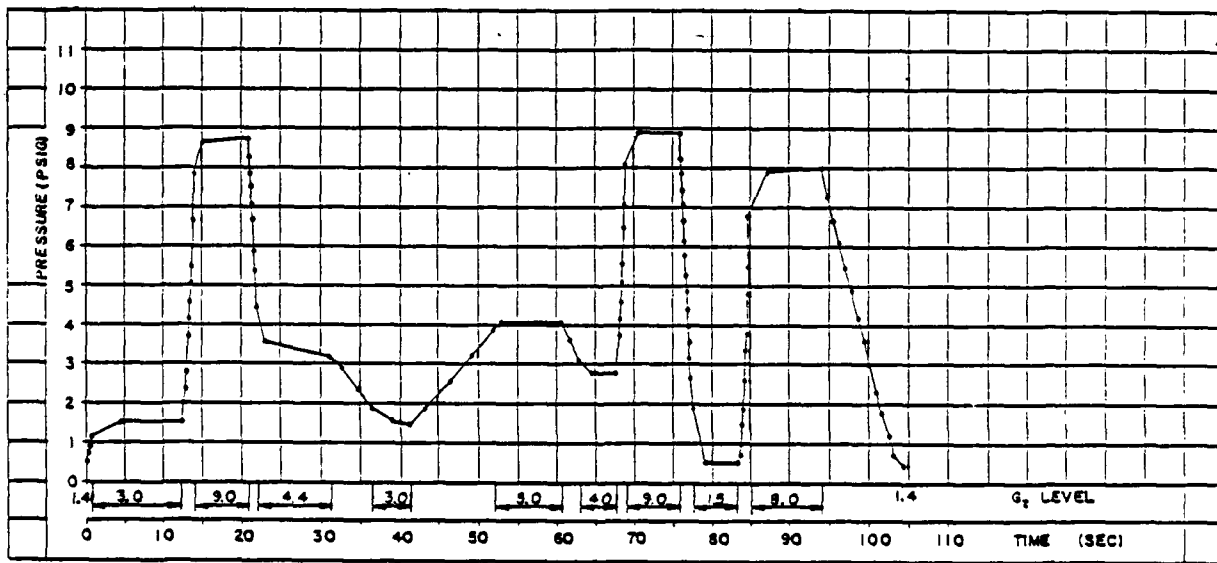


Figure 4.2-15. "Suit" pressures produced during SACM by ALAR HFRP anti-G valve under conditions of: 150-psig source pressure; 10-liter volume; 30° angle.

The effects of source pressure upon performance of the ALAR HFRP valve under SACM conditions were examined. Minimum (30 psig) and maximum (300 psig) source pressures were used. The simulated suit volume was 14 liters for the minimum pressure and 6 liters for the maximum pressure. At a source pressure of 30 psig (Fig. 4.2-16), the valve displayed pressure at 1.4 G with 0.3 psig in the suit volume; this was accompanied by an oscillation of 0.2 psig p-p up to 3 G. The suit pressure rose to 1.2 psig at 3 G, then leveled off at 2 psig. A rapid-onset acceleration to 9 G caused the suit pressure to increase to 9 psig, accompanied by an oscillation of 0.3 psig p-p. Deceleration to 4.4 psig caused the pressure to decrease rapidly to 5.6 psig, with an oscillation between 9 G and 6 G. The pressure leveled off at 4.0 psig within about 9 s and then decreased to 2.3 psig at 3 G. Acceleration to 5 G produced an initial pressure of 4.7 psig, which leveled off at 4.8 psig. Subsequent deceleration to 4.0 G yielded a pressure of 3.6 psig. The second rapid onset acceleration to 9 G produced a suit pressure of 8.2 psig which then leveled off at 9.6 psig. This acceleration also caused an oscillation of 0.9 psig p-p between 4 G and 8.5 G. Rapid deceleration to 1.5 G dropped the suit pressure to 3.5 psig; this was also accompanied by an oscillation between 9 G and 6 G. After 5 s at the 1.5-G level, the suit pressure dropped to 0.5 psig. A subsequent high-onset acceleration to 8 G resulted in the suit pressure leveling off at 8.6 G; oscillation (0.7 psig p-p) was observed between 1.5 G and 6 G. A fast-offset deceleration from 8 G to 1.4 G dropped the suit pressure to 0.5 psig which persisted until the end of the run. The valve oscillated (0.2 psig p-p) during this entire deceleration.

At a source pressure of 300 psig (and 6 liters suit volume), shown in Figure 4.2-17, the valve performed essentially the same as when 150 psig source pressure and suit volume of 10 liters were employed (Fig. 4.2-15). Differences were that suit pressures at the high-G levels were about 0.5 psig lower than under 150 psig, and oscillation occurred intermittently throughout the entire profile.

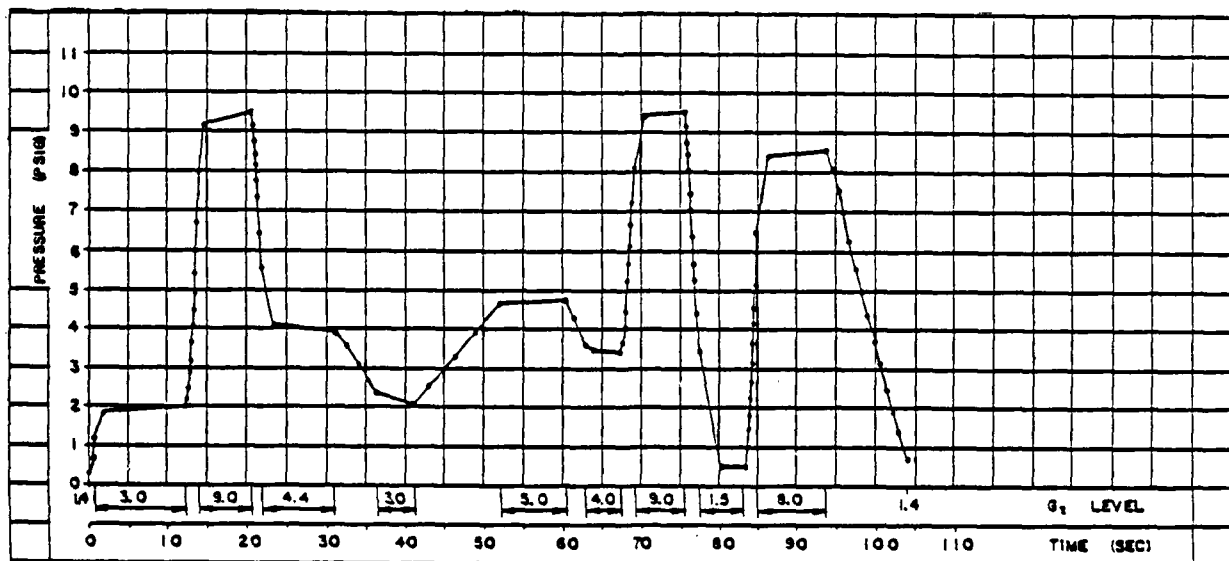


Figure 4.2-16. "Suit" pressures produced during SACM by ALAR HFRP anti-G valve under conditions of: 30-psig source pressure; 14-liter volume; 0° angle.

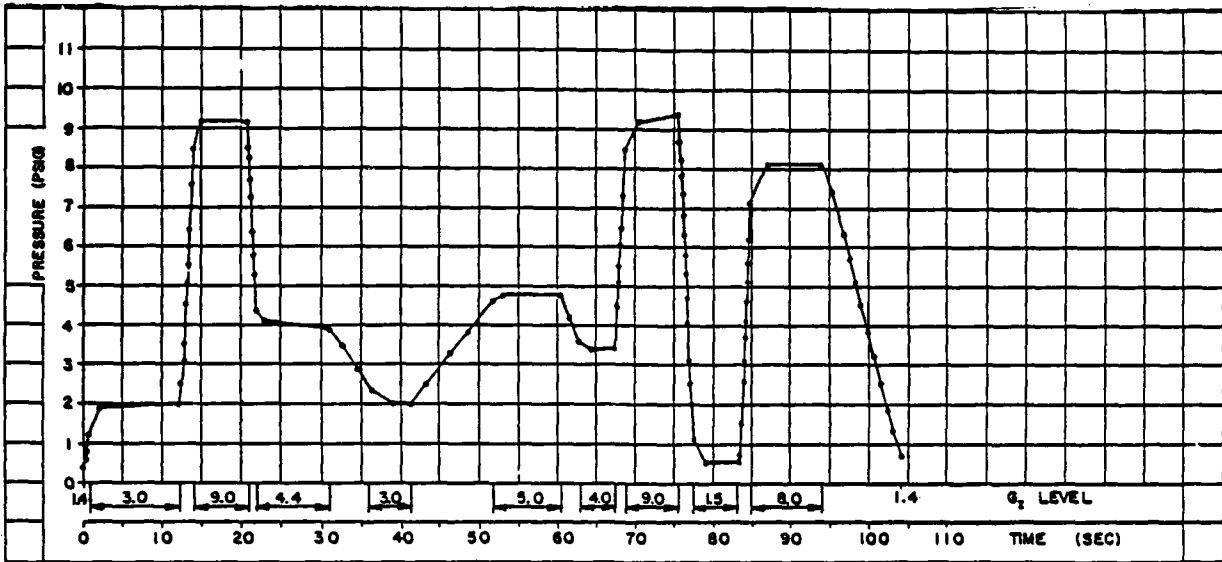


Figure 4.2-17. "Suit" pressures produced during SACM by ALAR HFRP anti-G valve under conditions of: 300-psig source pressure; 6-liter volume; 0° angle.

4.3 ALAR High-Flow Anti-G Valve

4.3.1 Description

The ALAR High-flow anti-G valve (Fig. 4.3-1) is a modified form of the standard ALAR 8400A anti-G valve (section 4.1). Modifications included enlargement of the orifices, and adjustment of the first stage regulator internal pressure and G-level opening point. These changes were designed to: increase airflow by 50 %; increase first stage pressure from 10 to 19 psig; and provide initiation of airflow at 1.25 G rather than 2 G. The valve tested was modified to open at 1.5 G (instead of 1.25 G) to avoid activating the valve at the USAFSAM centrifuge G threshold of 1.4 G_z.

The optimum source pressures for the ALAR High-flow anti-G valve were: 300 psig, maximum; 150 psig, median; and 30 psig, minimum.

4.3.2 Phase I - Determination of Maximum Flow Capacity

Maximum flow capacity of the ALAR High-flow valve was determined as described in Testing Procedures, section 3.2.1. Briefly, the median source pressure for this valve (150 psig) and a valve angle of 0° were used for three trapezoidal runs at 0.5 G_z s⁻¹ onset and offset rates. The unobstructed flow of air (in SCFM) through the valve, the valve output pressure (psig), and the source pressure (psig) were measured.

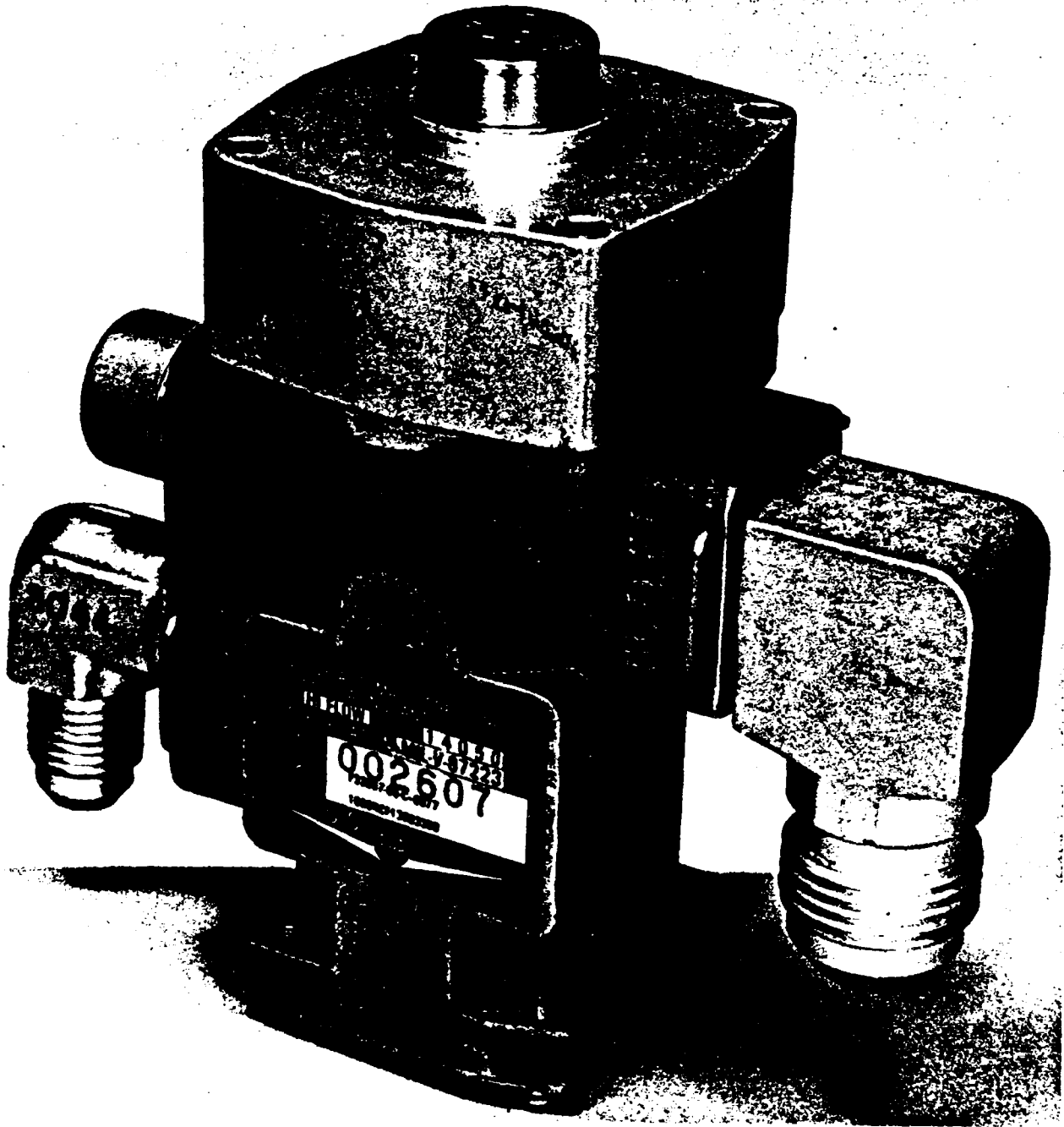


Figure 4.3-1. ALAR High-Flow Anti-G Valve.

The relationship between G_z level and maximum flow is shown in Figure 4.3-2, where each data point is the mean of the values obtained from the three runs. Flow was initiated when 2 G was attained; this initial flow was 1.5 SCFM. Flow then increased linearly with G level between 2 G and 3 G, yielding a flow of 8.6 SCFM at 3 G. At this point, the rate of increase in flow began to lessen, again becoming linear--but with reduced slope--from 4.5 G to 7.5 G (12.9 to 20.1 SCFM). At 7.5 G flow began to plateau, measuring 21.6 SCFM upon reaching 11 G and 21.8 SCFM at the end of the interval at 11 G. Upon initiation of deceleration, flow did not begin to decrease until after 8 G was passed. Flow was 20.7 SCFM at 7.5 G and decreased linearly to 11.3 SCFM at 4 G; immediately after this point, flow jumped up slightly (11.8 SCFM at 3.9 G) then began to decrease at a more rapid rate and ceased as 1.4 G was attained.

4.3.3 Phase II - Determination of Dynamic Response Capability

The dynamic response capability of the ALAR High-flow anti-G valve was determined as described in Testing Procedures, section 3.2.2. Pressure delivered by the valve was measured at the output port and inside the simulated anti-G suit volume. As used here, the term "output pressure" refers to the pressure within the suit volume, unless otherwise noted.

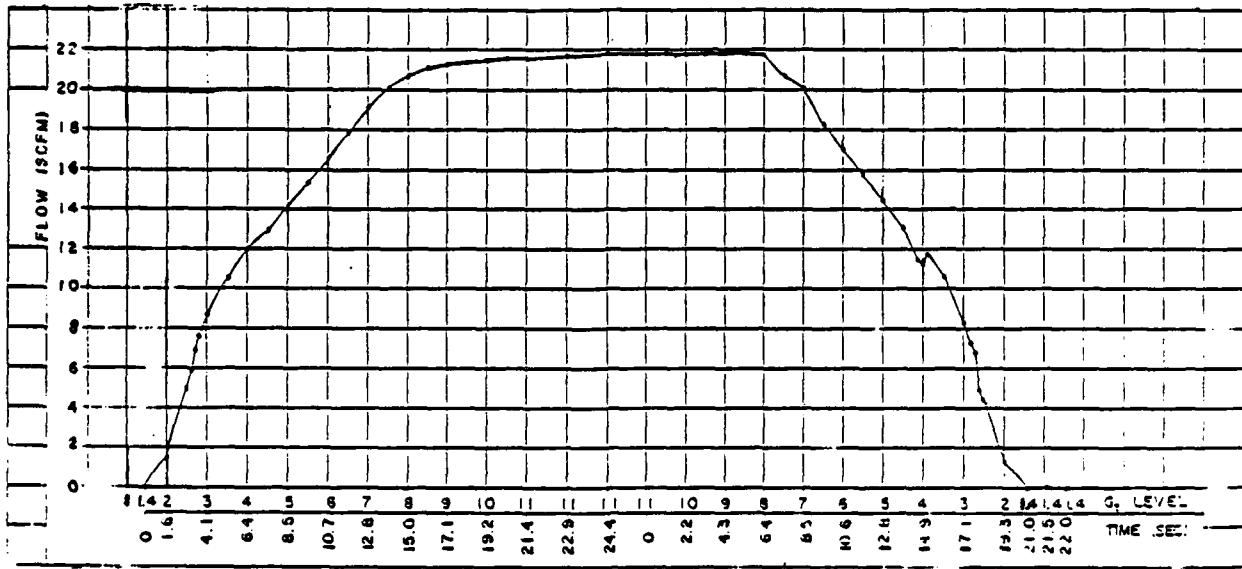
4.3.3.1 Low G_z -Onset-Rate Conditions

The 0.1 $G\ s^{-1}$ trapezoidal profile was used for all low G_z -onset tests for this valve.

Holding the source pressure at the median value of 150 psig while varying the valve angle, produced the results shown in Figures 4.3-3 through 4.3-5. When the valve angle was 0°, the suit pressures produced by this valve as G_z level was varied were as shown in Figure 4.3-3. The suit pressure was 0 psig at 1.4 G and 0.2 psig at 2 G; pressure then increased linearly as G level was increased, reaching 8 psig at 7.5 G. The rate of increase in suit pressure then began to curve to yield 10.6 psig as G level reached the 11-G level. While at 11 G, suit pressures varied approximately 0.2 psig. With deceleration, suit pressure began to decrease when G level fell to 9.5 G and continued to decrease in a linear fashion until reaching 0.3 psig at 1.4 G; after 1 s at 1.4 G, suit pressure was zero.

When the valve angle was changed to 15° while all other conditions were held constant (Fig. 4.3-4), the response of the ALAR High-flow valve was almost identical to that at 0° (Fig. 4.3-3). The principal difference between the two valve angles was that at 15° the maximum suit pressure at maximum G level was slightly higher than at 0° valve angle (11.5-11.6 psig vs. 10.6-10.8 psig).

A valve angle of 30° produced a similar response (Fig. 4.3-5), but the rate of suit pressure buildup and the maximum suit pressure reached were reduced; the maximum G level (11 G) yielded maximum suit pressures of 9.2-9.4 psig.



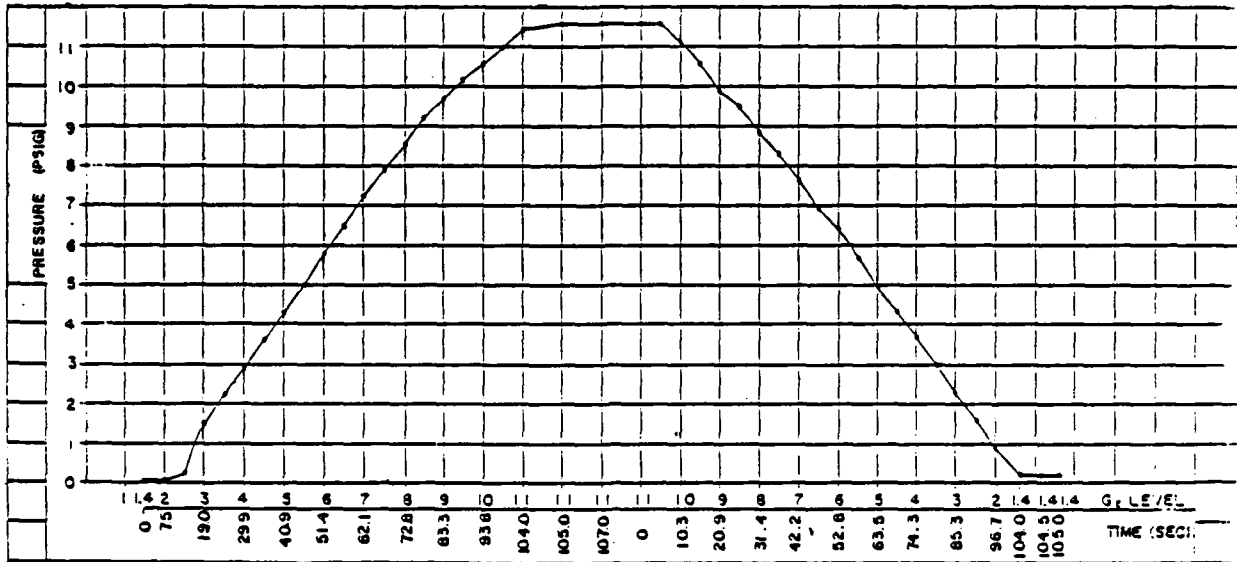


Figure 4.3-4. "Suit" pressures produced during acceleration/deceleration by ALAR High-flow anti-G valve under conditions of: 150-psig source pressure; low G onset; 10-liter volume; 15° angle.

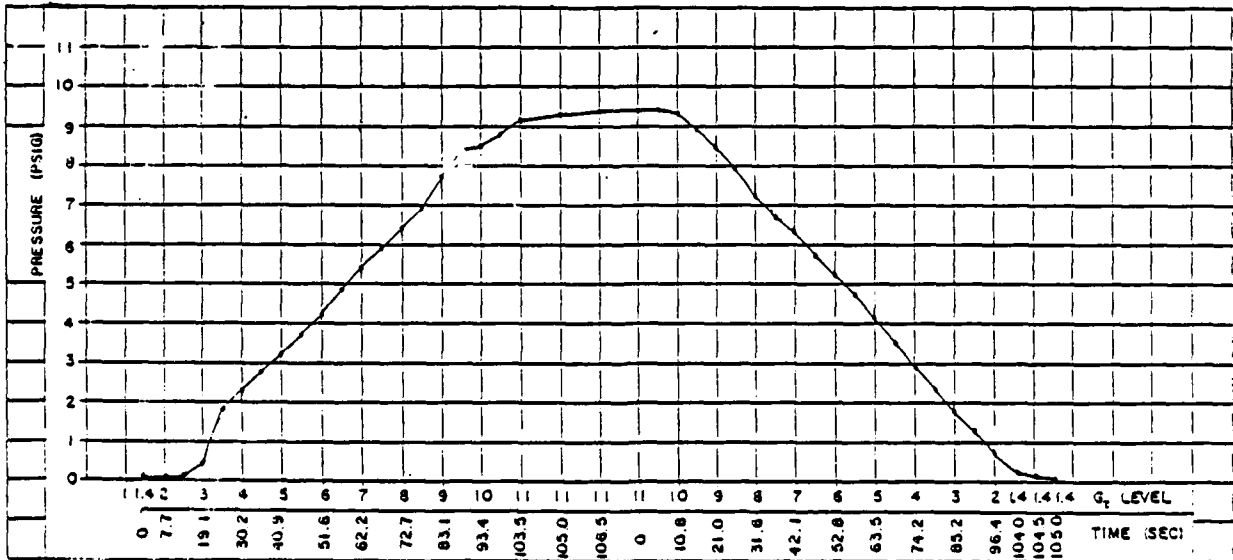


Figure 4.3-5. "Suit" pressures produced during acceleration/deceleration by ALAR High-flow anti-G valve under conditions of: 150 -psig source pressure; low G onset; 10-liter volume; 30° angle.

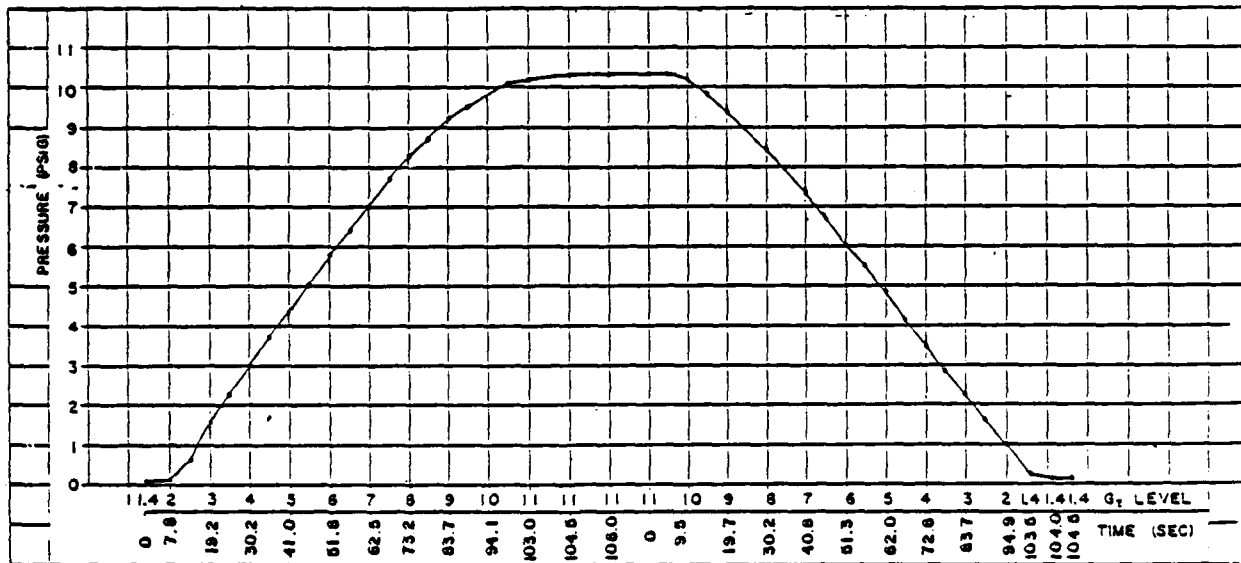


Figure 4.3-6. "Suit" pressures produced during acceleration/deceleration by ALAR High-flow anti-G valve under conditions of: 30-psig source pressure; low G onset; 10-liter volume; 0° angle.

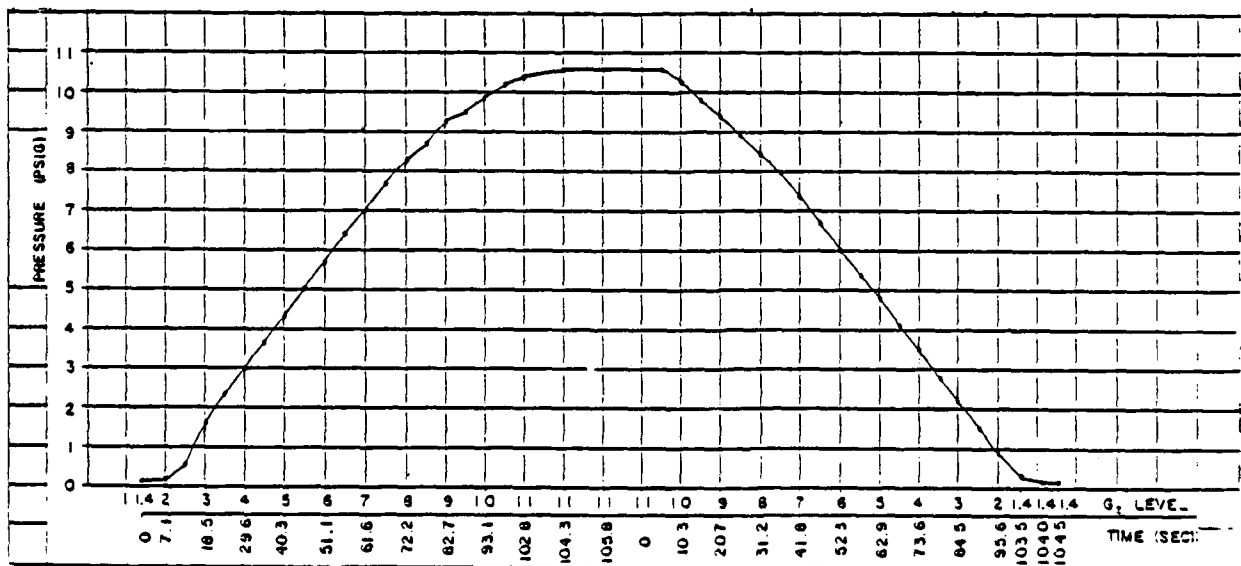


Figure 4.3-7. "Suit" pressures produced during acceleration/deceleration by ALAR High-flow anti-G valve under conditions of: 300-psig source pressure; low G onset; 10-liter volume; 0° angle.

The source pressure was varied while holding the valve angle at 0°. The response profile for the minimum source pressure of 30 psig (Fig. 4.3-6) and that for the maximum source pressure of 300 psig (Fig. 4.3-7) can be compared with that for the median source pressure of 150 psig just discussed (Fig. 4.3-3). At the minimum source pressure (Fig. 4.3-6), the suit pressures generated as a function of G_z level were almost identical to those produced when the median source pressure was used (Fig. 4.3-3); the only difference being a slightly lower maximum suit pressure at 11 G (10.2-10.3 psig vs. 10.6-10.8 psig). The maximum source pressure also produced a response pattern (Fig. 4.3-7) which was essentially identical to those of the median and minimum source pressures; maximum suit pressures of 10.4-10.6 psig were observed at 11 G.

4.3.3.2 High G_z -Onset-Rate Conditions

For high G_z -onset-rate testing of the ALAR High-flow anti-G valve, conditions were: a simulated suit volume of 10 liters, and acceleration and deceleration rates of $6 G_z s^{-1}$. The pressure delivered by the valve was measured at both the output port and inside the simulated suit volume; however, only suit volume pressures are presented and discussed here.

The effects of valve angle upon performance of the ALAR High-flow valve were explored by varying the valve angle (0°, 15°, 30°) while maintaining the source pressure at the median value for this valve (150 psig). When the valve angle was 0°, the suit pressurization profile was as shown in Figure 4.3-8. Pressurization started at 2 G with a suit pressure 0.2 psig, increasing to 0.8 psig at 3 G; the increase in suit pressure was then linear up to 10.5 G where pressure was 10.2 psig. The pressure buildup then began to slow, measuring 11.5 psig upon reaching 11 G, and plateauing at 12.2-12.4 psig during the time at 11 G. Upon deceleration, suit pressure began to decrease immediately and decreased linearly down to 3.3 psig at 2 G; it then dropped sharply to 0 psig as 1.4 G was reached.

When the valve angle was 15° (Fig. 4.3-9), the rate of suit pressurization and the maximum pressure produced were both reduced. There was an initial lag phase so that pressure increase did not become linear until after 5 G was attained; the maximum suit pressure produced was 10.7 psig at 11 G vs. 12.4 psig for a valve angle of 0° (Fig. 4.3-8). The slopes of the deceleration phases were similar for both conditions.

When the valve angle was 30°, a similar shift in the curve was observed (Fig. 4.3-10). The initial lag phase was longer than for the 15° angle (Fig. 4.3-9), with the result that the rate of pressurization did not become linear until 6.5 G was attained. The maximum suit pressure produced was slightly under 10 psig (at 11 G) vs. 10.7 psig at 15°, and 12.4 psig at 0°.

Under conditions of minimum source pressure and a valve angle of 0°, the suit pressurization was as seen in Figure 4.3-11. After an initial lag phase, the rate of pressure buildup was linear from 3.5 to 11 G. Pressure plateaued at 11 psig within 1.5 s at 11 G and remained at this level until deceleration was initiated. During deceleration suit pressure decreased linearly to 2.2 psig at 2 G. The pressure then decreased further to 1.2 psig at 1.4 G and fell further within 3 s at baseline G to 0.3 psig.

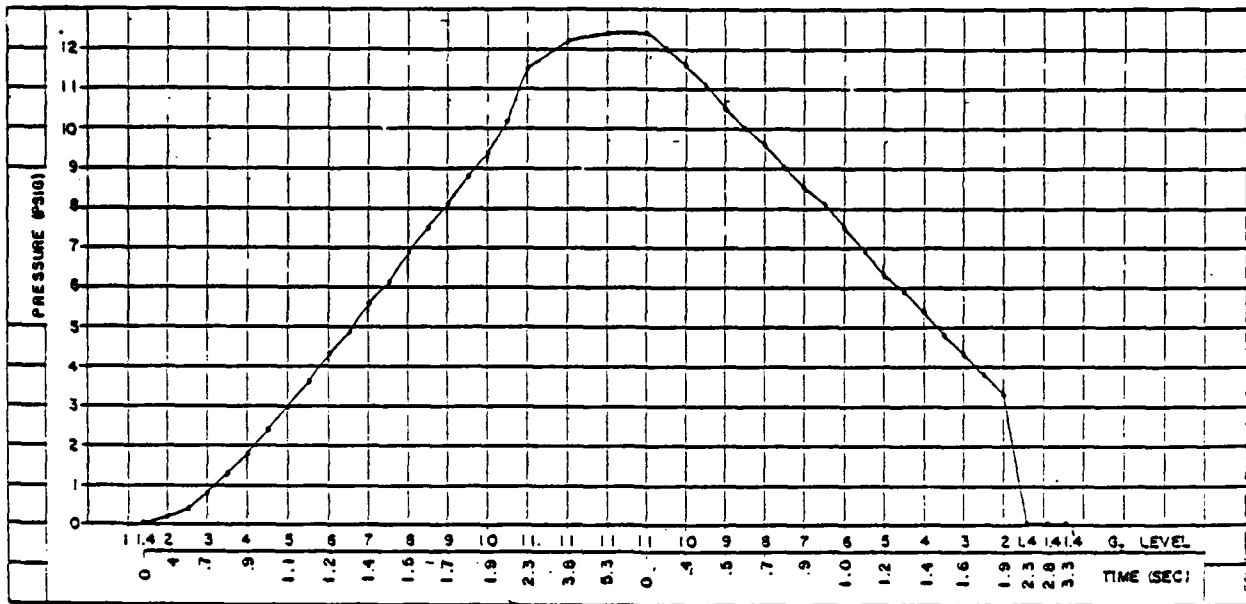


Figure 4.3-8. "Suit" pressures produced during acceleration/deceleration by ALAR High-flow anti-G valve under conditions of: 150-psig source pressure; high G onset; 10-liter volume; 0° angle.

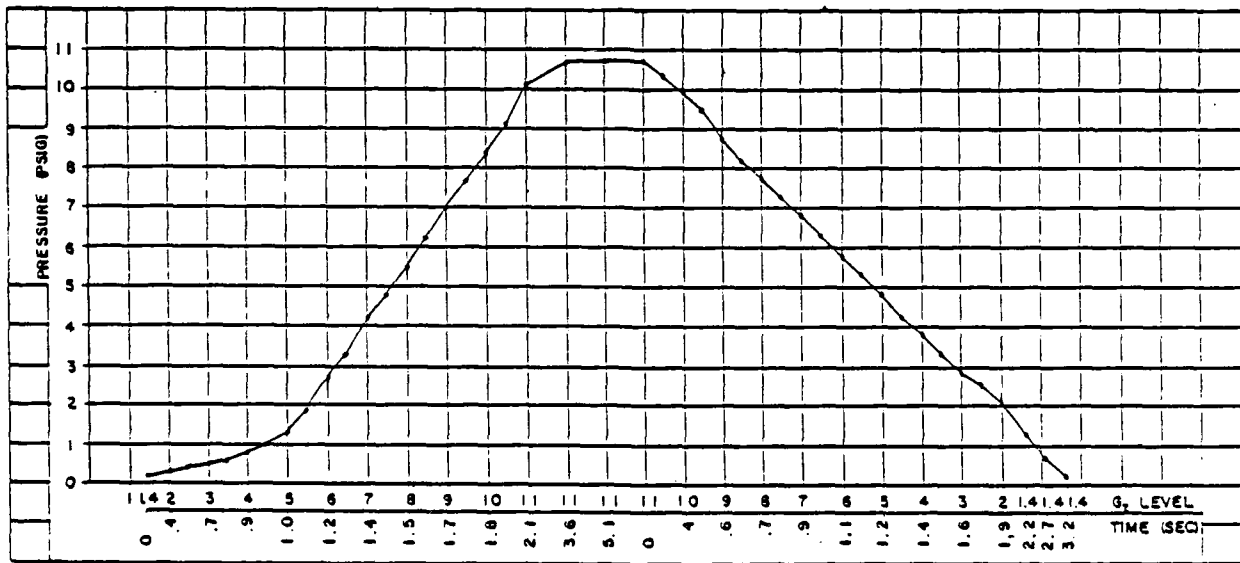


Figure 4.3-9. "Suit" pressures produced during acceleration/deceleration by ALAR High-flow anti-G valve under conditions of: 150-psig source pressure; high G onset; 10-liter volume; 15° angle.

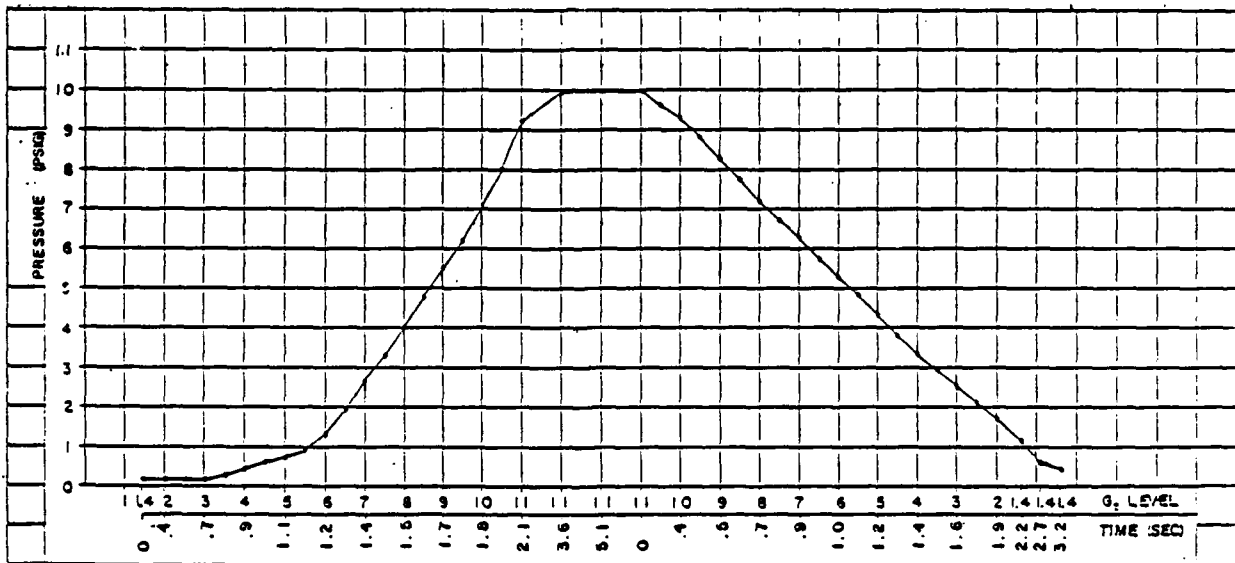


Figure 4.3-10. "Suit" pressures produced during acceleration/deceleration by ALAR High-flow anti-G valve under conditions of: 150-psig source pressure; high G onset; 10-liter volume; 30° angle.

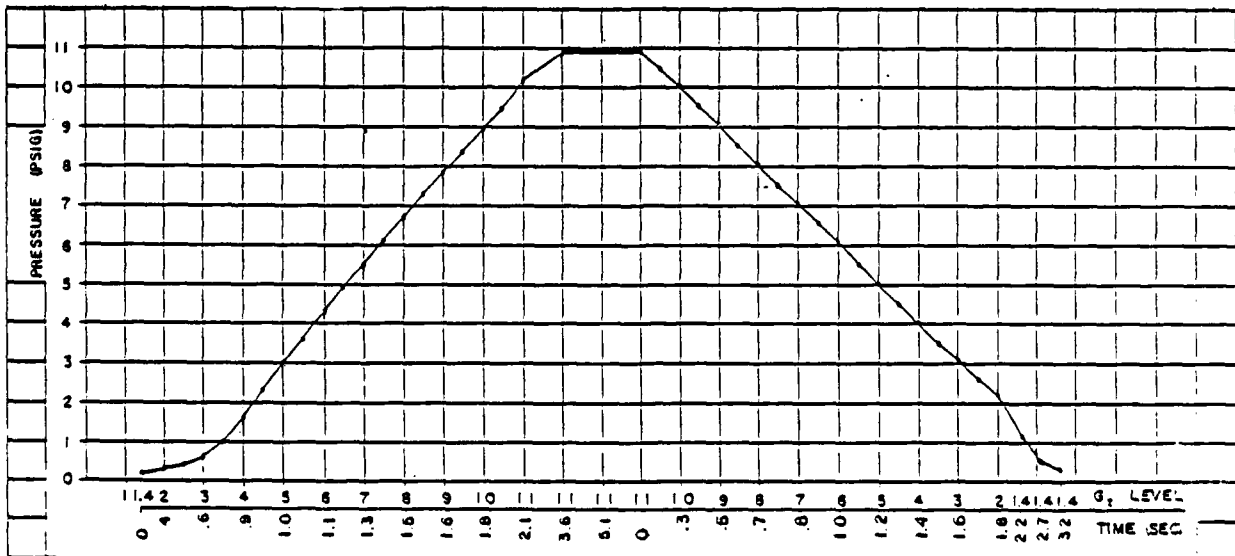


Figure 4.3-11. "Suit" pressures produced during acceleration/deceleration by ALAR High-flow anti-G valve under conditions of: 30-psig source pressure; high G onset; 10-liter volume; 0° angle.

At maximum source pressure (300 psig) and 0° angle (Fig. 4.3-12), the pressurization profile was more like that observed at minimum source pressure and 0° (30 psig, Fig. 4.3-11), than that at median pressure and 0° (150 psig, Fig. 4.3-8). The initial lag phase persisted up to 5 G and the pressurization was slightly less linear (Fig. 4.3-12) than for the minimum source pressure (Fig. 4.3-11). Maximum suit pressure attained and the deceleration profiles were essentially identical in these two cases (minimum and maximum); however, a higher maximum suit pressure was produced by the median source pressure (Fig. 4.3-8).

4.3.4 Phase III - Determination of Complex Dynamic Response Capability

Performance of the ALAR High-flow anti-G valve under SACM conditions and 0° valve angle and median source pressure is presented in Figure 4.3-13. At the 3-G level, suit pressure increased to 1.5 psig within 2.2 s then continued to increase to 2.4 psig by 12.4 s. Upon acceleration to 9 G, suit pressure built up to 8.9 psig and increased to 9.6 psig within 6 s. A subsequent deceleration to 4.4 G caused suit pressure to drop to 4.8-3.9 psig. The G level was then dropped to 3 G, causing suit pressure to fall to 2.4-2.1 psig. Slow-onset acceleration to 5 G brought suit pressure up to 4.5-4.9 psig; decreasing G to 4 G then dropped pressure to 3.6-3.4 psig. Rapid-onset acceleration to 9 G resulted in an increase in suit pressure to 9.2-9.6 psig, and rapid-offset deceleration to 1.5 G brought suit pressure down to 1.8-0.3 psig. Another rapid-onset acceleration to 8 G produced suit pressures of 7.9-8.6 psig. During the final descent to baseline G (1.4), suit pressure decreased linearly to 0.3 psig.

When the valve angle was changed to 15° while other conditions remained constant, the SACM performance of this valve was as shown in Figure 4.3-14. All features of the SACM suit-pressurization profile were essentially identical to that observed when the valve angle was 0° (Fig. 4.3-13). However, when the valve angle was 30° (Fig. 4.3-15), suit pressures were generally lower throughout the SACM protocol than for either of the first two angles.

Suit pressurization profiles for conditions of both maximum (14 liter) suit volume combined with minimum (30 psig) source pressure (Fig. 4.3-16) and minimum (6 liter) suit volume combined with maximum (300 psig) source pressure (Fig. 4.3-17) were similar. Maximum suit pressures attained and rates of pressure increase and decrease were almost identical for these two sets of conditions. Both of these figures were also similar to that yielded under conditions of median (150 psig) source pressure with median (10 liter) suit volume (Fig. 4.3-13); although maximum suit pressures attained were slightly lower for the median conditions (Fig. 4.3-13).

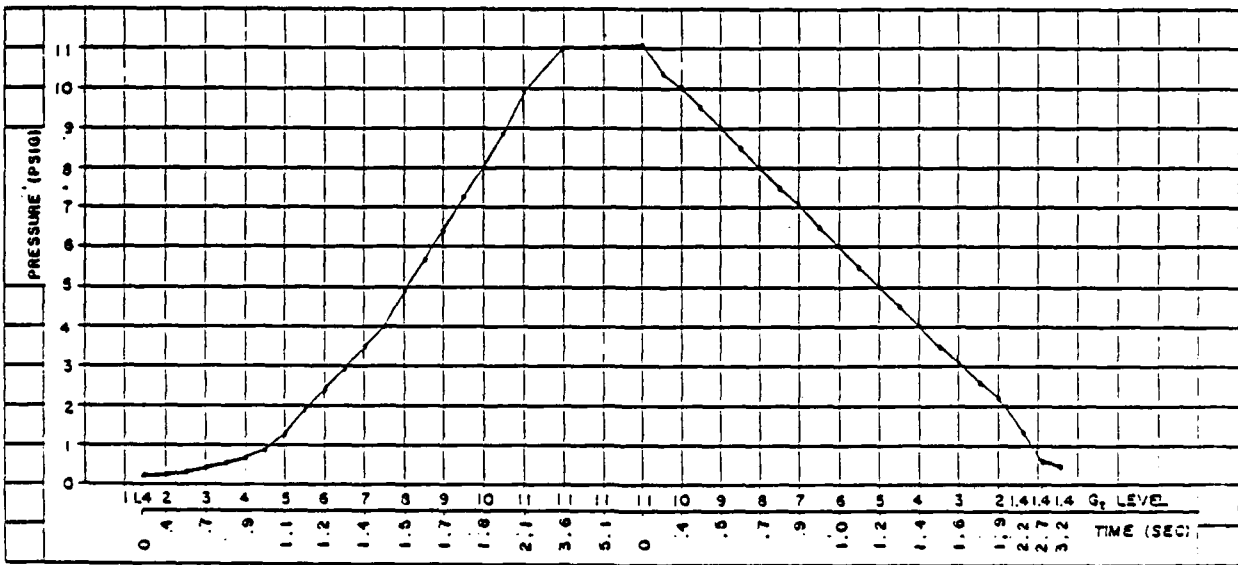


Figure 4.3-12. "Suit" pressures produced during acceleration/deceleration by ALAR High-flow anti-G valve under conditions of: 300-psig source pressure; high G onset; 10-liter volume; 0° angle.

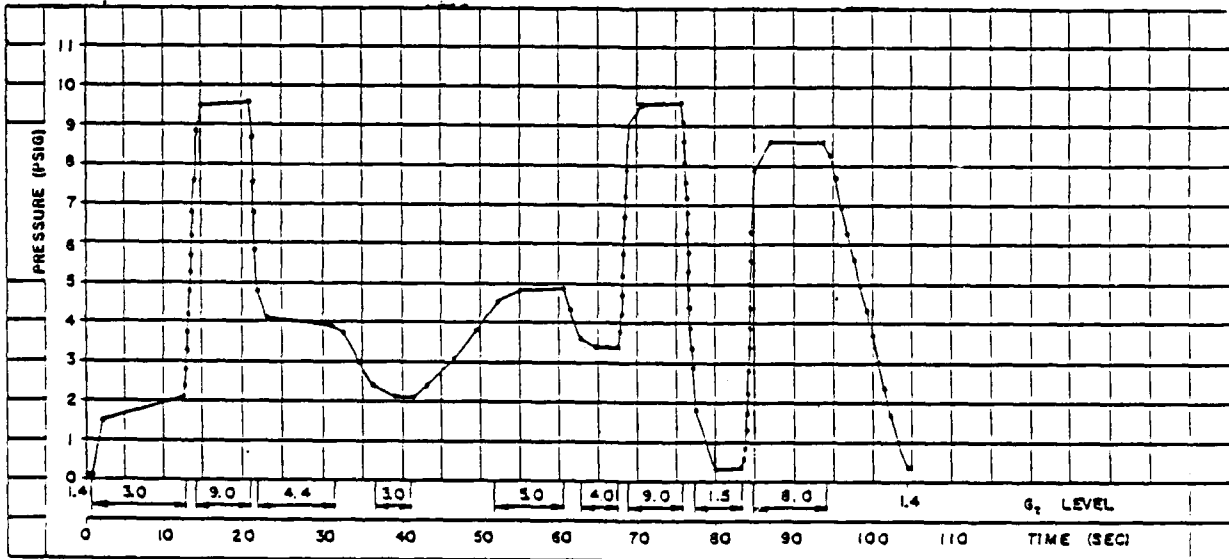


Figure 4.3-13. "Suit" pressures produced during SACM by ALAR High-flow anti-G valve under conditions of: 150-psig source pressure; 10-liter volume; 0° angle.

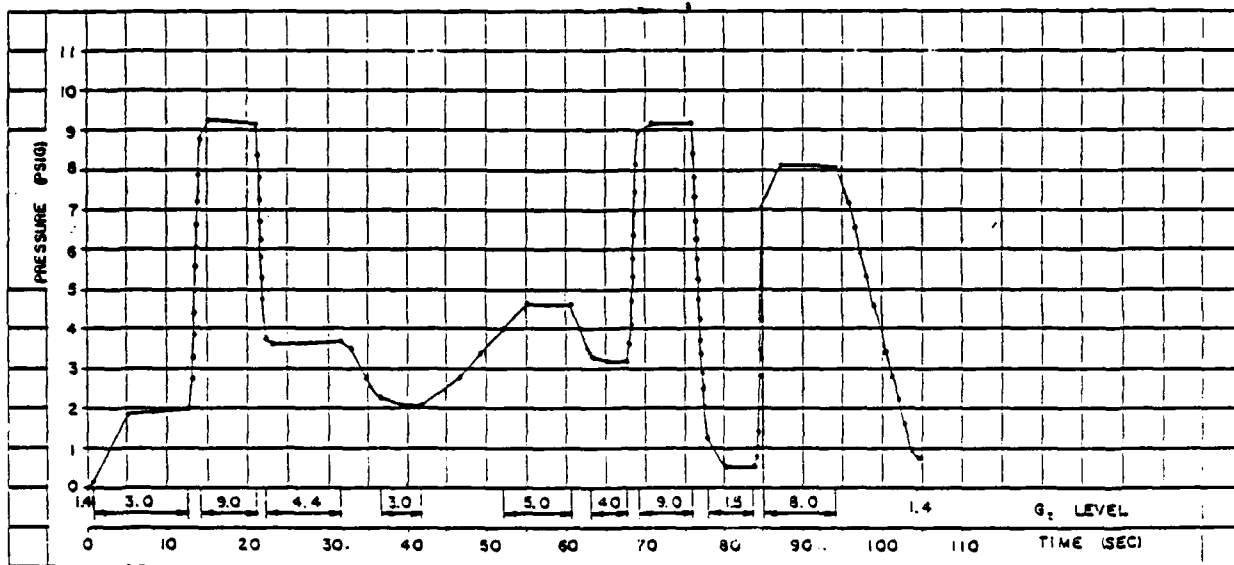


Figure 4.3-14. "Suit" pressures produced during SACM by ALAR High-flow anti-G valve under conditions of: 150-psig source pressure; 10-liter volume; 15° angle.

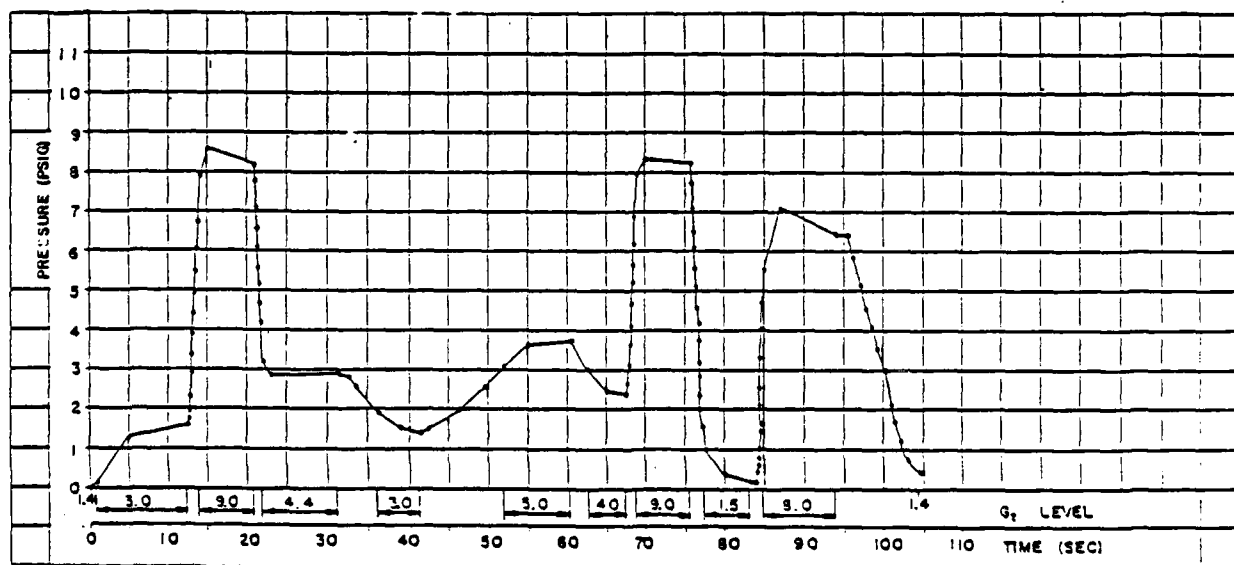


Figure 4.3-15. "Suit" pressures produced during SACM by ALAR High-flow anti-G valve under conditions of: 150-psig source pressure; 10-liter volume; 30° angle.

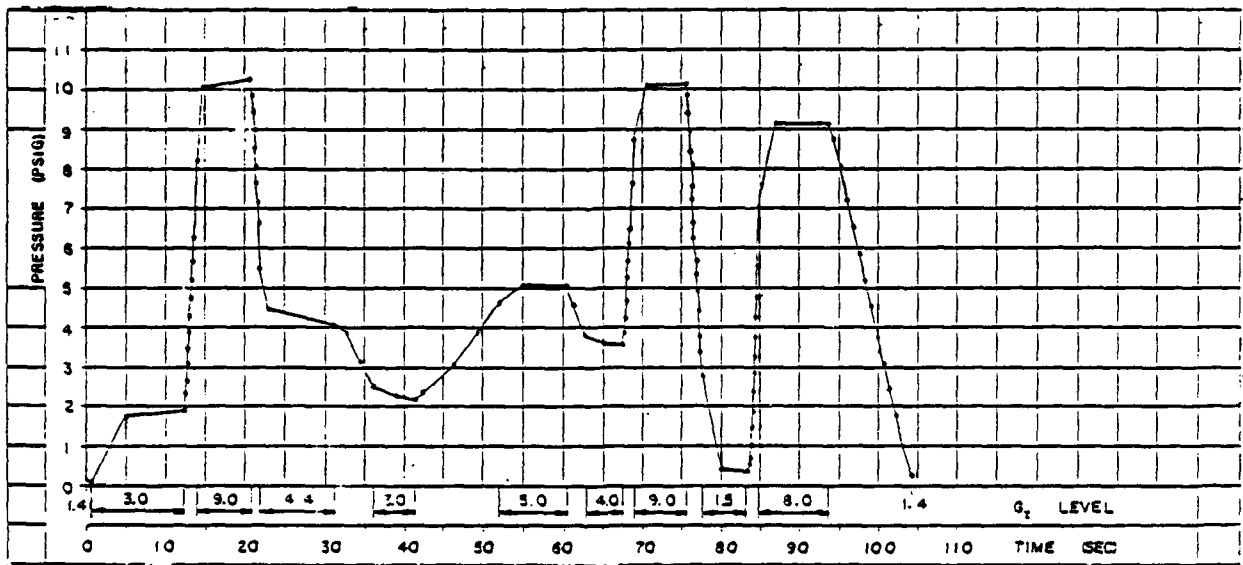


Figure 4.3-16. "Suit" pressures produced during SACM by ALAR High-flow anti-G valve under conditions of: 30-psig source pressure; 14-liter volume; 0° angle.

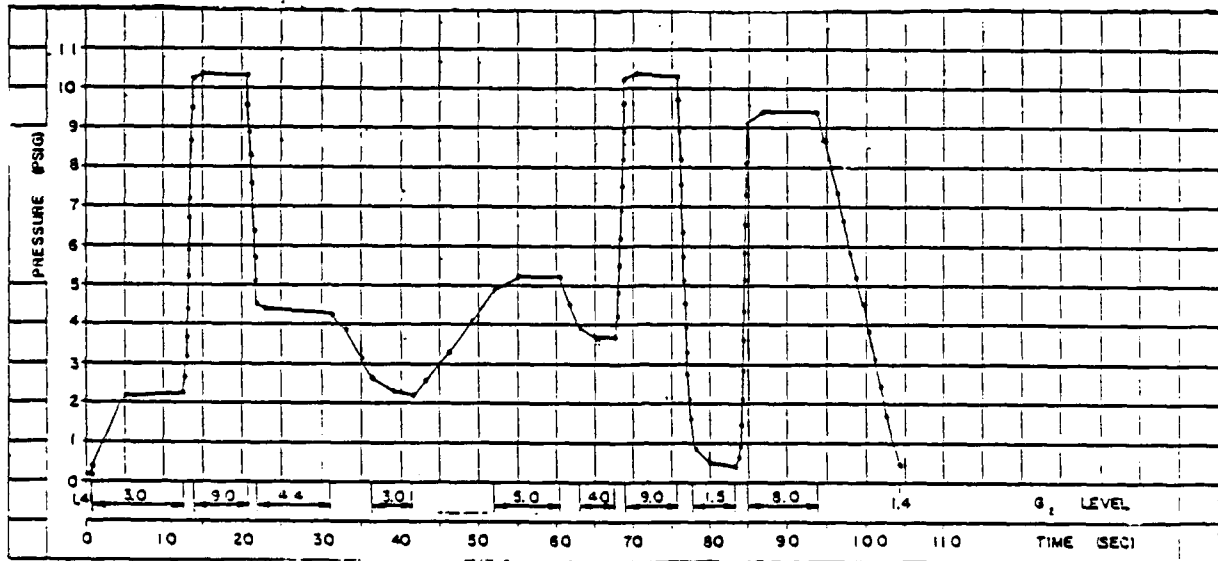


Figure 4.3-17. "Suit" pressures produced during SACM by ALAR High-flow anti-G valve under conditions of: 300-psig source pressure; 6-liter volume; 0° angle.

4.4 Garrett Electronic/Pneumatic Anti-G Valve

4.4.1 Description

The Garrett Electronic/Pneumatic (Servo-controlled) anti-G valve (S. N. 59364) (Fig. 4.4-1) is a poppet-type, acceleration-biased pressure regulator, which is controlled by a torque motor and balanced for inlet pressure. This valve is manufactured by the Garrett Corporation, Phoenix, Arizona. This valve is designed to sense acceleration along one axis only, and to regulate pressure to an external anti-G suit according to a predetermined schedule which is based on the magnitude of the sensed acceleration. The valve incorporates an overpressure relief valve, a reference pressure regulator, a manual test switch, and a provision for remote acceleration simulation.

This valve is designed so that supply air enters the unit at the inlet port and is directed to the poppet valve (which is spring loaded, closed) and to the reference pressure regulator. The reference pressure regulator supplies a constant pressure to the torque motor inlet nozzle; in the absence of current, the torque motor lever arm blocks the inlet nozzle and vents the chamber through the vent nozzle. Thus, the spring load on the diaphragm actuator lifts the actuator off the poppet valve vent seat to cause suit pressure to be vented to the ambient environment.

As the accelerometer senses acceleration along the control axis, a voltage proportional to the magnitude of acceleration is generated. The valve electronic controller receives this voltage signal and provides current to the torque motor. As the current increases, the motor lever moves to restrict the vent nozzle and to control the reference regulator outlet pressure flowing into the chamber. The pressure in the chamber causes the diaphragm actuator to first overcome the spring load, closing the poppet valve vent seat; and then to begin pushing the poppet valve off the fill seat. These actions allow inlet air to flow past the fill seat and into the anti-G suit.

The suit-pressure-feedback transducer senses anti-G suit pressure and supplies the valve electronic controller with a voltage proportional to that pressure. The valve electronic controller compares transducer voltage and accelerometer voltage, and adjusts the current supplied to the motor as required to maintain the specified relationship between sensed acceleration and anti-G suit pressure.

A relief valve is provided to limit suit pressure to a safe level. A "Test" switch allows the unit to be tested by supplying a simulated acceleration signal to the valve electronic controller. In addition, an electrical circuit is provided to allow external application of a voltage to simulate any level of acceleration.

4.4.2 Phase I - Determination of Maximum Flow Capacity

The maximum flow capacity of the Garrett Electronic/Pneumatic anti-G valve was measured under open-flow conditions where the terminating suit volume was omitted, but the normal hose remained attached to the output port of the flow transducer. This hose was terminated by the female quick-disconnect fitting used for attaching the simulated anti-G suit volume.

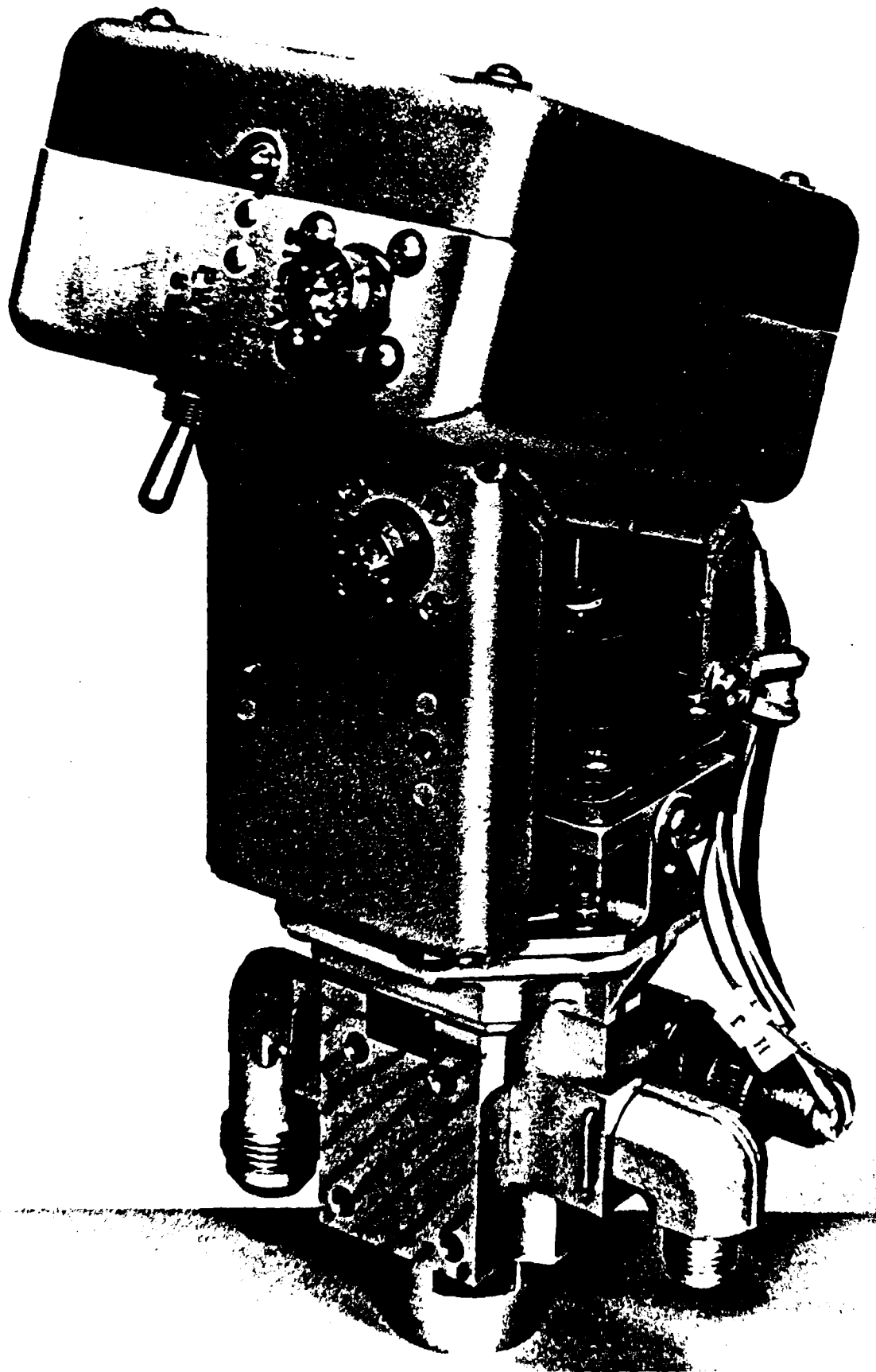


Figure 4.4-1. Garrett Electronic/Pneumatic Anti-G Valve.

Results of the open-flow testing are shown in Figure 4.4-2. With the valve designed to produce ready pressure, the airflow at baseline G (1.4 G) was 8 SCFM. As the G level increased, the flow was 12.3 SCFM at 2 G and 22 SCFM at 4 G. As G level continued to increase, flow increased to a maximum of 28.4 SCFM at 5.7 G, then dropped to 26.5 SCFM at 5.8 G; it then stabilized, reading 25.5 SCFM at 8 G, and 25.8 SCFM at 11 G. Upon deceleration, flow initially increased somewhat up to 26.3 SCFM, and continued to increase to 26.8 SCFM as the G level decreased to 5.5 G; flow then began to decrease rapidly reaching 7.9 SCFM at 1.4 G.

4.4.3 Phase II - Determination of Dynamic Response Capability

The dynamic response capability of the Garrett Electronic/Pneumatic anti-G valve was determined as described in Testing Procedures (section 3.2.2). The pressure delivered by the valve was measured at the output port and inside the simulated anti-G suit volume. "Output pressure" refers to the pressure within the simulated suit volume, unless otherwise noted.

4.4.3.1 Low G_z -Onset-Rate Conditions

The 0.1 G s⁻¹ trapezoidal profile was used for all low-onset tests. When this valve was tested under low G_z -onset conditions at 150-psig source pressure and a valve angle of 0°, the results shown in Figure 4.4-3 were obtained. The suit pressure was 0.8 psig at 1.4 G. At 1.5 G the pressure began to increase and maintained an essentially linear rate of increase up to 7 G, with a pressure of 3.3 psig at 3 G; 6.5 psig at 5 G; and 9.5 psig at 7 G. After 7 G, the rate of increase slowed somewhat, reaching a maximum of 10.3 psig at 7.7 G and remaining at this pressure as G level increased to 11 G. The source pressure was turned off during the interval between when G level reached 7.7 on acceleration and 7.5 on deceleration due to excessive flow. Upon deceleration the suit pressure decreased linearly from 10.3 psig at 7.5 G to 0.8 psig at 1.4 G. The average pressurization rate was 1.6 psig G⁻¹ over the useful range of this valve.

The effect of valve angle upon low G_z performance of the Garrett Servo-controlled valve was explored using valve angles of 15° and 30°, and the median source pressure of 150 psig. At a valve angle of 15° (Fig. 4.4-4), suit pressure was 0.6 psig at 1.4 G and started to increase at 1.5 G. From 1.5 G to 7.5 G, suit pressure increased linearly; pressure was 3.1 psig at 3 G, 6.1 psig at 5 G, 9.3 psig at 7.5 G, and 10.2 psig at 7.8 G. Suit pressure remained at the maximum value of 10.2 psig as G level increased to 11 G, and during the time at 11 G. As G level decreased, the suit pressure decreased linearly from 10.2 psig at 11 G to 0.6 psig at 1.4 G.

When the valve angle was 30° (Fig. 4.4-5), there was no suit pressure measured at 1.4 G; the valve initiated flow at 1.5 G and pressure was 0.5 psig at 1.6 G. Suit pressure increased linearly from 2 to 8 G, with pressure readings of 2.5 psig at 3 G and 5.3 psig at 5 G. At 8 G the rate of pressurization began to level off, measuring 9.5 psig at 8 G and reaching a maximum pressure of 10.3 psig at 8.8 G. Suit pressure remained at 10.3 psig as the G level increased to 11 G and remained there. Upon deceleration from 11 G to 1.4 G, suit pressure decreased linearly down to 0 psig at 1.4 G.

The effect of source pressure upon performance of the Garrett Electronic/Pneumatic anti-G valve during low G_z -onset was determined by testing at both the minimum and maximum source pressures; i.e., 30 and 300 psig, respectively. At a source pressure of 30 psig (Fig. 4.4-6), the valve produced a suit pressure of 0.7 psig at 1.4 G. Suit pressure increased linearly as G level increased to 7 G; pressures of 1.6 psig at 2 G, 6.5 psig at 5 G, and 9.6 psig at 7 G were recorded. The pressure did not climb further after reaching 9.6 psig, but remained at this level as G increased to, and remained at, 11 G. When G level decreased from 11 to 1.4, the suit pressure decreased linearly from 9.6 psig to 0.7 psig.

When a source pressure of 300 psig was employed (Fig. 4.4-7), a suit pressure of 0.7 psig was measured at 1.4 G. The pressure immediately began to increase linearly as G level increased to 7.5 G, reading 1.6 psig at 2 G, 6.4 psig at 5 G, and peaking at 10.3 psig at 7.5 G. At this maximum source pressure, the rate of suit pressurization lagged the rate measured at the minimum source pressure (30 psig, Fig. 4.4-6) by 0.1 psig.

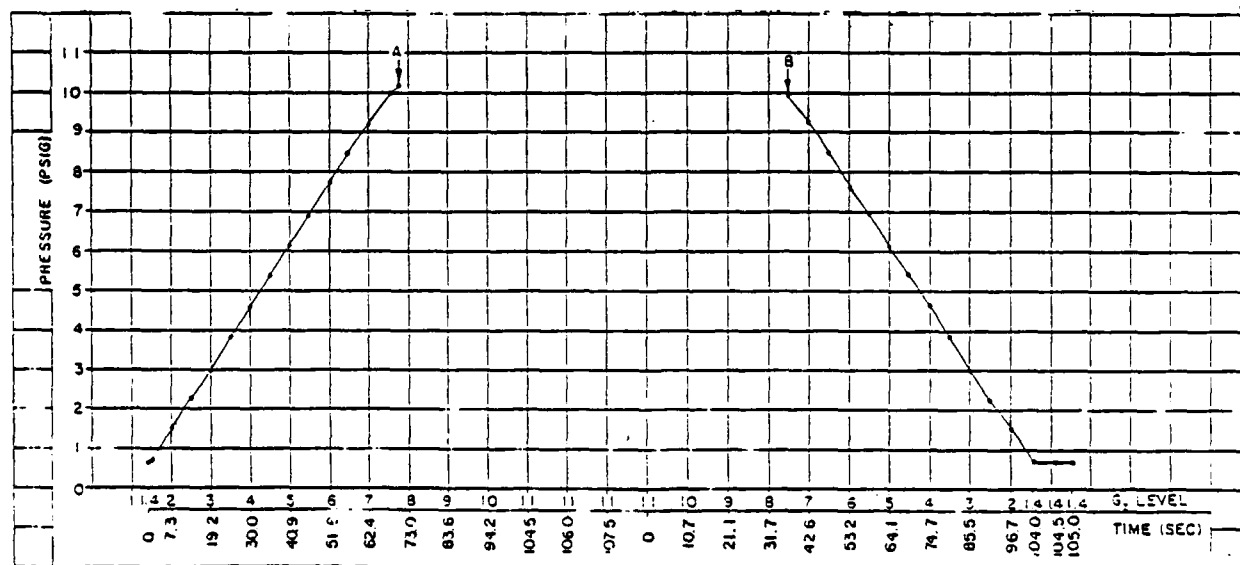
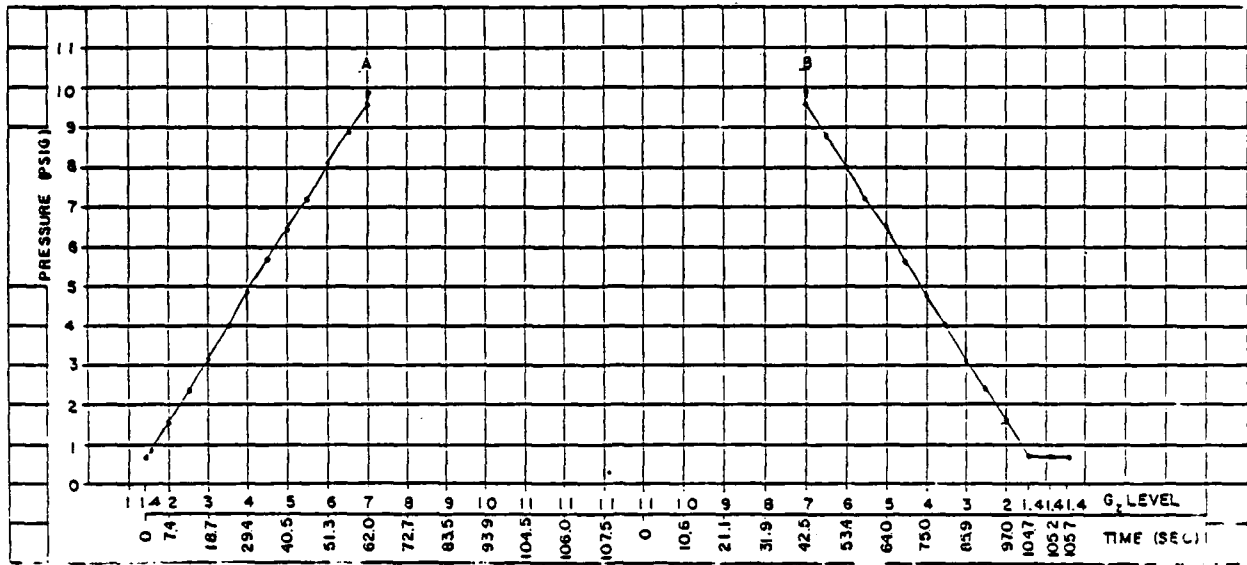


Figure 4.4-4. "Suit" pressures produced during acceleration/deceleration by Garrett Electronic/Pneumatic anti-G valve under conditions of: 150-psig source pressure; low G onset; 10-liter volume; 15° angle. Source pressure turned off between points "A" and "B" due to excessive flow.



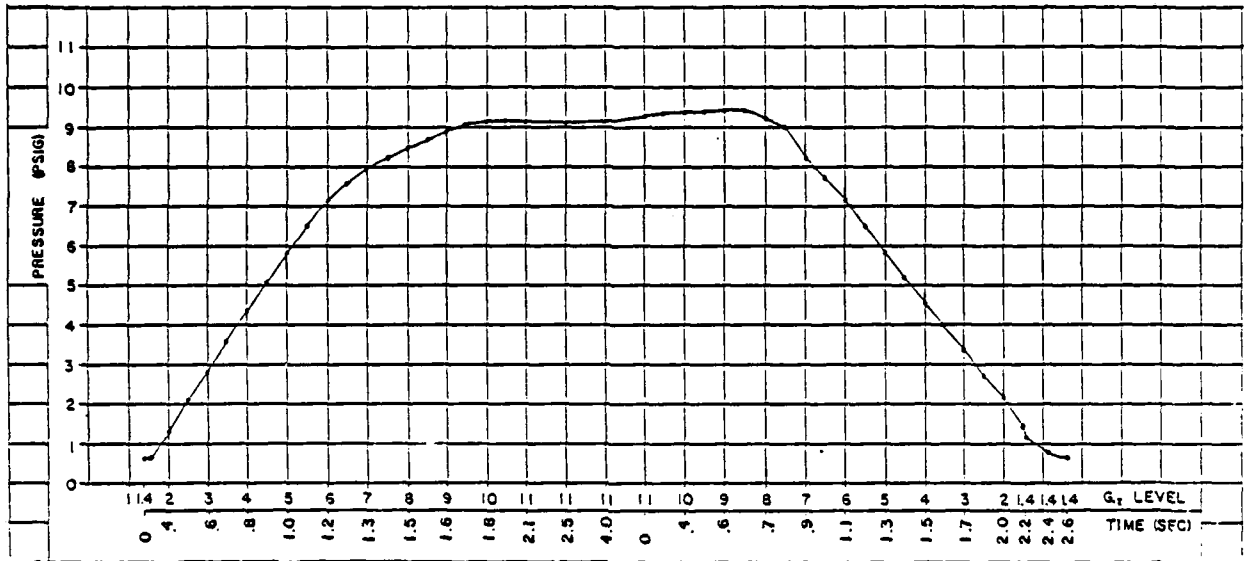


Figure 4.4-8. "Suit" pressures produced during acceleration/deceleration by Garrett Electronic/Pneumatic anti-G valve under conditions of: 150-psig source pressure; high G onset; 10-liter volume; 0° angle.

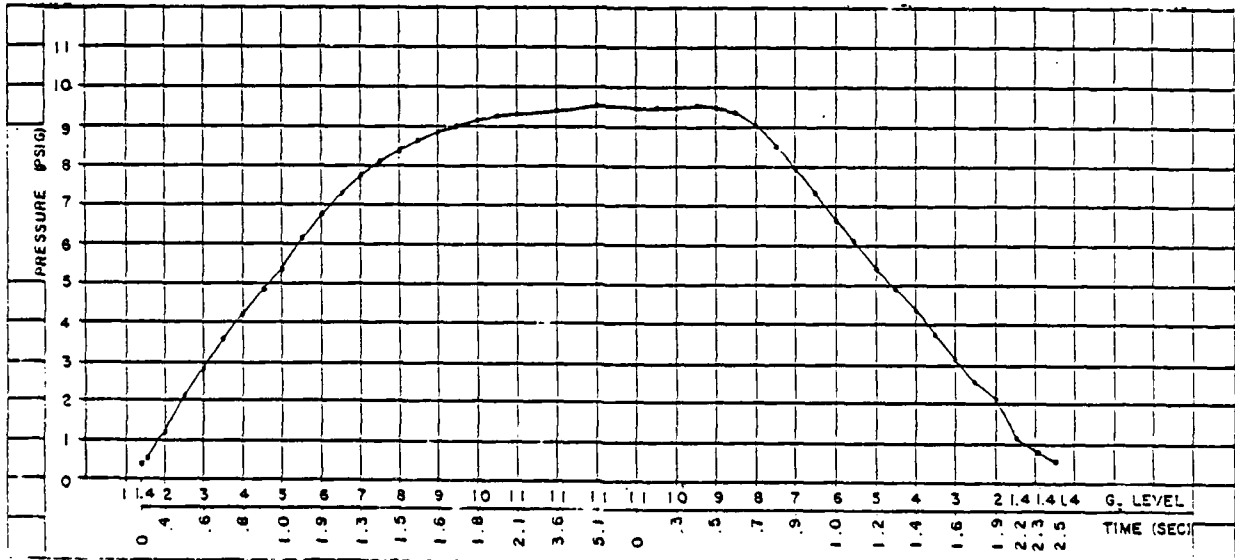


Figure 4.4-9. "Suit" pressures produced during acceleration/deceleration by Garrett Electronic/Pneumatic anti-G valve under conditions of: 150-psig source pressure; high G onset; 10-liter volume; 15° angle.

(Fig. 4.4-9), a low-frequency oscillation (of amplitude 1.4 psig p-p) was again observed as the G level increased from 1.4 G to 6 G. The suit pressurization schedule was similar to that just observed for the 0° angle. The slope of the increase in suit pressure with increasing G_z level approached linearity until 7 G was attained (Fig. 4.4-9); the slope of the line then decreased, plateauing at 9.3 psig at 11 G. The suit pressure was 0.5 psig at 1.5 G, 2.9 psig at 3 G, 6.8 psig at 6 G, 8.9 psig at 9 G, and 9.3 psig at 11 G. Suit pressure increased slightly during the interval at 11 G so that prior to initiation of deceleration, pressure was 9.5 psig. Upon deceleration, suit pressure began to decrease at 8.5 G; the decrease was then linear until 1.4 G was reached. Pressure was 4.3 psig at 4.5 G, and 1.0 psig at 1.4 G.

For a valve angle of 30° (Fig. 4.4-10), suit pressurization began slowly, with zero pressure at 1.5 G and 0.5 psig at 2 G. The rate of pressurization as a function of increasing G_z level was approximately linear until 8 G was attained, although a small decrease in slope occurred at 4 G. Pressures of: 2.3 psig at 3 G, 4.7 psig at 5 G, and 6.9 psig at 7 G were observed. Suit pressure leveled off at 9.3 psig at 10.5 G, then increased to a maximum of 9.6 psig after 10 s at 11 G. Oscillation (1.2 psig p-p) occurred as G_z level increased from 1.4 G to 7 G, then ceased. During deceleration, the suit pressure remained at the maximum level (9.6 psig) until the G level decreased to 9.5 G; pressure then decreased linearly with decreasing G level down to 0.9 psig upon reaching 1.4 G; after 0.5 s at 1.4 G, pressure began to decrease slowly to the final value 0.3 psig. A low-frequency oscillation (0.75 psig p-p), starting at 9.5 G and continuing until 4.5 G, was again observed during deceleration; suit pressure decreased from 9.6 psig to 4.9 psig in the presence of the oscillation.

The effects of source pressure upon high G_z -onset performance of this Garrett valve were explored by testing at both the minimum (30 psig) and the maximum (300 psig) source pressures, while keeping the valve angle at 0°. When the source pressure was 30 psig (Fig. 4.4-11), the suit pressurization schedule was roughly linear from 1.4 G to 7 G, although the slope of the line decreased slightly at 5 G. Suit pressure was initially 0.6 psig at 1.4 G; it increased to 3.6 psig at 3.5 G, then 6.9 psig at 6 G, and leveled off at 8.7 psig at 9.5 G. Within 5 s of reaching 11 G, suit pressure increased to 9 psig; upon deceleration, suit pressure did not begin to decrease until G level had decreased to 7.5 G; it then decreased linearly to 1.3 psig at 1.4 G and dropped slowly to 0.6 psig after 0.5 s. Oscillations were observed upon acceleration (1.0 psig p-p) during the interval between 1.4 G and 3.5 G, and upon deceleration (0.9 psig p-p) from 7.5 G to 4 G.

When the source pressure was 300 psig (Fig. 4.4-12), the suit pressurization schedule was approximately linear from 1.4 G to 7 G; at this point, the slope decreased slightly and continued in a positive linear fashion to 9 G, curving to a very gradual slope which increased throughout the interval at 11 G and the initial stages of deceleration. The suit pressure was 0.6 psig at 1.4 G, 8.3 psig at 7 G, and 11.3 psig at 11 G which increased to 11.9 psig after 5 s "on top" (at 11 G). Upon deceleration, the suit pressure did not change until G level had dropped to 9 G; the pressure then decreased linearly to a value of 1.4 psig at 1.4 G. The slope of the increase and decrease in suit pressure observed here was identical to the slopes observed for a source pressure of 30 psig (Fig. 4.4-10), up to 7 G during acceleration, and from 6.5 G to 1.4 G during deceleration. The significant difference between these two conditions

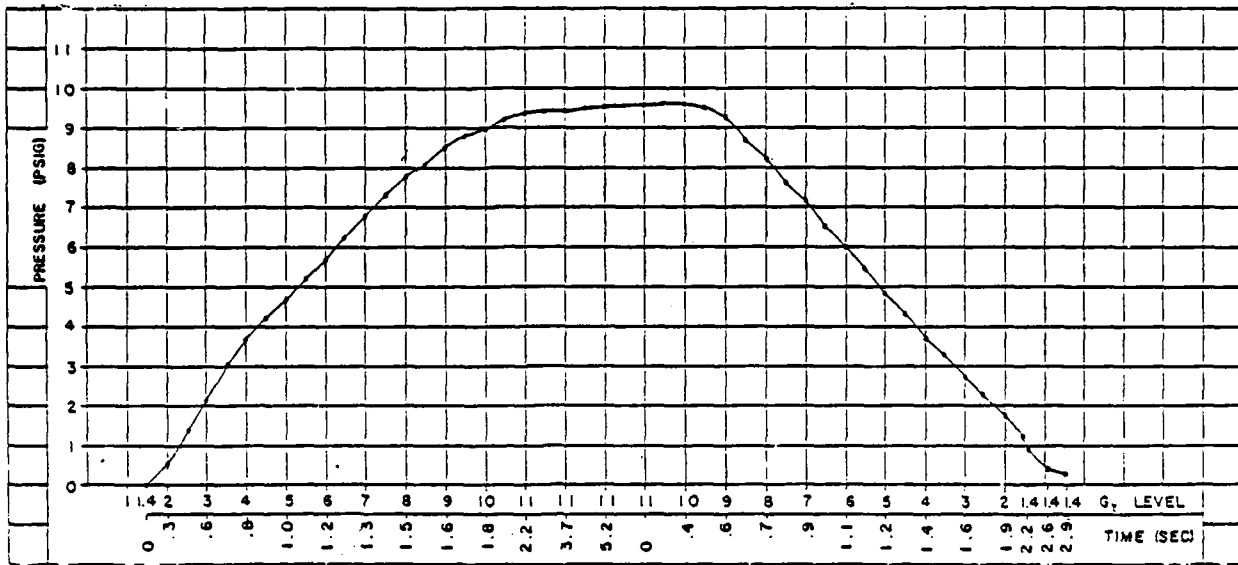


Figure 4.4-10. "Suit" pressures produced during acceleration/deceleration by Garrett Electronic/Pneumatic anti-G valve under conditions of: 150-psig source pressure; high G onset; 10-liter volume; 30° angle.

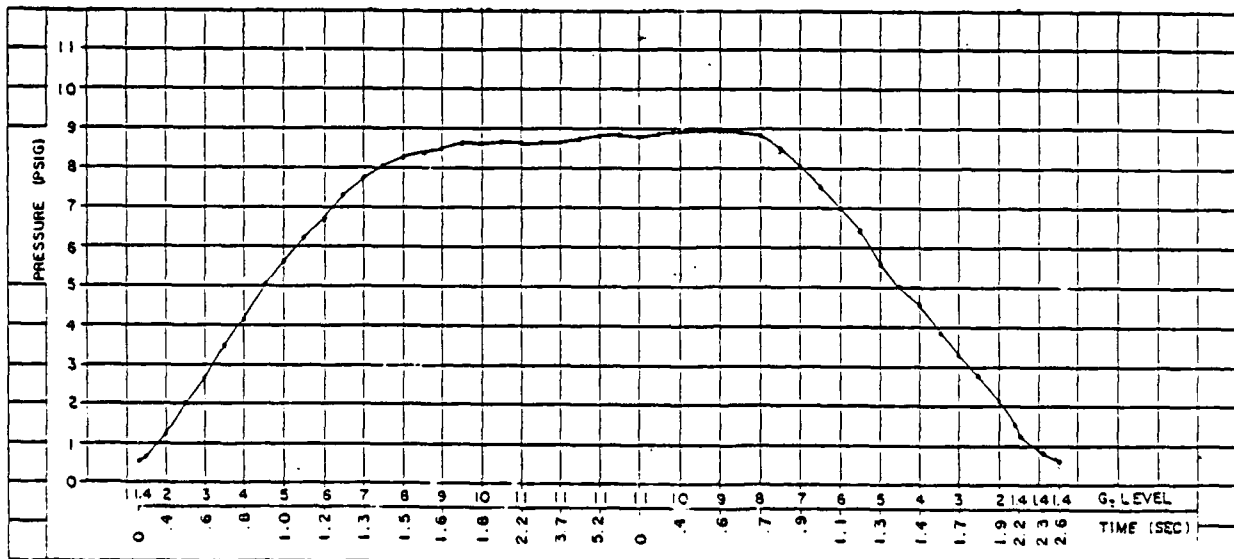


Figure 4.4-11. "Suit" pressures produced during acceleration/deceleration by Garrett Electronic/Pneumatic anti-G valve under conditions of: 30-psig source pressure; high G onset; 10-liter volume; 0° angle.

of source pressure was the maximum suit pressures obtained, which were 9 psig at a source pressure of 30 psig vs. 12 psig at a source pressure of 300 psig. Low-frequency oscillations were again observed during acceleration (1.05 psig p-p) from 1.4 G to 7 G, and during deceleration (0.75 psig p-p) from 9 G to 4.5 G.

4.4.4 Phase III - Determination of Complex Dynamic Response Capability

The Phase III testing under SACM conditions was performed as described in Testing Procedures (section 3.2.3). Initially, median values of source pressure and suit volume were selected and the valve angle varied; subsequently, valve angle was maintained at 0° and the combinations of: minimum source pressure with maximum suit volume, and maximum source pressure with minimum suit volume were evaluated.

For the median source pressure (150 psig) and valve angle of 0° (Fig. 4.4-13), the valve started with 0.6 psig suit pressure at 1.4 G. With a high onset to 3 G (3 psig) the valve showed oscillation of 0.9 psig p-p from 1.4 G to 3 G. Upon rapid-onset acceleration to 9 G, the suit pressure increased to 9.6 psig at 9 G and leveled off at 9.7 psig; oscillation occurred between 3 G and 6.5 G (1.2 psig p-p). Decreasing rapidly down to 4.4 G and 5.1 psig, low-level oscillation (1.05 psig p-p) was present between 8.5 G and 4.4 G.

Dropping off to 3 G the suit pressure dropped to 3.1 psig. Upon acceleration to 5 G suit pressure increased to 6.1 psig; subsequent deceleration to 4 G resulted in a suit pressure of 4.6 psig. With a rapid-onset acceleration to 9 G the suit pressure increased to 9.6 psig with a slight oscillation (1.0 psig p-p) occurring between 4 G and 6 G; the pressure leveled off at 9.7 psig at 9 G. With a rapid-offset deceleration from 9 G to 1.5 G the suit pressure decreased to 1.5 psig, and after 6 s at 1.5 G the pressure leveled off at 0.9 psig; oscillation (1.2 psig p-p) occurred from 9 G down to 4.5 G. With a rapid-onset acceleration to 8 G the suit pressure increased to--and leveled off at--9.8 psig with oscillation (1.1 psig p-p) between 1.5 G and 6.5 G. Decelerating from 8 G to 1.4 G, the pressure dropped off to 0.7 psig--with oscillation (0.6 psig p-p) from 7.8 G down to 1.4 G.

The angular-dependent studies of the Garrett valve during the Phase III SACM testing used valve angles of 15° and 30° while the source pressure and simulated G-suit volume remained at their median values (150 psig and 10 liters), respectively. At a valve angle of 15° (Fig. 4.4-14), the valve started to flow at 1.4 G with 0.5 psig suit pressure, and at 3 G the pressure was 2.8 psig; a slow oscillation of 2.9 psig p-p was observed between 1.4 G and 3 G.

With a high onset to 9 G the pressure in the G-suit volume increased rapidly to 9.4 psig with a low-frequency oscillation of 1.2 psig p-p. After 1 s on top at 9 G the pressure increased to 9.6 psig with an oscillation of 0.9 psig p-p. A rapid offset down to 4.4 G produced a suit pressure of 4.9 psig. A slow further offset to 3 G brought the pressure to 2.9 psig, while a slow-onset back up to 5 G resulted in a pressure of 5.8 psig. A slow offset down to 4 G dropped the pressure to 4.4 psig. With a high onset to 9 G the pressure increased to 9.6 psig with oscillation (0.9 psig p-p) between 4 G and 6.5 G; after 3.5 s on top at 9 G the pressure increased to 9.7 psig. With a high-offset

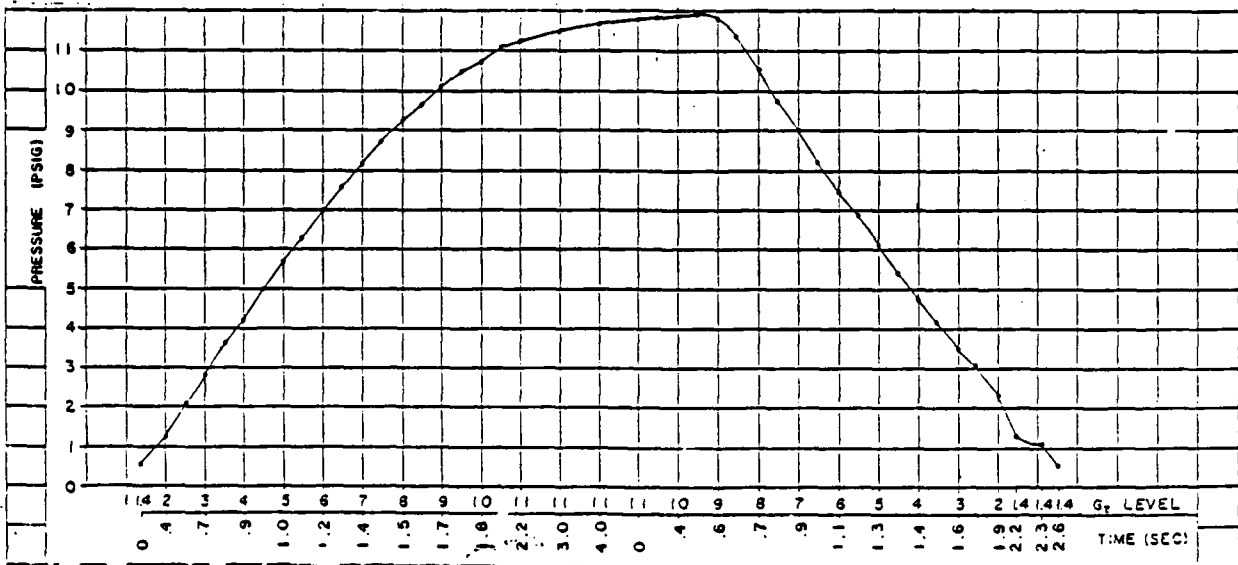


Figure 4.4-12. "Suit" pressures produced during acceleration/deceleration by Garrett Electronic/Pneumatic anti-G valve under conditions of: 300-psig source pressure; high G onset; 10-liter volume; 0° angle.

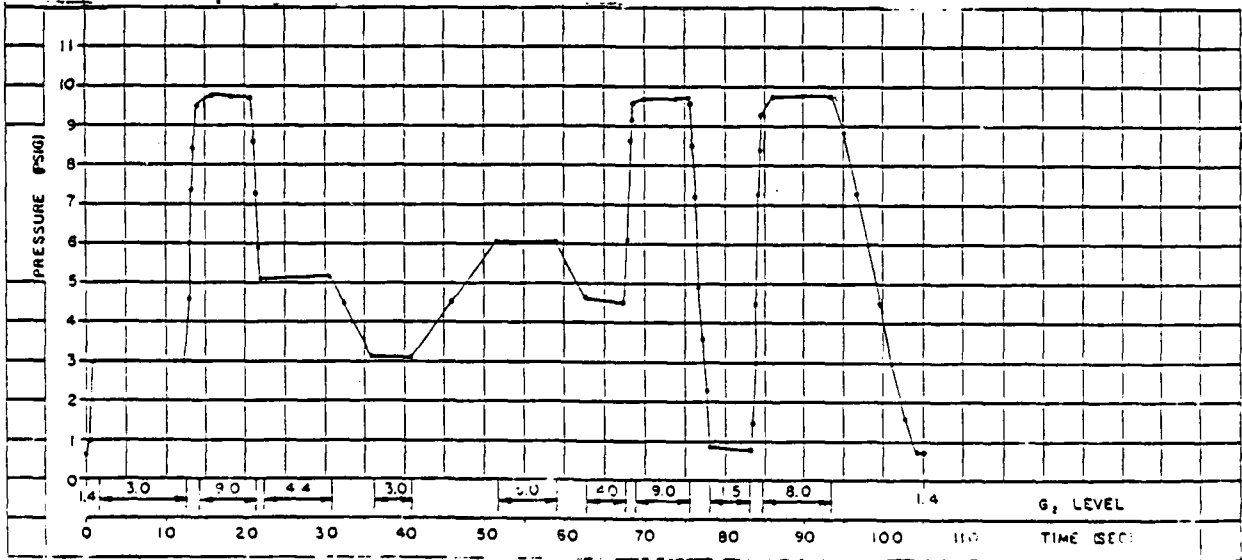


Figure 4.4-13. "Suit" pressures produced during SACM by Garrett Electronic/Pneumatic anti-G valve under conditions of: 150-psig source pressure; 10-liter volume; 0° angle.

from 9 G to 1.5 G, the pressure decreased rapidly to 0.8 psig, with a low-frequency oscillation of 0.8 psig p-p. A rapid-onset acceleration to 8 G produced a suit pressure of 9.3 psig with oscillation between 1.5 G and 6 G; and after 3.5 s the pressure leveled at 9.7 psig. Upon deceleration from 8 G down to 1.4 G the pressure decreased to 0.6 psig; oscillation (0.5 psig p-p) occurred from 8 G to 1.4 G.

At a valve angle of 30° (Fig. 4.4-15) the valve started flowing at 2 G, and at 3 G the pressure was 1.1 psig; oscillation of 0.8 psig p-p occurred between 1.4 G and 3 G. After 4.5 s at 3 G the pressure settled down at 2.5 psig. With a high onset to 9 G the pressure increased rapidly to 9.5 psig and after 6.5 s the pressure was 9.8 psig. Oscillation (1.1 psig p-p) was observed between 9 G and 7 G. Upon deceleration from 9 G down to 4.4 G the pressure decreased to 4.1 psig with oscillation (0.9 psig p-p) between 9 G and 4.4 G. A further decrease to 3 G resulted in a pressure of 2.4 psig. A slow onset to 5 G brought the pressure to 5 psig. Upon slow deceleration to 4 G the pressure decreased to 3.7 psig. A high onset to 9 G, with oscillation (0.9 psig p-p) between 4 G and 7.5 G, produced a suit pressure of 9.5 psig to 9.7 psig. Decelerating rapidly from 9 G to 1.5 G the pressure decreased to 0.9 psig, and after 0.5 s settled at 0.3 psig; oscillation (0.9 psig p-p) occurred between 9 G and 4.5 G. With a high onset to 8 G the pressure increased to 9.1 psig and then dropped off to 8.3 psig within 0.5 s; oscillation (0.9 psig p-p) occurred between 1.5 G and 7 G. From 8 G down to 1.4 G the pressure decreased to 0.2 psig; oscillation (0.5 psig p-p) was again observed between 7.5 G and 2 G.

Two source pressure-dependent studies were conducted in this phase on the Garrett valve. While the valve angle was at 0°, one experiment combined a source pressure of 30 psig with a 14-liter simulated suit volume, and the other combined 300-psig source pressure with a simulated suit volume of 6 liters. At a source pressure of 30 psig and a volume of 14 liters (Fig. 4.4-16), the suit volume pressure was 0.6 psig at 1.4 G, and 2.7 psig at 3 G—but leveled off at 3.1 psig within 1 s. Oscillation (1.2 psig p-p) was observed between 1.4 G and 3 G. With a rapid onset to 9 G, the pressure increased to 8.7 psig with oscillation (0.9 psig p-p) between 3 G and 5 G. Leaving 9 G with a high offset rate to 4.4 G, the pressure rapidly decreased to 5.3 psig; after 9 s at 4.4 G the pressure further decreased to 5.1 psig. Oscillation (0.8 psig p-p) was observed between 8.5 G and 4.4 G. Deceleration to 3 G produced a pressure of 3.1 psig; a subsequent increase to 5 G increased suit pressure to 6 psig, and another decrease to 4 G dropped the pressure to 4.5 psig. With a high onset rate to 9 G the suit pressure increased rapidly to 8.8 psig and leveled off at 8.9 psig with a small oscillation (1 psig p-p) between 4 G and 5 G. Upon rapid offset down to 1.5 G the suit pressure decreased rapidly to 2.4 psig, and after about 6 s the pressure decreased to 0.8 psig. Oscillation (0.8 psig p-p) was observed between 8.5 G and 5 G. With a high onset rate to 8 G the suit pressure climbed to 8.4 psig, and after 9 s at 8 G it leveled off at 9 psig; oscillation (1 psig p-p) was present between 1.4 G and 3 G. With a high offset down to 1.4 G the pressure decreased rapidly to 0.8 psig, with oscillation (0.3 psig p-p) between 7 G and 1.4 G.

At a source pressure of 300 psig and suit volume of 6 liters (Fig. 4.4-17) the suit pressure was 0.6 psig at 1.4 G; at 3 G the pressure was 3.1 psig and oscillation (1 psig p-p) was observed between 1.4 G and 3 G. With a high onset from 3 G to 9 G, the suit pressure increased rapidly to 11.7 psig and leveled off at 12.4 psig after about 6.5 s; an oscillation (1.2 psig p-p) occurred from 3 G to 7.5 G. Upon subsequent high offset

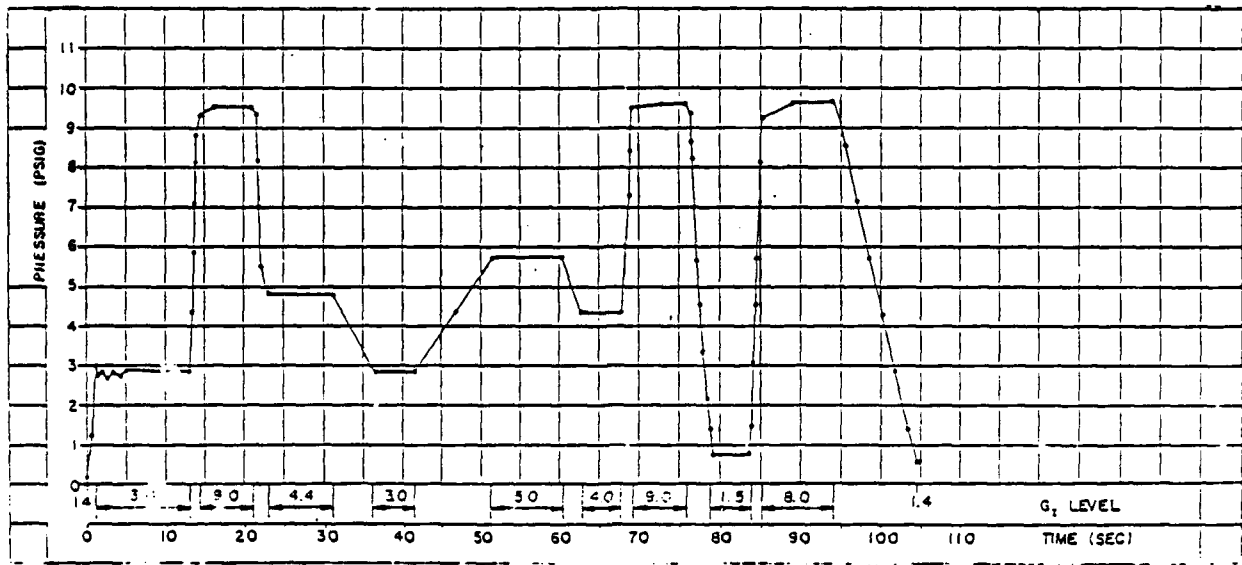


Figure 4.4-14. "Suit" pressures produced during SACM by Garrett Electronic/Pneumatic anti-G valve under conditions of: 150-psig source pressure; 10-liter volume; 15° angle.

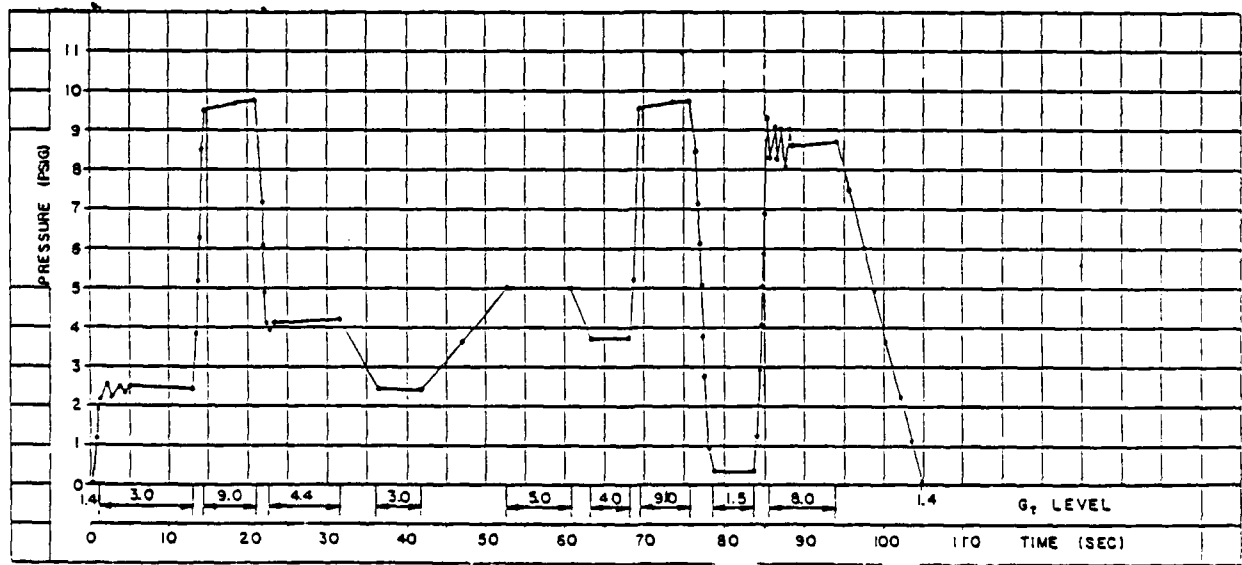


Figure 4.4-15. "Suit" pressures produced during SACM by Garrett Electronic/Pneumatic anti-G valve under conditions of: 150-psig source pressure; 10-liter volume; 30° angle.

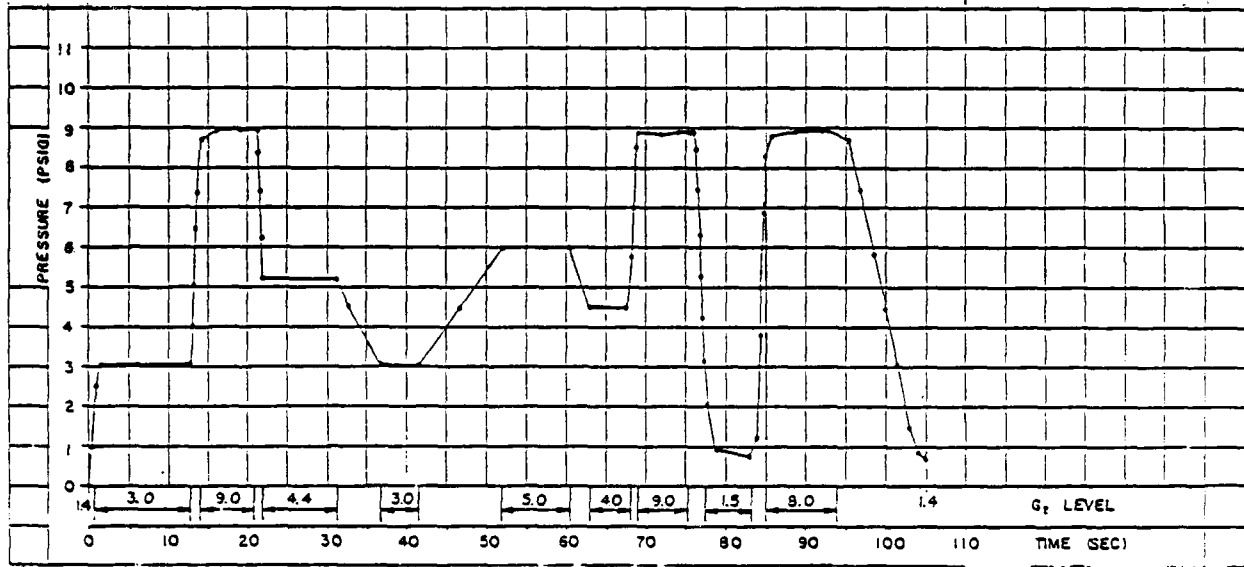


Figure 4.4-16. "Suit" pressures produced during SACM by Garrett Electronic/Pneumatic anti-G valve under conditions of: 30-psig source pressure; 14-liter volume; 0° angle.

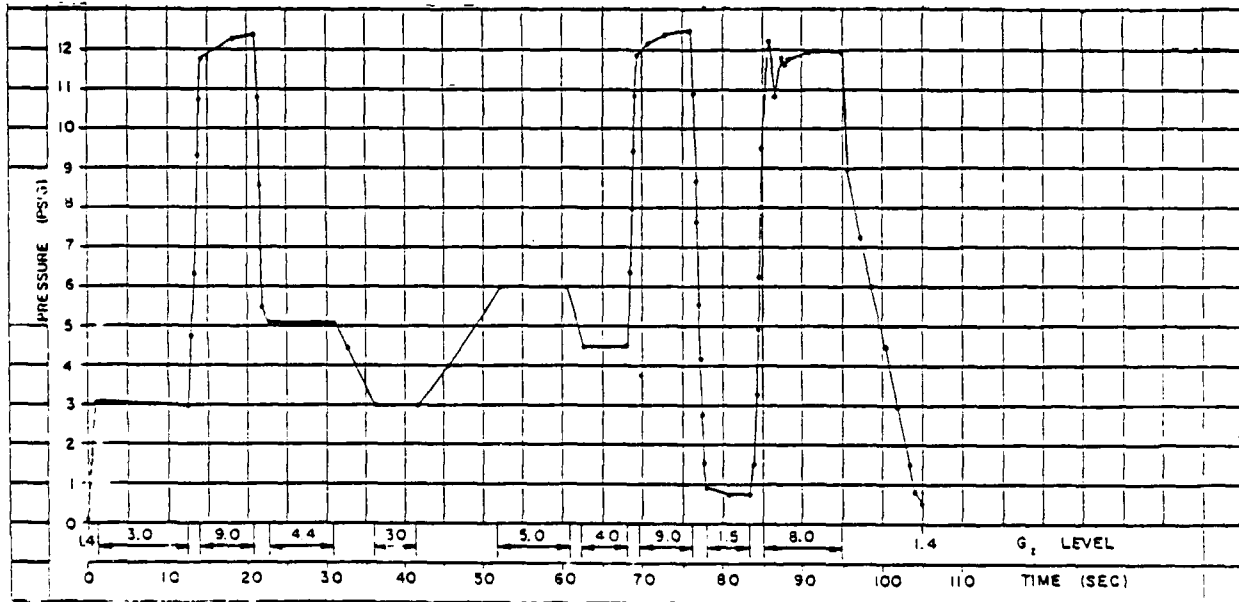


Figure 4.4-17. "Suit" pressures produced during SACM by Garrett Electronic/Pneumatic anti-G valve under conditions of: 300-psig source pressure; 6-liter volume; 0° angle.

down to 4.4 G the pressure decreased to 5.1 psig, with oscillation (1 psig p-p) between 8.7 G and 4.4 G. Further decrease to 3 G dropped the pressure to 3 psig. Acceleration to 5 G brought the pressure to 6 psig, and the next deceleration to 4 G reduced the pressure to 4.5 psig. With a high onset to 9 G the suit pressure increased to 11.9 psig and leveled off at 12.5 psig after about 6.5 s; a low-level oscillation (1.3 psig p-p) was observed between 4 G and 7.5 G. With a high offset rate to 1.5 G the suit volume pressure decreased rapidly to 0.9 psig and leveled off at 0.8 psig; oscillation (0.9 psig p-p) was again observed between 8.7 G and 2.5 G. With a rapid-onset acceleration to 8 G the pressure increased to 10.8 psig, with oscillations (1 psig p-p) observed between 1.5 G and 7.5 G; after about 8.5 s at 8 G the pressure leveled off at 12 psig. With a high offset down to 1.4 G the pressure decreased to 0.6 psig, with a 0.5 psig p-p oscillation observed between 7.9 G and 1.4 G.

4.5 Hymatic VAG-110-022 Anti-G Valve

4.5.1 Description

The Hymatic VAG-110-022 anti-G valve (SN 276AS) (Fig.4.5-1) was manufactured by Hymatic Engineering Co., Ltd. (Redditch, England), for use by British military personnel. This valve has an inlet filter; a nonreturn valve; a manually operated two-position ("On/Off") valve; a spring-loaded G-sensitive main valve assembly; a diaphragm which incorporates a filter; an outlet connection containing a cleanable brazed-in filter; and a spring-loaded relief valve (which prevents overpressurization of the anti-G suit). The valve body, main piston, and mass constitute one matched assembly; the stop valve and stop valve body make up another matched assembly.

This valve is designed so that placing the stop valve lever in the "Off" position closes the valve to inlet airflow, thus preventing air from entering the valve body. The anti-G suit is vented to ambient pressure through vents in the valve body, and through ports drilled to a vent in the stop valve barrel. Placing the stop valve lever in the "On" position (in the absence of G forces) prevents air from entering the anti-G suit because the valve piston is oriented across the flow passage. Again, the suit is vented to ambient pressure through the valve body vents.

As G forces are applied to the valve, the mass pushes down the main and lower pistons against the spring loads, resulting in closing of the bleed-air vents on the sides of the valve body and allowing inlet air to enter the valve. The inlet air enters both the valve outlet to the anti-G suit and the main piston (through cross holes); pressure is exerted on the lower piston, forcing it down to the lower stop assembly. The main piston is then suspended between the lifting forces of the upper spring pressure plus air pressure and the depressing forces of the mass acted upon by G forces. The resultant of these vectors produces a steady suit pressure; the leakage of air past the main piston and through the bleed-air vents is equal to the inlet airflow. As G forces decrease, the piston and mass are returned to the static condition (by spring pressure) and the suit pressure again exhausts to ambient atmosphere through the gauze-covered vents in the valve body.

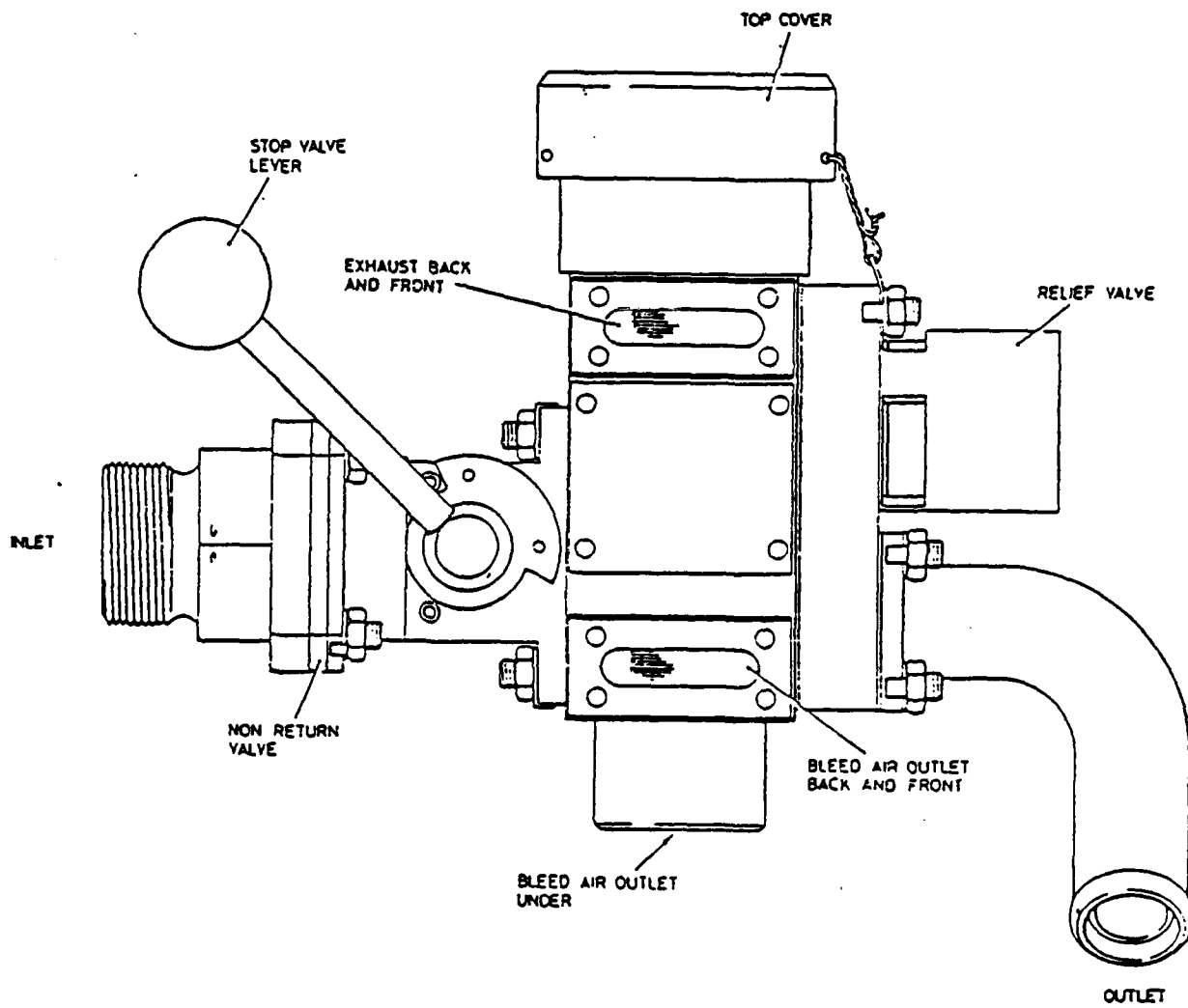


Figure 4.5-1. Hymatic VAG-110-022 anti-G valve.

Overpressurization of the suit causes air pressure to act upon a spring-loaded relief valve set on the outlet side of the anti-G valve. When this action occurs, the relief valve is lifted from its seat and excess pressure is vented directly to the ambient atmosphere. The relief valve contains a friction spring which ensures smooth operation by damping out small spring movement.

If the air supply should fail during a G_z maneuver, deflation of the pressurized suit would be controlled by a nonreturn valve adjacent to the inlet filter. A preflight check of valve function can be performed when engines are running by manually depressing the diaphragm assembly in the top cover.

Performance of the Hymatic VAG anti-G valve was evaluated over the range of source pressures specified by the manufacturer: 120 psig, maximum; 30 psig, minimum; and 60 psig, median.

4.5.2 Phase I - Determination of Maximum Flow Capacity

The maximum flow capacity of the British Hymatic VAG-110-022 anti-G valve was measured with a source pressure of 60 psig, the median source pressure for this valve. The G_z -onset conditions were $0.5 G_z s^{-1}$, and the valve angle was 0° . The results of the maximum-flow testing are shown in Figure 4.5-2. At baseline G (1.4 G), flow was 0.4 SCFM. As the G level increased, the flowrate did not change until 2 G was reached when the flow was 0.75 SCFM; flow then increased rapidly, reaching 7.3 SCFM at 2.4 G. At this point, the rate of increase slowed, but remained essentially linear up to 7 G, where the flowrate was 17.8 SCFM. Flow plateaued at 17.8 SCFM while G level increased to--and remained at--11 G for 4.5 s; flow did not change until approximately 6.5 G was reached during deceleration. The rate of decrease in pressure during deceleration closely mirrored the rate of increase during acceleration; a linear decrease occurred from 17.8 SCFM (11 G) to 2.5 SCFM (7.3 G). At this point, flow began to drop exponentially to 1.6 SCFM at 2 G, followed by a minimal flow of 0.5 SCFM from 1.7 G throughout the time at baseline G (1.4 G).

4.5.3 Phase II - Determination of Dynamic Response Capability

The dynamic response capability of the Hymatic VAG-110-022 anti-G valve was determined as described in Testing Procedures (section 3.2.2). Pressure delivered by the valve was measured at the output port and inside the simulated anti-G suit volume. "Output pressure" refers to the pressure within the simulated suit volume, unless otherwise noted.

4.5.3.1 Low G_z -Onset-Rate Conditions

The $0.1 G_z s^{-1}$ trapezoidal profile was used for all low-onset tests.

Under conditions of low G_z -onset, median source pressure (60 psig), and a valve angle of 0° , the results shown in Figure 4.5-3 were observed. As G_z level began to

increase from the baseline of 1.4 G, there was no increase in suit pressure until after 2 G; the increase in pressure was then rapid, reaching 1.5 psig at 2.3 G, whereupon the rate of pressure increase slowed and became linear from this point up to 9 G where it was 9.2 psig. The increase in suit pressure then became slightly erratic, but reached the maximum value of 10.4 psig when 11 G was attained. The pressure remained stable at 10.5 psig while 11 G was maintained. Upon deceleration, suit pressure began to decrease immediately with a linear slope which mirrored the increase upon acceleration, except that the drop at the low end was more gradual than the initial jump in pressure with acceleration; at 2.5 G the suit pressure was 2 psig, at 2 G it was 1.1 psig, at 1.8 G it was 0.2 psig, and at 1.4 G (baseline) suit pressure was 0 psig.

The effects of valve angle upon low- G_z performance of the Hymatic VAG valve were explored by using valve angles of 15° and 30° while maintaining source pressure at the median value of 60 psig. When the valve angle was 15° , the results shown in Figure 4.5-4 were observed. Upon acceleration, suit pressurization did not start until G level was increased from 1.4 G to 2.4 G (0.2 psig); pressure then jumped up rapidly to 2.1 psig at 2.6 G and increased slightly to 2.2 psig at 3 G. From this point, the increase in suit pressure became consistently linear with the increase in G_z level up to 10.2 psig at 11 G; however, a small shoulder was observed in the region of 9.5-10 G. Suit pressure then remained stable at the maximum value of 10.2 psig while G level was maintained at 11 G. Upon deceleration, suit pressure began to drop at 10.5 G (10.2 psig), with an essentially linear decrease down to 2 G (1 psig); pressure then dropped rapidly to 0 psig at 1.7 G.

The results obtained when the valve angle was 30° are shown in Figure 4.5-5. Pressurization of the suit was not initiated until 2.9 G was reached. Suit pressure was 0.4 psig at 3 G; it then climbed rapidly to 2.6 psig at 3.3 G, whereupon it dropped slightly before beginning a nearly linear increase up to 8.1 psig at 10 G. At this point the suit pressure buildup faltered slightly but reached 8.8 psig as 11 G was attained. During the time interval at 11 G, the pressure continued to increase slightly, reaching 9.4 psig just before deceleration was initiated. As deceleration began, suit pressure did not change significantly down to approximately 9.7 G; from this point, pressure began to decrease essentially linearly while decelerating to 2.5 G (1.6 psig). At 2 G, pressure was 0.2 psig, and at 1.7 G it was 0 psig.

The effects of source pressure upon low G_z -onset performance of the Hymatic VAG valve were observed by testing at both the minimum and maximum source pressures for this valve (30 psig and 120 psig, respectively) while keeping all other conditions constant. At a source pressure of 30 psig, the valve performed as shown in Figure 4.5-6. Upon acceleration, suit pressure was 0 psig until after 2 G was reached; it then jumped up to 1.9 psig at 2.5 G where it began a linear increase up to 8.9 psig at 9 G; it then continued to increase in a somewhat erratic fashion, reaching 10.1 psig at 10.6 G, and stabilizing at 10.2 psig throughout the time at 11 G. Upon deceleration, the suit pressure did not begin to fall until approximately 9.3 G was reached; after this point pressures of 9.9 psig at 9.3 G, 9.5 psig at 9 G, and 9.2 psig at 8.5 G were observed. Suit pressure then decreased linearly with G level until 2 G (1.1 psig) was reached; after this point, the pressure dropped to 0.7 psig at 1.9 G and continued down to 0 psig at 1.6 G.

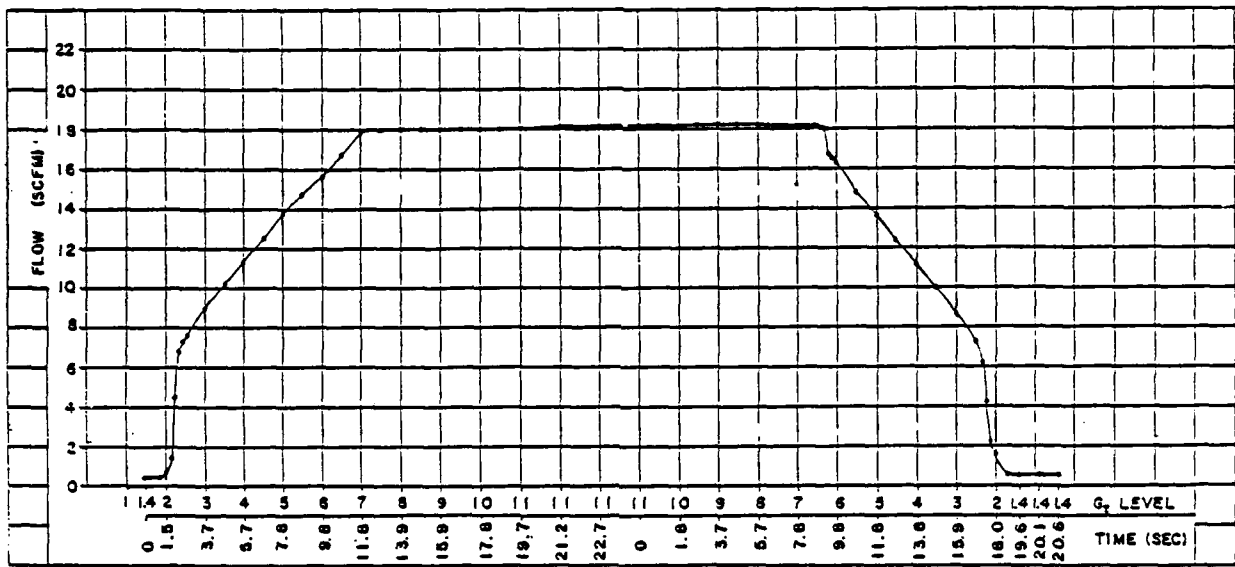


Figure 4.5-2. Maximum flow through Hymatic VAG-110-022 anti-G valve.

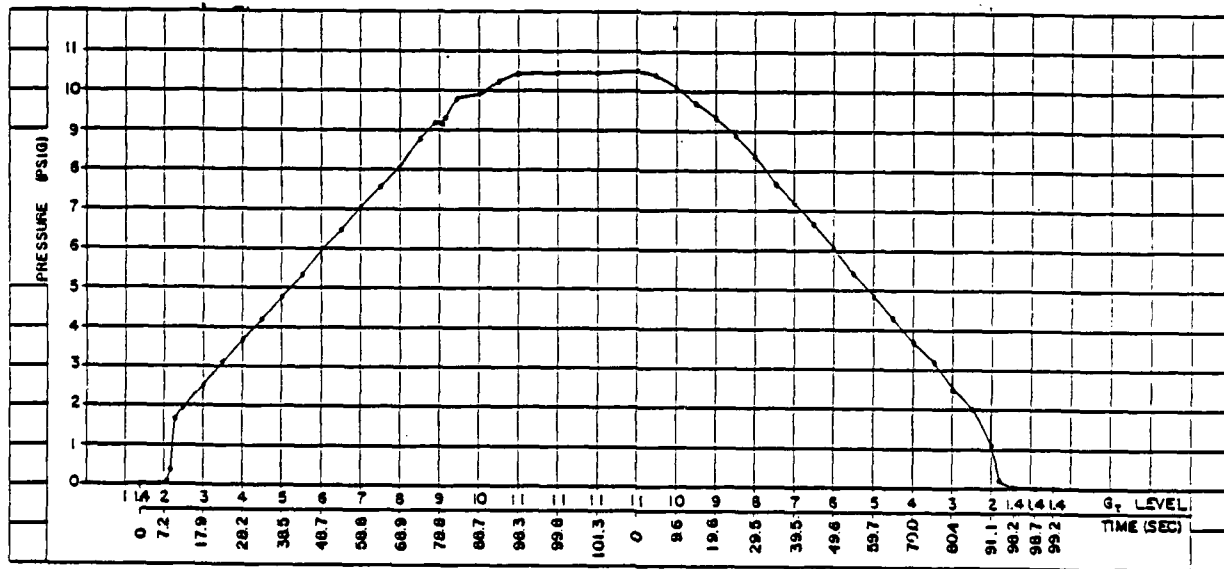


Figure 4.5-3. "Suit" pressures produced during acceleration/deceleration by Hymatic VAG-110-022 anti-G valve under conditions of: 60-psig source pressure; low G onset; 10-liter volume; 0° angle.

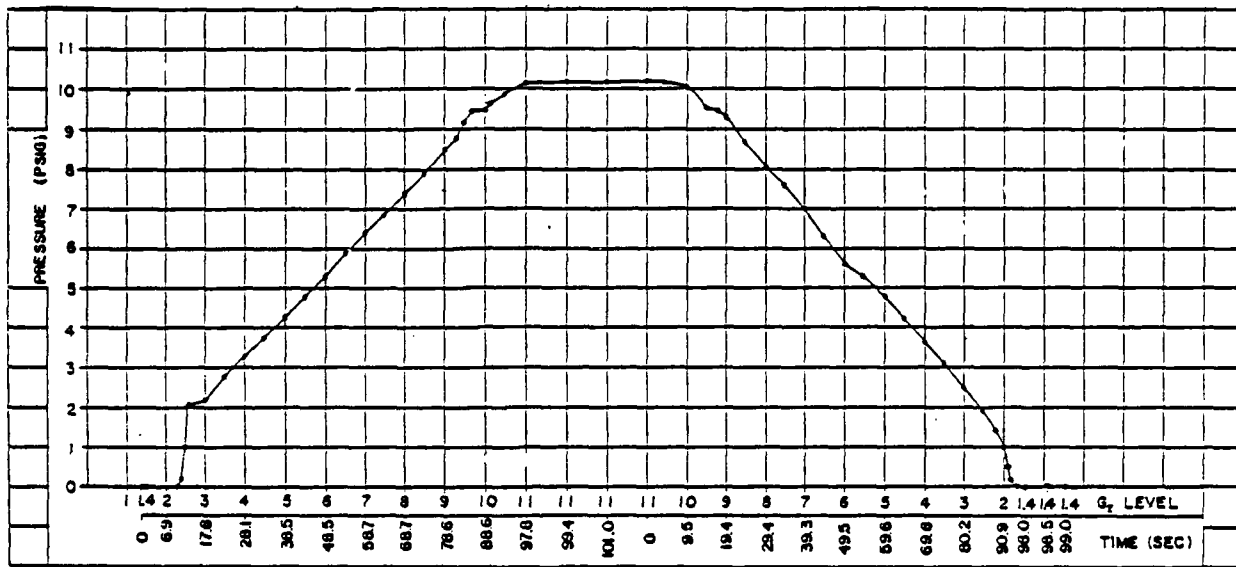


Figure 4.5-4. "Suit" pressures produced during acceleration/deceleration by Hymatic VAG-110-022 anti-G valve under conditions of: 60-psig source pressure; low G onset; 10-liter volume; 15° angle.

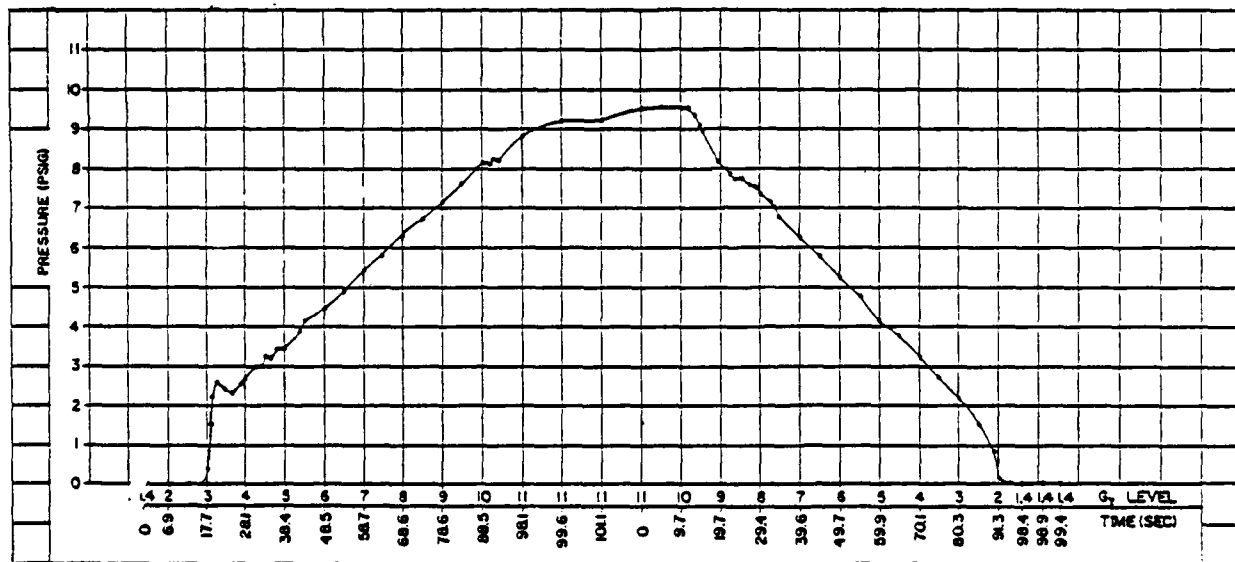


Figure 4.5-5. "Suit" pressures produced during acceleration/deceleration by Hymatic VAG-110-022 anti-G valve under conditions of: 60-psig source pressure; low G onset; 10-liter volume; 30° angle.

When the source pressure was 120 psig, the Hymatic VAG valve performed as shown in Figure 4.5-7. Suit pressure did not begin to increase until G force had increased from 1.4 G to 2 G; after 2 G pressure jumped up rapidly to 1.9 psig at 2.5 G before beginning a smooth linear increase up to 9.8 psig at 9.6 G. Pressure then continued to increase more slowly, reaching 10.4 psig at 11 G. During the time that G level was maintained at 11 G, the pressure continued to increase slightly, reaching a maximum of 10.5 psig at the end of this period. Pressure began to decrease immediately upon deceleration and dropped to 10 psig at 10 G, thence to 9.5 psig at 9 G. From 9 G down to 2.5 G, the pressure decreased linearly to a value of 2 psig at 2.5 G; pressure then decreased more rapidly to 1.1 psig at 2 G and 0 psig at 1.6 G.

4.5.3.2 High G_z -Onset-Rate Conditions

For high G_z -onset testing of the Hymatic VAG anti-G valve, conditions were: a simulated suit volume of 10 liters and high acceleration and deceleration rates. The pressure delivered by the valve was measured at both the output port and inside the simulated suit volume; however, only suit pressures are presented and discussed here.

The effects of valve angle upon performance of the Hymatic anti-G valve were explored by varying the valve angle (0° , 15° , and 30°) while maintaining the source pressure at the median value for this valve (60 psig). When the valve angle was 0° , suit pressure did not begin to increase until G level had increased from baseline (1.4 G) to 2.5 G (Fig. 4.5-8). Once pressurization began, suit pressure increased in a smooth linear fashion up to 10 psig at 11 G; while G level was maintained at 11 G, the pressure increased further to 10.5 psig within 1.5 s, then remained at 10.5 psig until after deceleration was initiated. Upon deceleration, pressure did not begin to fall until after 9.5 G was attained; it fell to 10.2 psig at 9 G, then 9.5 psig at 8 G. After this point, pressure decreased linearly with G_z down to 3.8 psig at 2 G; it then dropped more rapidly to 2.5 psig at 1.4 G (baseline) and after 1 s at baseline G the pressure was 0.4 psig.

When the valve angle was set to 15° (Fig. 4.5-9), test performance under median source pressure was essentially identical to that at a valve angle of 0° (Fig. 4.5-8).

For a 30° valve angle and median source pressure (Fig. 4.5-10), test performance was also similar to the other two valve angles, although in the region from 6 G to 11 G (3.8 psig to 9.3 psig) the pressure increase became nonlinear. As acceleration reached 11 G, suit pressure was 9.3 psig but jumped to 10.5 psig within 1.5 s. Upon deceleration, suit pressure began to decrease immediately and the rate of decrease approached linearity down to the 2-G level (3.4 psig), whereupon the decrease became exponential. Suit pressure was 1.8 psig as 1.4 G (baseline) was reached, then fell further to 0.8 psig within 0.5 s, followed by 0.3 psig after another 0.5 s at 1.4 G.

The effects of source pressure upon performance of the Hymatic VAG valve were explored by testing under conditions of minimum (30 psig) and maximum (120 psig) source pressure while holding the valve angle constant at 0° . (These results can be compared to those obtained under the median source pressure of 60 psig and valve angle of 0° , shown in Fig. 4.5-8.) When a minimum source pressure was used under

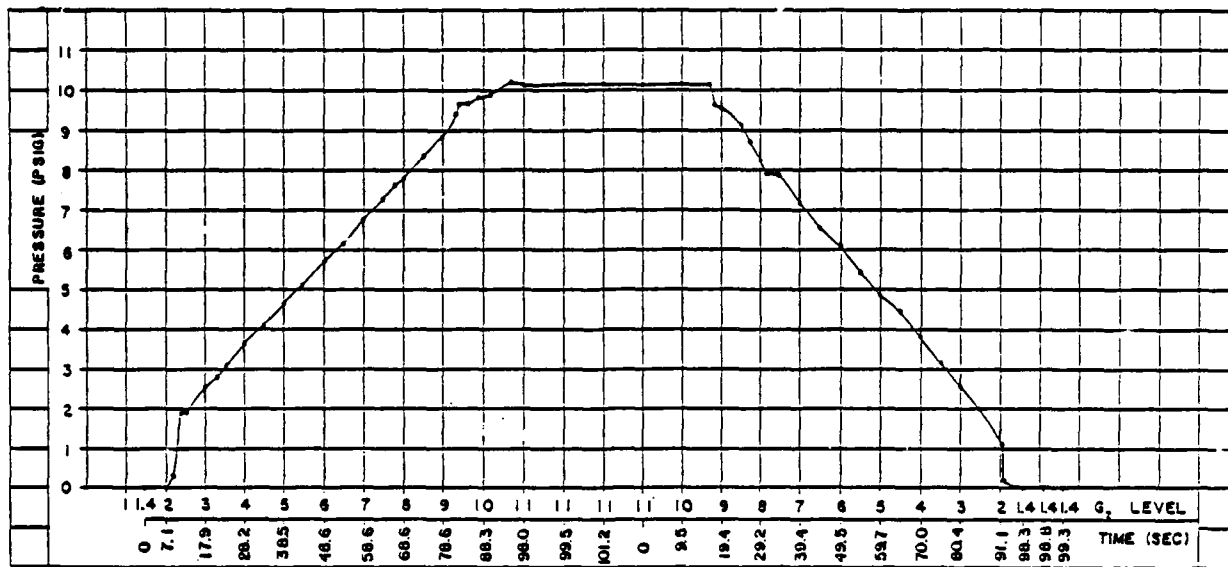


Figure 4.5-6. "Suit" pressures produced during acceleration/deceleration by Hymatic VAG-110-022 anti-G valve under conditions of: 30-psig source pressure; low G onset; 10-liter volume; 0° angle.

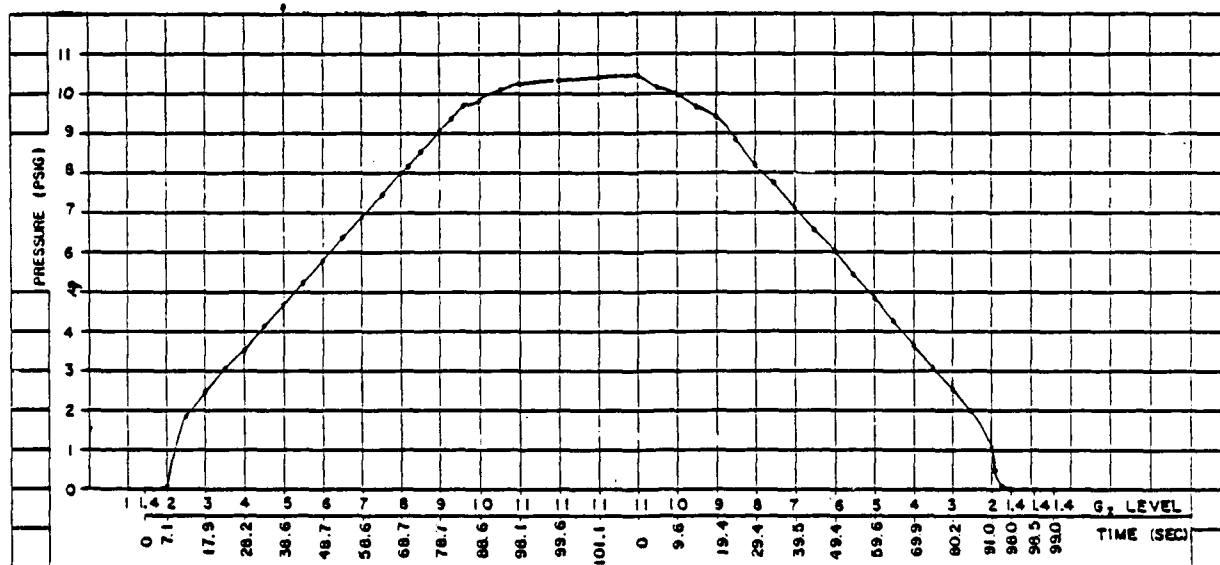


Figure 4.5-7. "Suit" pressures produced during acceleration/deceleration by Hymatic VAG-110-022 anti-G valve under conditions of: 120-psig source pressure; low G onset; 10-liter volume; 0° angle.

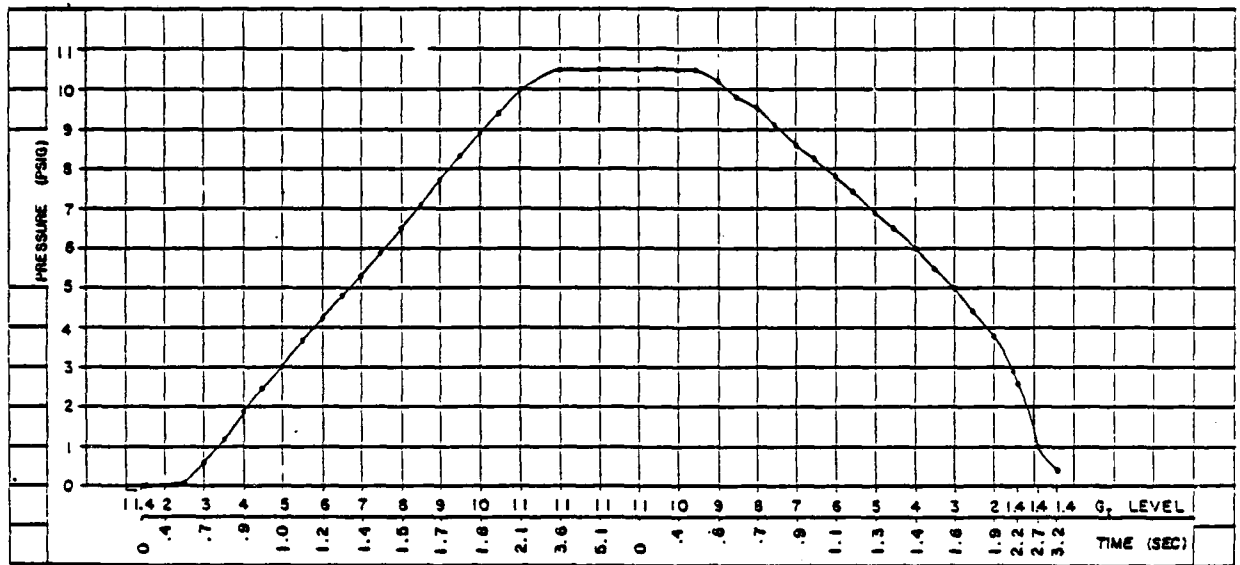


Figure 4.5-8 "Suit" pressures produced during acceleration/deceleration by Hymatic VAG-110-022 anti-G valve under conditions of: 60-psig source pressure; high G onset; 10-liter volume; 0° angle.

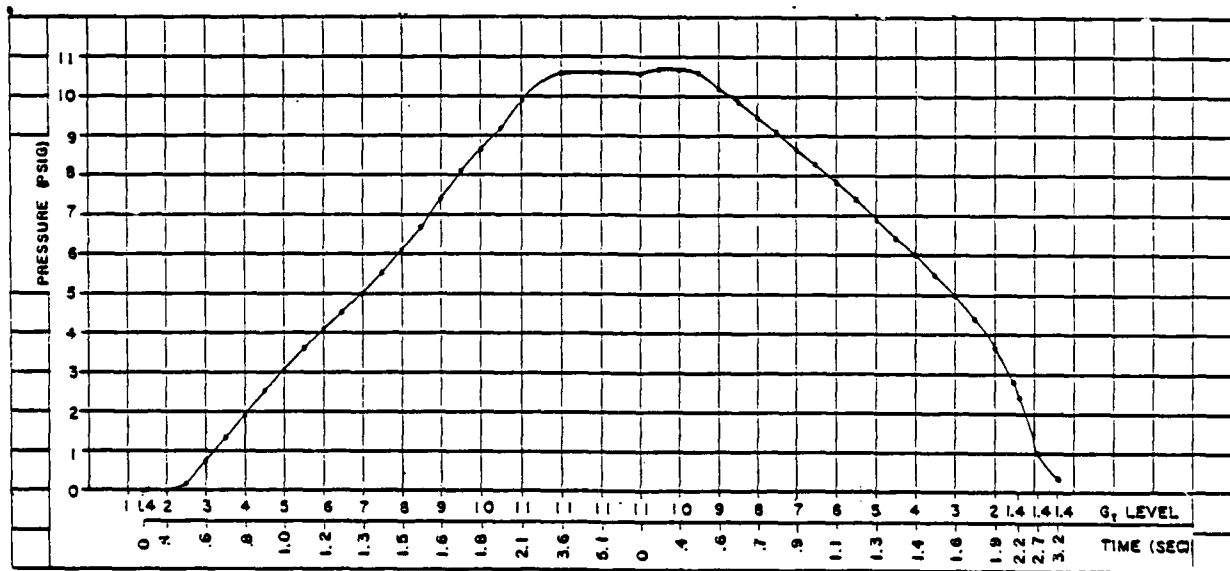


Figure 4.5-9. "Suit" pressures produced during acceleration/deceleration by Hymatic VAG-110-022 anti-G valve under conditions of: 60-psig source pressure; high G onset; 10-liter volume; 15° angle.

these high G-onset conditions, valve performance was as shown in Figure 4.5-11. On acceleration, suit pressure did not begin to increase until after 2.5 G, then increased linearly up to 2.8 psig at 5.5 G. After this point, the pressure buildup became nonlinear, measuring 3.8 psig at 7 G, 5.2 psig at 9 G, and 7.4 psig initially at 11 G; after 1.5 s at 11 G, however, the pressure jumped to 10 psig and stabilized at this level until well after deceleration had started. After deceleration to 8.5 G the pressure began to drop, becoming approximately linear from 7.5 G (9.1 psig) to 2 G (3.7 psig). After the 2-G point, the pressure fell more rapidly, measuring 2.5 psig as 1.4 G was reached; within 1 s at 1.4 G the pressure had fallen to 0.3 psig.

At the maximum source pressure (120 psig), pressure in the suit started to build up when the G-level reached 2-2.5 G (Fig. 4.5-12). The increase in pressure was consistently linear as G level increased to 11 G, measuring 2.7 psig at 5 G and 9.8 psig at 11 G. After 1.5 s at 11 G, the pressure increased further to 10.5 psig where it remained throughout the interval at 11 G. Upon deceleration, suit pressure started falling immediately and followed a gentle convex curve as G level decreased down to 2 G; pressures measured 10.1 psig at 10 G, 9.1 psig at 8 G, 7.7 psig at 6 G, and 3.8 psig at 2 G. After 2 G the pressure decreased exponentially, reading 1.3 psig as baseline G (1.4 G) was reached; after 1 s at this level pressure dropped further to 0.2 psig.

4.5.4 Phase III - Determination of Complex Dynamic Response Capability

The response pattern of the Hymatic VAG anti-G valve under SACM conditions was examined by varying the valve angle while holding the source pressure at the median value of 60 psig. (Suit volume was always the median value of 10 liters unless specified otherwise.) Subsequently, the minimum source pressure was combined with a maximum suit volume of 14 liters, and the maximum source pressure was combined with a minimum suit volume of 6 liters, while the valve angle was held at 0°.

The effects of varying the valve angle (while holding source pressure at 60 psig and suit volume at 10 liters) are shown in Figures 4.5-13 through 4.5-15. At an angle of 0°, the pattern shown in Figure 4.5-13 was observed. Under 3 G, pressure increased to 2.7 psig within 2-3 s and stabilized at this level. The first high-onset rate to 9 G produced a buildup of suit pressure from 2.7 G to 9.9 G within 2-3 s; the pressure then fell slightly to approximately 9.7 psig within 6-7 s. Rapid deceleration from 9 G to 4.4 G caused an immediate drop to 4.4 psig within 3 s. Further deceleration to 3 G again yielded a suit pressure of 2.7-2.8 psig. A subsequent slow acceleration to 5 G produced a pressure of 5 psig; a deceleration to 4 G then resulted in a pressure of 3.9-4 psig. Another rapid-onset acceleration to 9 G caused the pressure to increase to 9.9 psig, and then to decrease slightly to 9.7 psig within approximately 6 s. Rapid deceleration to 1.5 G was accompanied by a sharp drop in pressure to 2.2 psig, then to 0.1 psig within 5 s. A subsequent rapid acceleration to 8 G resulted in an immediate pressure increase to 8.8 psig; the pressure then drifted down to approximately 8.6 psig within about 8 s. The return to baseline G (1.4 G) produced an essentially linear fall in suit pressure to 0.3 psig (Fig. 4.5-13).

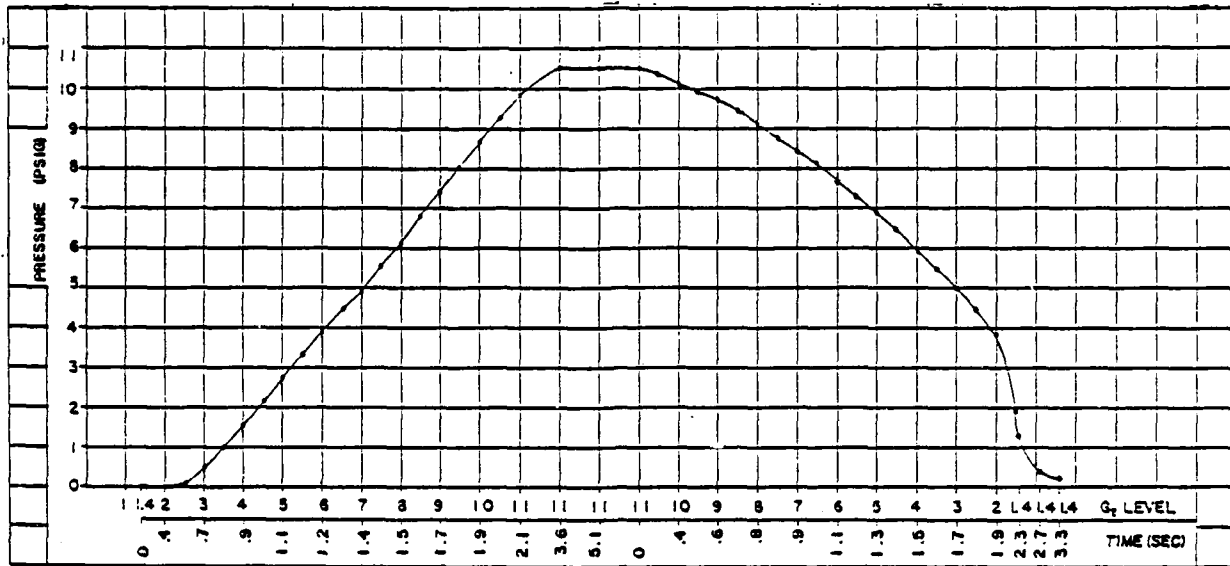


Figure 4.5-12. "Suit" pressures produced during acceleration/deceleration by Hymatic VAG-110-022 anti-G valve under conditions of: 120-psig source pressure; high G onset; 10-liter volume; 0° angle.

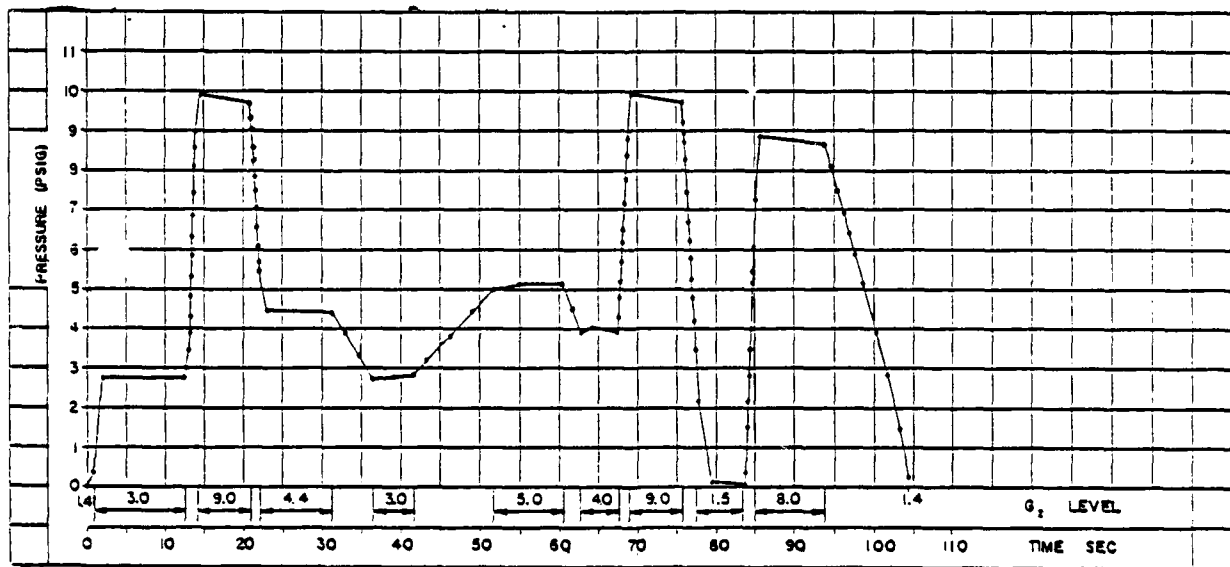


Figure 4.5-13. "Suit" pressures produced during SACM by Hymatic VAG-110-022 anti-G valve under conditions of: 60-psig source pressure; 10-liter volume; 0° angle.

When the valve angle was 15°, the SACM profile observed (Fig. 4.5-14) was almost identical to that for the 0° angle (Fig. 4.5-13). The only apparent difference between the two patterns was that when the angle was 15°, the rapid deceleration from 9 G to 4.4 G caused the suit pressure to fall slightly further--i.e., to 4.1 psig vs. 4.5 psig at 0°.

For a valve angle of 30° (Fig. 4.5-15), the SACM profile was also similar to that for angles of 0° and 15°; however, suit pressures were generally slightly lower at 30°.

When the maximum suit volume (14 liters) was used with the minimum source pressure (30 psig) and an angle of 0°, the SACM suit pressurization response (Fig. 4.5-16) was essentially identical to the response observed for conditions of 60-psig source pressure, 10-liter suit volume, and 0° angle shown in Figure 4.5-13. The conditions of maximum source pressure (120 psig), minimum suit volume (6 liters), and valve angle of 0°, shown in Figure 4.5-17, also produced a response pattern identical to that of Figures 4.5-13 and 4.5-16.

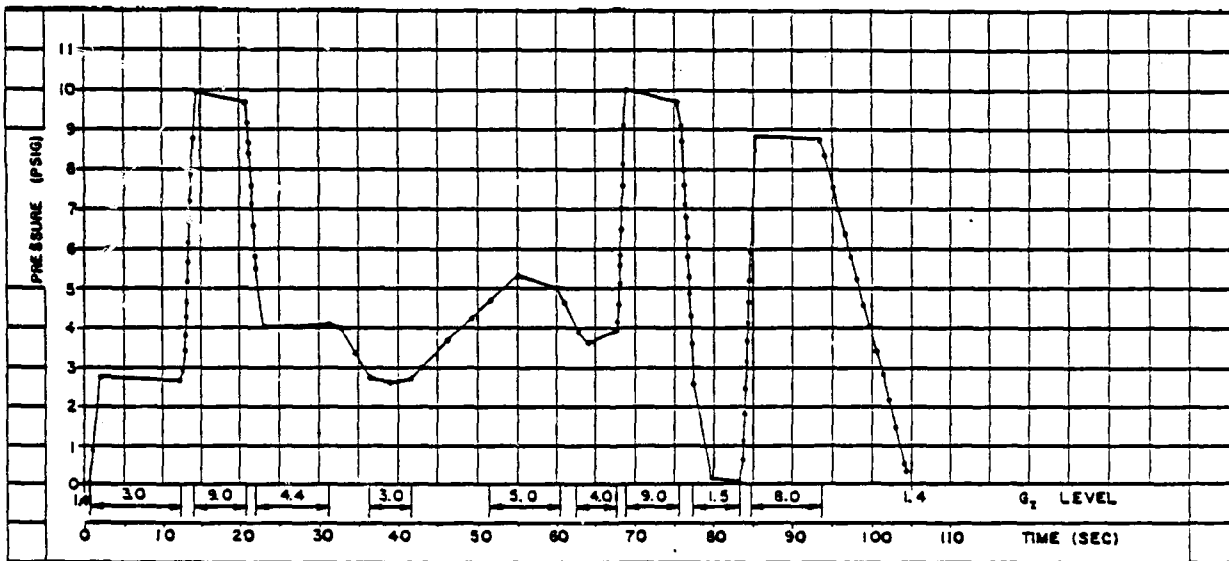


Figure 4.5-14. "Suit" pressures produced during SACM by Hymatic VAG-110-022 anti-G valve under conditions of: 60-psig source pressure; 10-liter volume; 15° angle.

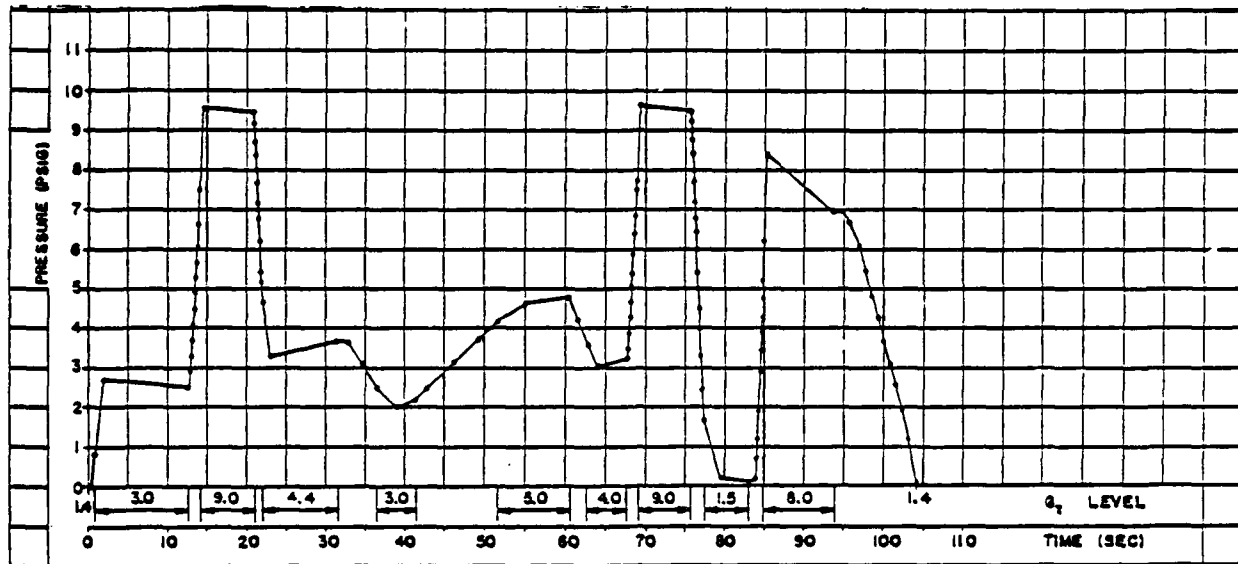


Figure 4.5-15. "Suit" pressures produced during SACM by Hymatic VAG-110-022 anti-G valve under conditions of: 60-psig source pressure; 10-liter volume; 30° angle.

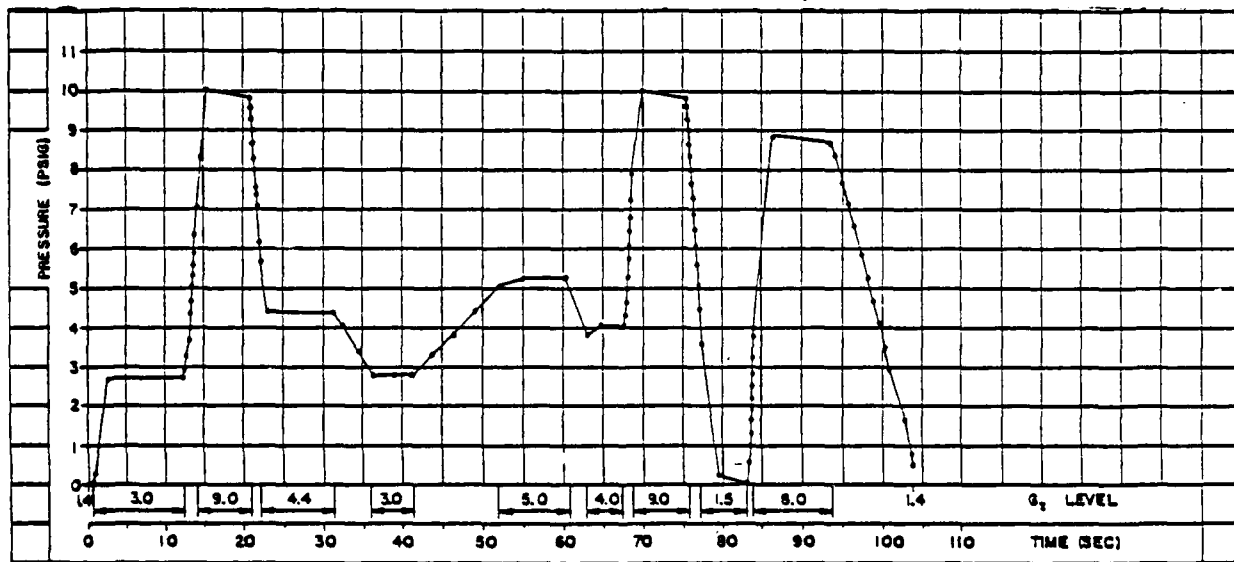


Figure 4.5-16. "Suit" pressures produced during SACM by Hymatic VAG-11-022 anti-G valve under conditions of: 30-psig source pressure; 14-liter volume; 0° angle.

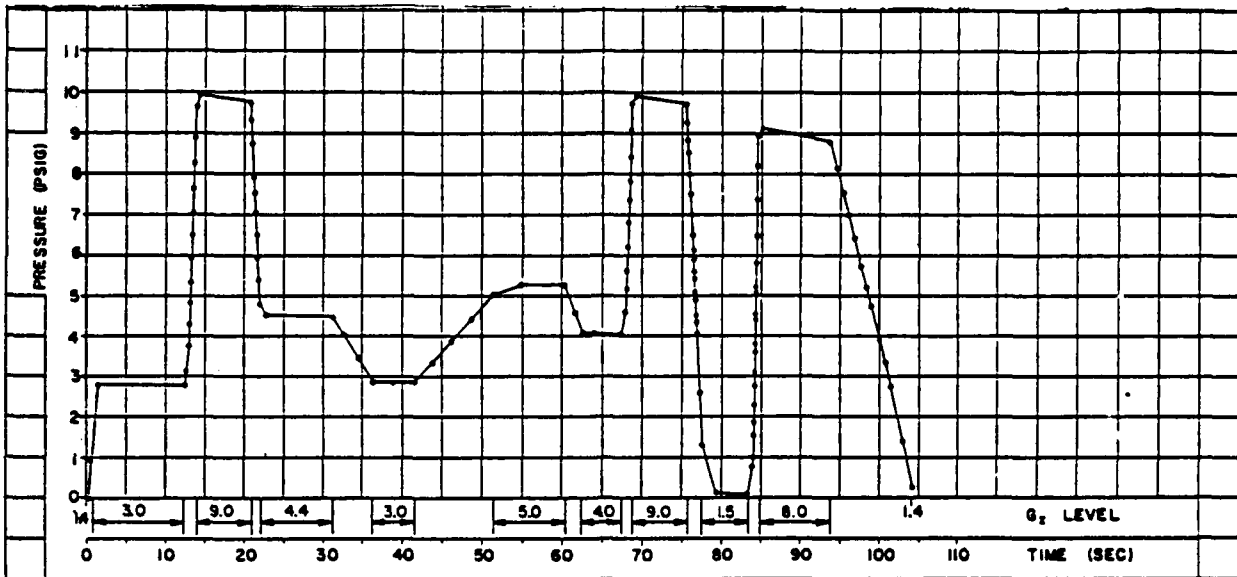


Figure 4.5-17. "Suit" pressures produced during SACM by Hymatic VAG-110-022 anti-G valve under conditions of: 120-psig source pressure; 6-liter volume; 0° angle.

4.6 AAMRL Anti-G Valve

4.6.1 Description

The Armstrong Aerospace Medical Research Laboratory (AAMRL), or "Bang Bang," anti-G valve (SN 002) (Fig. 4.6-1) is a modified ALAR High Flow (SN 107, see section 4.3) valve. A solenoid plunger was added to the ALAR High Flow valve and the "Press to Test" button was relocated. The modifications were made at AAMRL, Wright-Patterson Air Force Base, Ohio.

In operation, this valve uses an electronically controlled solenoid to drive the anti-G suit pressure to maximum when the level of acceleration exceeds both +2 G and an onset rate of 2 G s⁻¹. The maximum pressure is maintained for 2.5 s before the valve reverts back to normal operation. If the "trigger" conditions are encountered again, the solenoid will be activated again.

4.6.2 Phase I - Determination of Maximum Flow Capacity

The maximum flow capacity of the AAMRL anti-G valve was measured at: its median pressure of 150 psig; 0.5 G s⁻¹; valve angle of 0°; and with electronically controlled solenoid both on and off. The flow through the valve was the same for both cases; this can be seen from Figures 4.6-2 and 4.6-3. Flow was initiated between 1.7 G and 2 G, reaching 8.5 SCFM at 3 G; after this point flow increased linearly up to 7.5 G, then began to plateau at a maximum level of 21-22 SCFM. Maximum flow was maintained throughout the time at 11 G and until 8.5 G was reached during deceleration. The decrease in flow was approximately linear down to 3 G (8 SCFM) whereupon it began to fall rapidly to 0 SCFM at 1.5 G (Figs. 4.6-2 and 4.6-3).

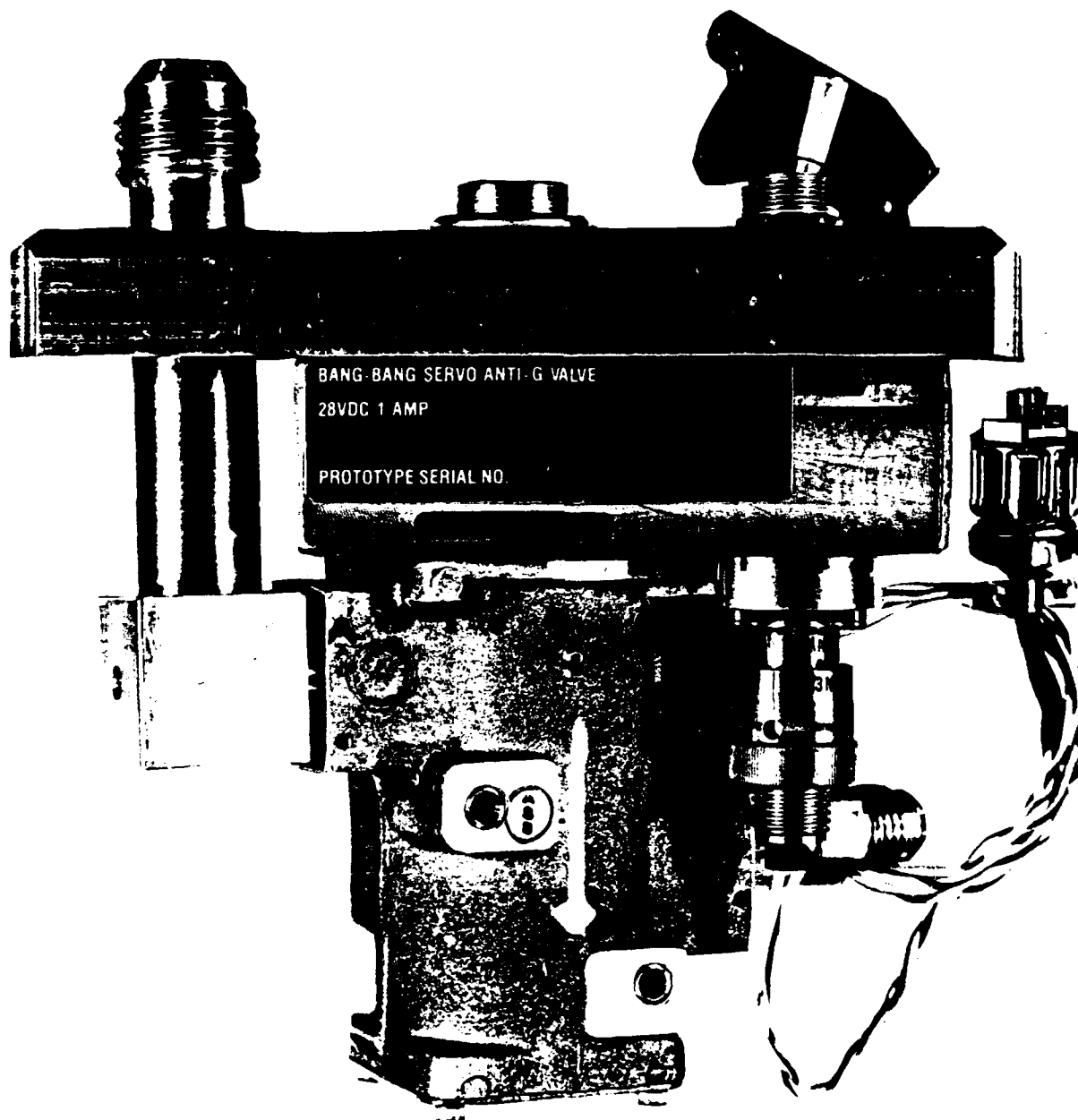


Figure 4.6-1. AAMRL anti-G valve ("Bang Bang").

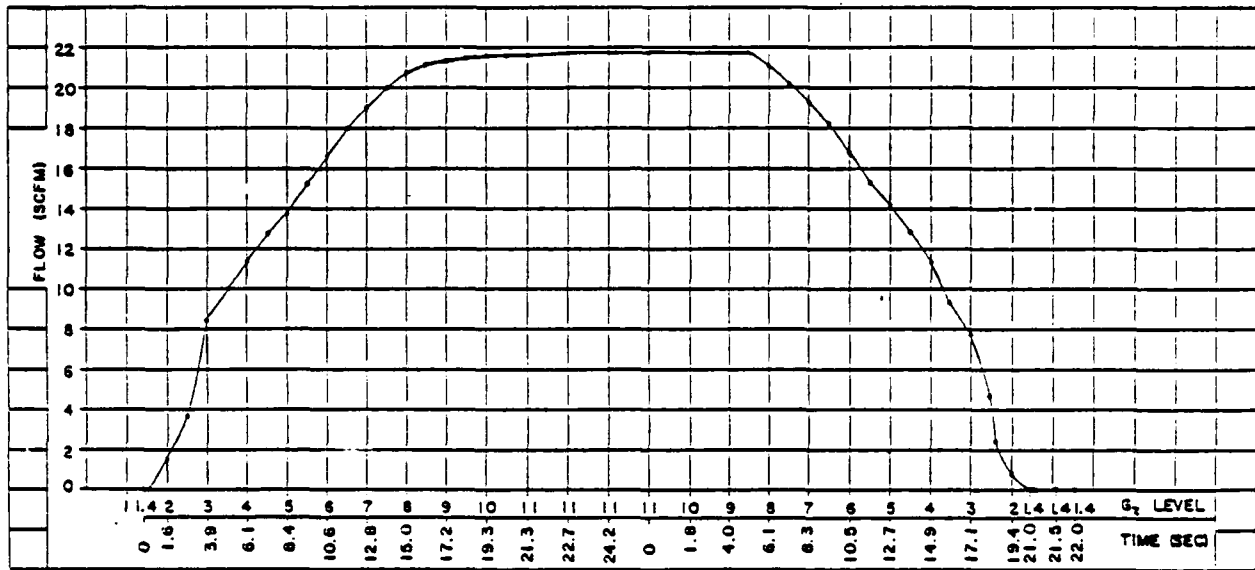


Figure 4.6-2. Maximum flow through AAMRL anti-G valve with pressure off.

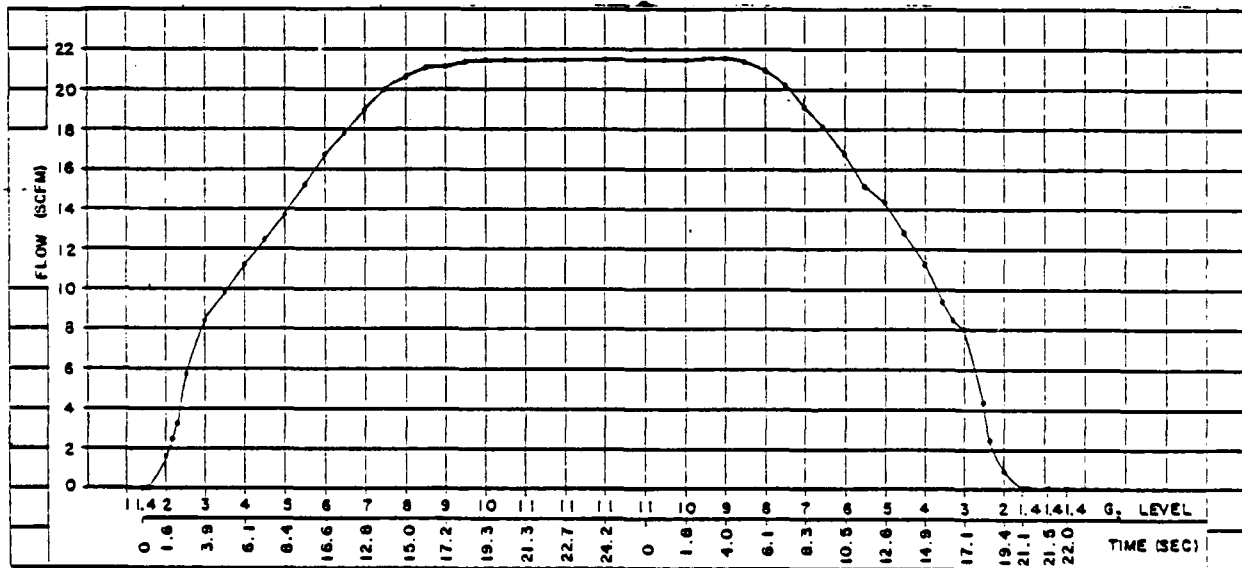


Figure 4.6-3. Maximum flow through AAMRL anti-G valve with pressure on.

4.6.3 Phase II - Determination of Dynamic Response Capability

The dynamic response capability of the AAMRL anti-G valve was determined as described in Testing Procedures (section 3.2.2). Pressure delivered by the valve was measured at the output port and inside the simulated anti-G suit volume. "Output pressure" refers to the pressure within the simulated suit volume, unless otherwise noted. This valve was tested under conditions of both high G-onset and low G-onset as described in Testing Procedures, section 3.2.2.

4.6.3.1 Low G_z-Onset-Rate Conditions

The 0.1 G_z s⁻¹ trapezoidal profile was used for all low-onset tests.

Under conditions of low G_z onset, median source pressure (150 psig), median suit volume (10 liters), and valve angle of 0°, the valve performed as shown in Figure 4.6-4. Suit pressurization did not begin until 2 G was reached; pressure then increased linearly to a value of 7.5 psig at 6.5 G. The rate of pressure increase with increasing G level then began to curve to a maximum level of 10.5-10.8 psig from 10-11 G. Maximum pressure was maintained throughout the time at 11 G; upon deceleration, pressure began to decrease at about 9.5 G and decreased linearly from 10.4 psig at 9 G to 0.4 psig at 1.5 G.

When the valve angle was changed to 15° while all other conditions were held constant, the valve performed as shown in Figure 4.6-5. The suit pressurization profile remained identical in all respects except that the maximum pressure attained at 15° was slightly lower--10.2 psig to 10.4 psig--than at 0° (10.5 psig to 10.8 psig, Fig. 4.6-4). Further increasing the valve angle to 30°, however, produced discontinuities in the suit pressurization profile, shown in Figure 4.6-6. In this case, suit pressurization was not initiated until 2.5 G and several breaks in pressure buildup were observed; maximum pressure (10.0 psig) was attained at 10.5 G and maintained until 10.5 G was reached upon deceleration. The decrease in suit pressure was again somewhat erratic, reaching 0 psig after 1 s at 1.4 G.

When the AAMRL anti-G valve was tested under conditions of low G onset, minimum source pressure (30 psig), median suit volume (10 liters), and 0° valve angle, the results shown in Figure 4.6-7 were observed. The valve opened between 1.5 G and 2 G to produce a suit pressure of 0.25 psig at 2 G. Pressure increase was linear up to 7.4 psig at 6.5 G; from this point the slope of the line decreased slightly to reach 10.4 psig at 9.5 G. The maximum pressure of 10.8 psig was attained at 11 G and did not change until deceleration to 9.5 G; the fall in suit pressure was then essentially linear down to 0.35-0.31 psig at 1.4 G.

Under conditions of low G-onset, maximum source pressure (300 psig), median suit volume and 0° valve angle, the suit pressurization profile--which is shown in Figure 4.6-8--was essentially identical to that produced by minimum source pressure and 0° angle (Fig. 4.6-7).

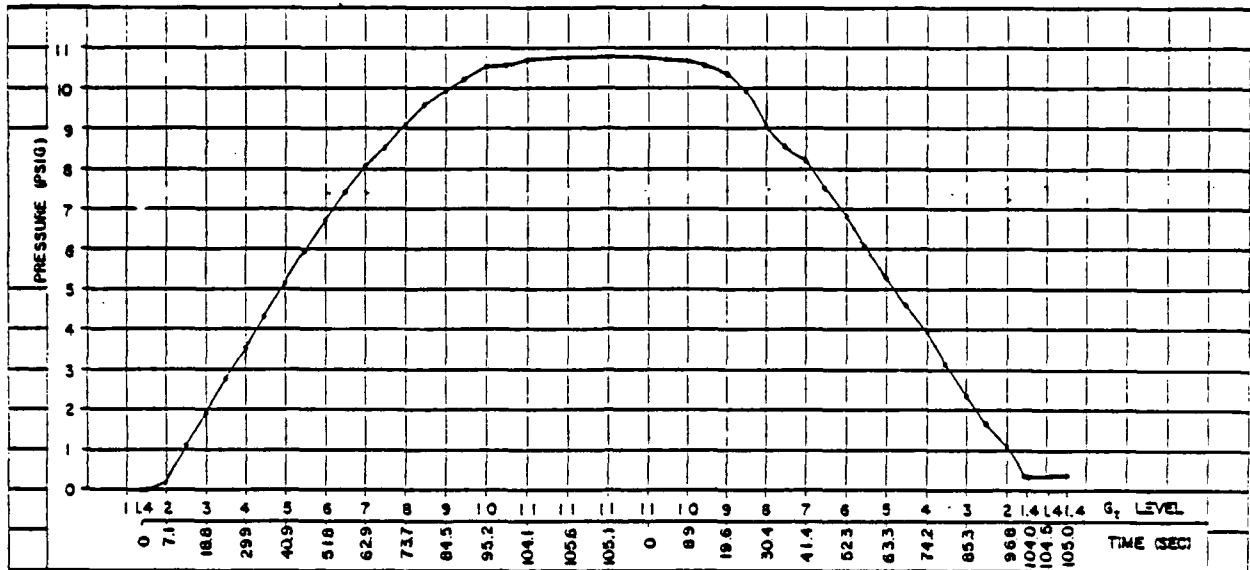


Figure 4.6-4. "Suit" pressures produced during acceleration/deceleration by AAMRL anti-G valve under conditions of: 150-psig source pressure; low G onset; 10-liter volume; 0° angle.

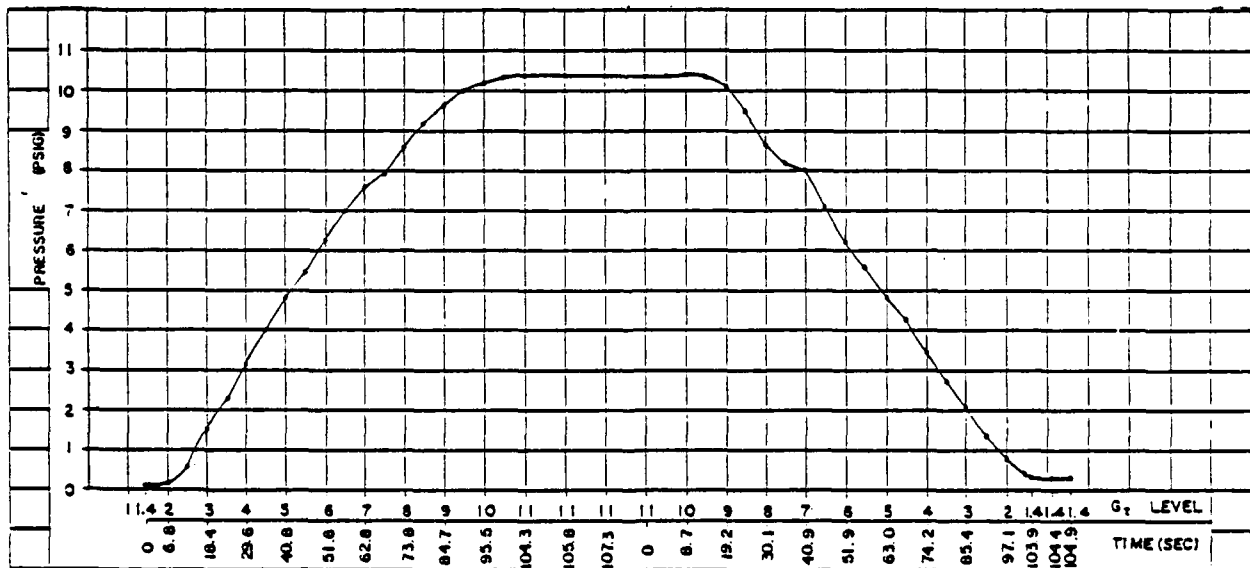


Figure 4.6-5. "Suit" pressures produced during acceleration/deceleration by AAMRL anti-G valve under conditions of: 150-psig source pressure; low G onset; 10-liter volume; 15° angle.

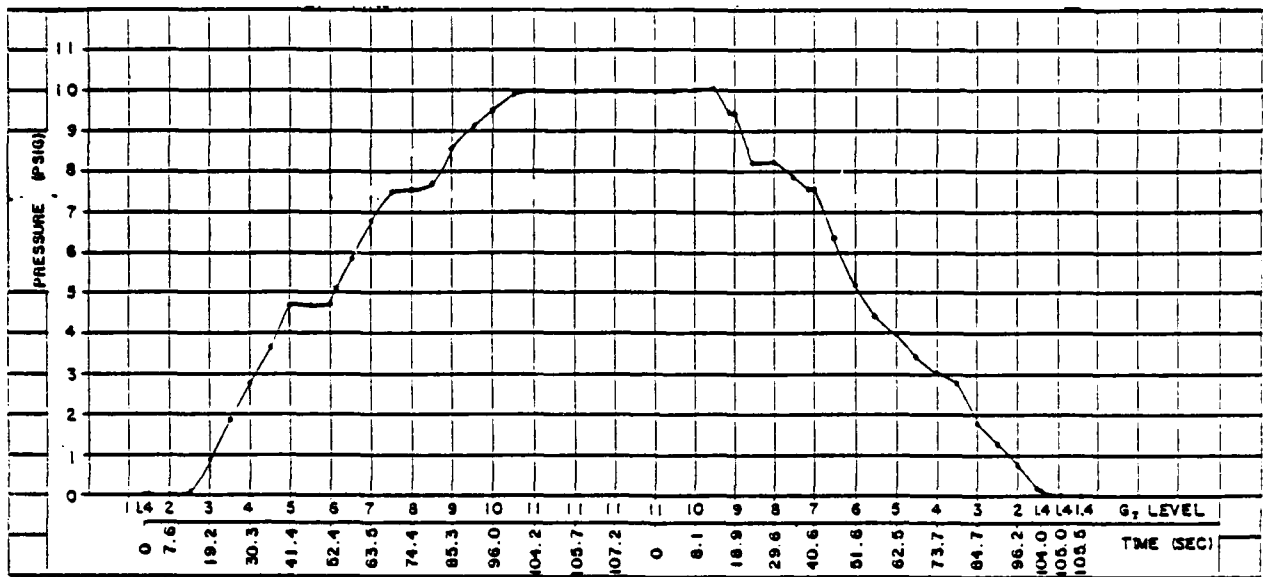


Figure 4.6-6. "Suit" pressures produced during acceleration/deceleration by AAMRL anti-G valve under conditions of: 150-psig source pressure; low G onset; 10-liter volume; 30° angle.

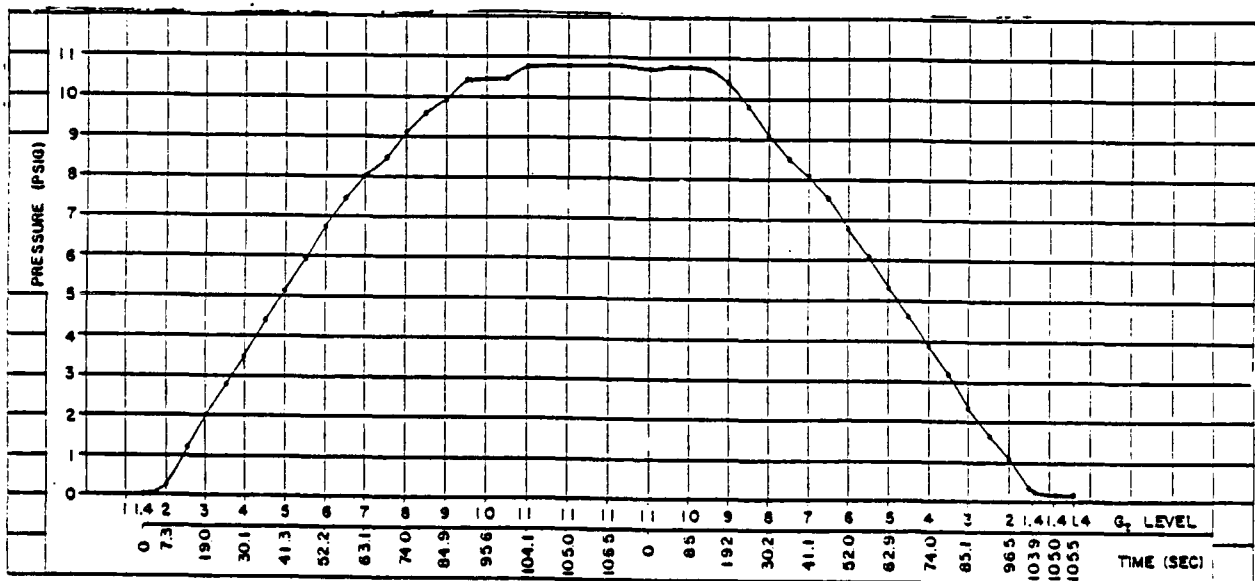


Figure 4.6-7. "Suit" pressures produced during acceleration/deceleration by AAMRL anti-G valve under conditions of: 30-psig source pressure; low G onset; 10-liter volume; 0° angle.

4.6.3.2 High G-Onset-Rate Conditions

The high G-onset conditions for the AAMRL anti-G valve were 4.42 G s^{-1} ; and source pressures of 30, 150, and 300 psig.

For conditions of high G onset, median source pressure (150 psig), 10-liter suit volume, and 0° valve angle, this valve produced the suit pressurization profile shown in Figure 4.6-9. During acceleration the valve opened quickly, producing a suit pressure of 0.34 psig at baseline G (1.4 G). Pressure then increased smoothly in a triphasic pattern; the slope was linear from: 1.4 G to 3 G (4 psig); 3 G to 5 G (7.2 psig); and 5.5 G to 11 G (10.8 psig). After reaching 11 G, pressure continued to increase linearly throughout the time at maximum G level--reaching 11.6 psig after 0.6 s. Upon deceleration, suit pressure began to decrease at 10 G, and continued to decrease linearly down to 3.6 psig at 2.5 G; the rate of pressure drop increased resulting in 2 psig as baseline G (1.4 G) was reached and a further drop to 0.4 psig within 0.6 s.

When the valve angle was set to 15° while all other conditions were unchanged, this valve performed as shown in Figure 4.6-10. There was an initial lag in pressurization so that suit pressure was 0 psig at 1.4 G but 0.3 psig at 2 G. Pressure then increased not quite as rapidly--but somewhat smoother--than when the angle was 0° (Fig. 4.6-9). As 11 G was first attained, suit pressure was 10.4 psig but jumped to the maximum value of 11.2 psig within 0.5 s; it was stable at this level while at 11 G. During deceleration, pressure decreased in a smooth linear manner from 10 G (11 psig) to 2 G (2.8 psig); it then dropped more rapidly to measure 1.7 psig upon reaching 1.4 G and stabilized at 0.2 psig after 1.2 s. Changing the valve angle to 30° produced the suit pressurization profile shown in Figure 4.6-11. This profile is essentially identical to that observed for a valve angle of 15° (Fig. 4.6-10).

With the minimum source pressure (30 psig), 10-liter suit volume, and 0° angle, data plotted in Figure 4.6-12 were obtained. Again there was an initial lag with suit pressure measuring only 0.14 psig at 2 G. From this point, pressure buildup followed a gentle curve which was really two line segments of decreasing slopes. Upon reaching 11 G, pressure was 10.4 psig but then jumped to 11.1 psig within 5 s and stabilized at this maximum level until after deceleration had started. During deceleration, suit pressure decreased smoothly and linearly from 11 psig at 10 G to 1.9 psig as 1.4 G was attained, then dropped to 0.4 psig within 1 s. By comparison with the suit pressurization profile produced at median source pressure (Fig. 4.6-9), minimum source pressure (Fig. 4.6-12) resulted in a somewhat slower, more linear increase in pressure which stabilized within 0.5 s at maximum G level instead of continuing to increase as in Figure 4.6-9.

Maximum source pressure (300 psig), 10-liter suit volume, and 0° valve angle yielded the plot shown in Figure 4.6-13. As for lower source pressures, the increase in suit pressure was multiphasic--with line segments of at least four different slopes. Maximum pressure (11.5 psig) was attained only after 0.6 s at 11 G. The drop in suit pressure during deceleration was essentially the same as for lower source pressures (Figs. 4.6-9 and 4.6-12).

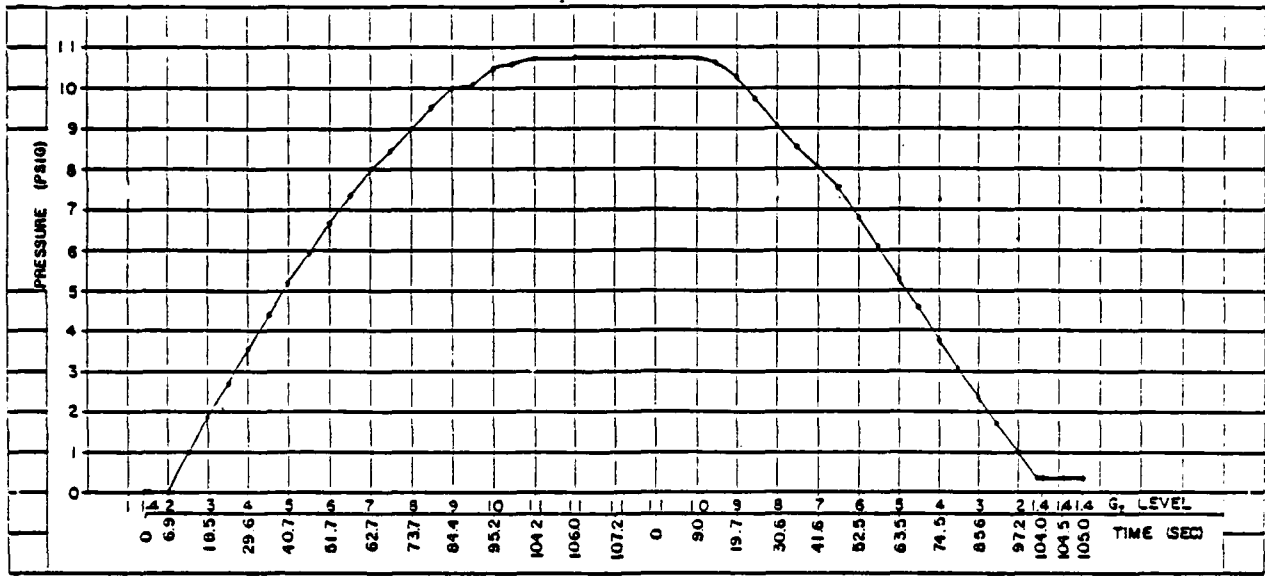


Figure 4.6-8. "Suit" pressures produced during acceleration/deceleration by AAMRL anti-G valve under conditions of: 300-psig source pressure; low G onset; 10-liter volume; 0° angle.

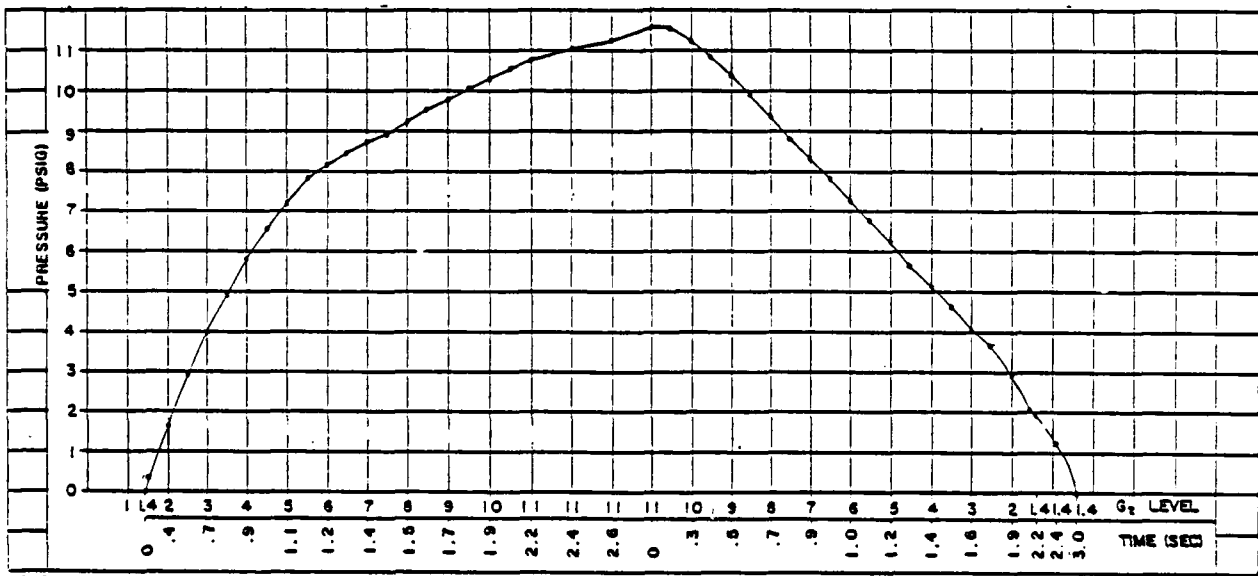


Figure 4.6-9. "Suit" pressures produced during acceleration/deceleration by AAMRL anti-G valve under conditions of: 150-psig source pressure; high G onset; 10-liter volume; 0° angle.

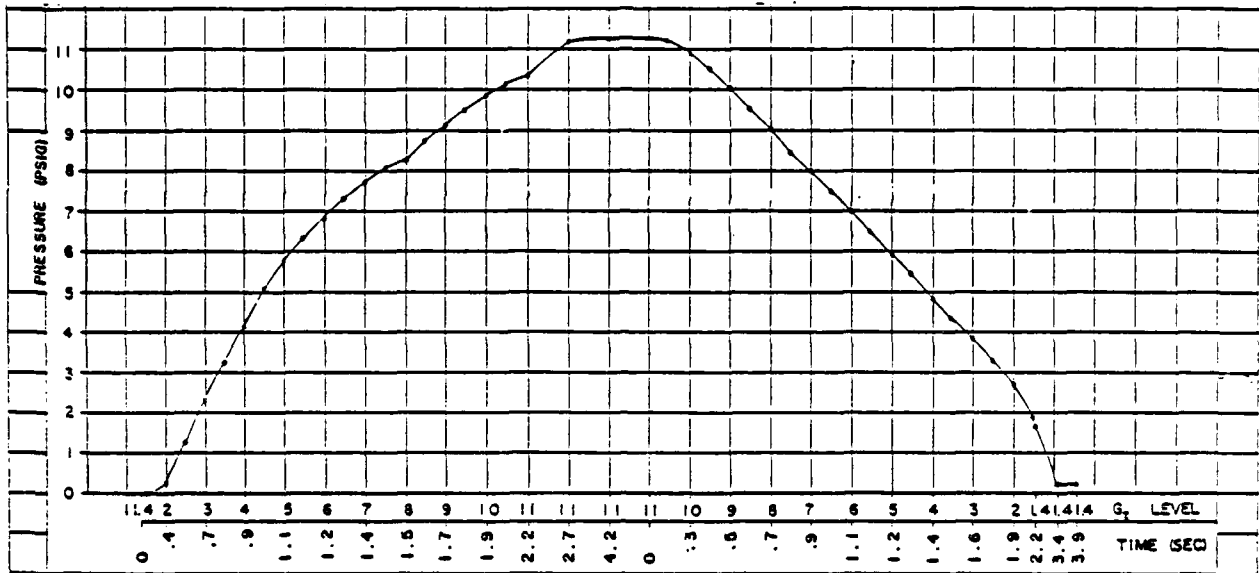


Figure 4.6-10. "Suit" pressures produced during acceleration/deceleration by AAMRL anti-G valve under conditions of: 150-psig source pressure; high G onset; 10-liter volume; 15° angle.

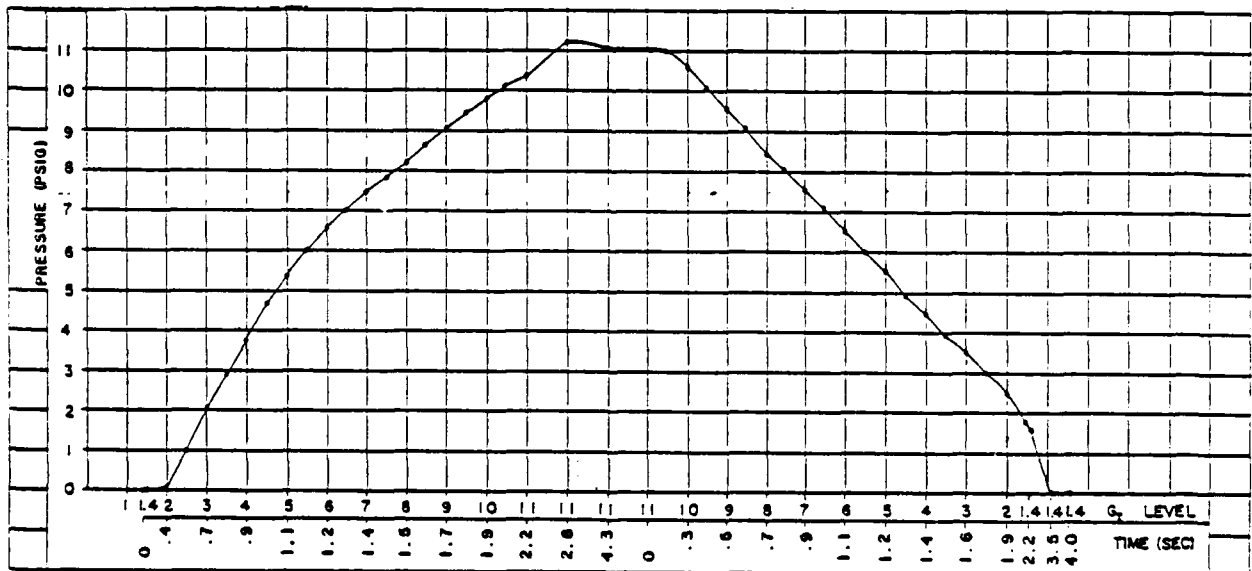


Figure 4.6-11. "Suit" pressures produced during acceleration/deceleration by AAMRL anti-G valve under conditions of: 150-psig source pressure; high G onset; 10-liter volume; 30° angle.

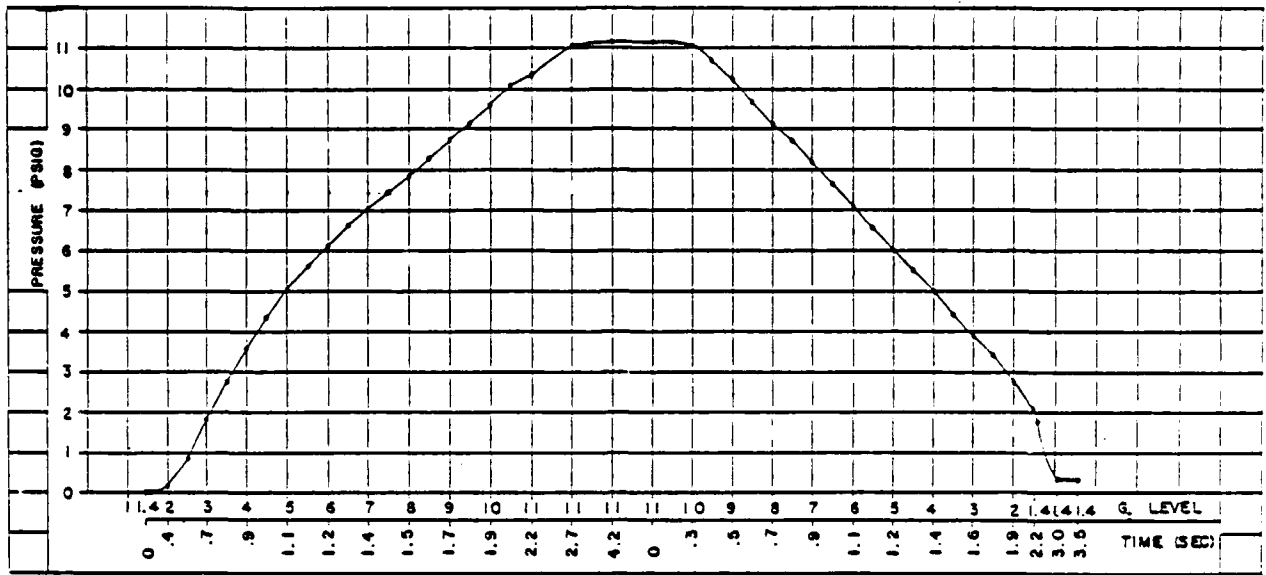


Figure 4.6-12. "Suit" pressures produced during acceleration/deceleration by AAMRL anti-G valve under conditions of: 30-psig source pressure; high G onset; 10-liter volume; 0° angle.

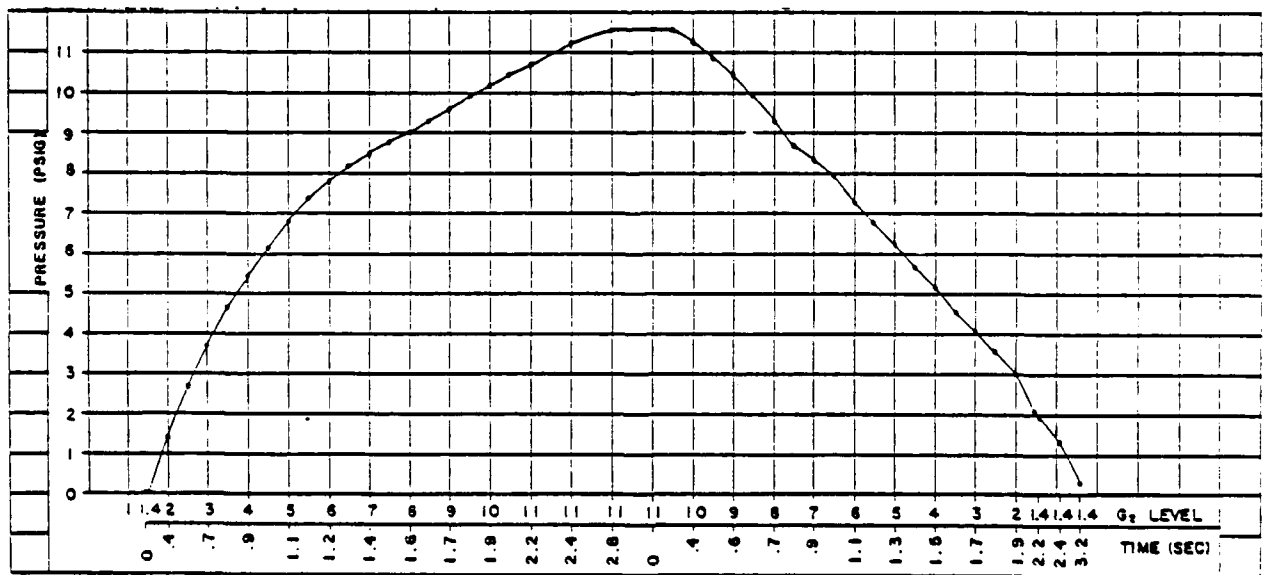


Figure 4.6-13. "Suit" pressures produced during acceleration/deceleration by AAMRL anti-G valve under conditions of: 300-psig source pressure; high G onset; 10-liter volume; 0° angle.

4.6.4 Phase III - Determination of Complex Dynamic Response Capability

Phase III testing under SACM conditions was performed as described in Testing Procedures (section 3.2.3). Initially, median values of source pressure and suit volume were selected and the valve angle varied; subsequently, valve angle was maintained at 0° and the combinations of minimum source pressure with maximum suit volume, and maximum source pressure with minimum suit volume were evaluated.

For median source pressure (150 psig), median suit volume (10 liters), and a valve angle of 0°, the SACM profile shown in Figure 4.6-14 was observed. During the initial period at 3 G the suit pressure spiked to 11.1 psig before settling back to 2.7-2.4 psig within 5 s. A rapid onset acceleration to 9 G caused the pressure to rise rapidly to 11.4 psig and then stabilize at 10.1 psig; deceleration to 4.4 G produced a rapid drop in suit pressure to 4.4 psig. Decelerating further to 3 G dropped the pressure to 2.4-2.5 psig. A slow onset acceleration to 5 G resulted in the pressure building up slowly to 5.1-5.2 psig, and a subsequent slowing to 4 G dropped the pressure to 3.9-3.8 psig. Another rapid acceleration to 9 G caused the pressure to increase rapidly to 11.4 psig then stabilize at 10.1 psig, while rapid deceleration to 1.5 G dropped the suit pressure to 0.4 psig immediately. The last rapid acceleration to 8 G resulted in the pressure rising to 11.2 psig then stabilizing at 8.8-8.9 psig. During the slower deceleration to baseline G (1.4 G), suit pressure dropped linearly to 0.3 psig.

When the valve angle was changed to 15° while all other conditions were held constant, the response pattern seen in Figure 4.6-15 was observed. This suit pressurization profile was similar to that observed for a valve angle of 0° (seen in Fig. 4.6-14); the differences were in the plateau pressures produced by various stationary G levels, which were consistently lower at the 15° valve angle (Fig. 4.6-15) than at the 0° angle (Fig. 4.6-14).

When the valve angle was 30°, the suit pressurization profile (Fig. 4.6-16) was also similar to those observed for the 0° and 15° angles (Fig. 4.6-14), in that the initial spikes in suit pressure were observed upon rapid acceleration; however, the subsequent plateau pressure levels (Fig. 4.6-16) were again lower than for even the 15° angle.

When the minimum source pressure was combined with the maximum suit volume (0° valve angle), the profile of Figure 4.6-17 was produced. Comparing these results to those obtained when median values of both source pressure and suit volume were used (Fig. 4.6-14), it can be seen that the conditions of minimum source pressure/maximum volume caused the initial spikes in suit pressure to be damped considerably, while the plateau suit pressures at stationary G levels were the same as for the median-value conditions (Fig. 4.6-14).

When maximum source pressure (300 psig) was combined with minimum suit volume (6 liters), suit pressurization was as shown in Figure 4.6-18. There was little difference between this pressurization profile and that observed for the median source pressure/median suit volume combination (Fig. 4.6-14); the only apparent difference was that the plateau suit pressure after the final rapid onset acceleration to 8 G was approximately 1 psig higher at maximum source pressure/minimum suit volume conditions (Fig. 4.6-18) than at the median-value conditions.

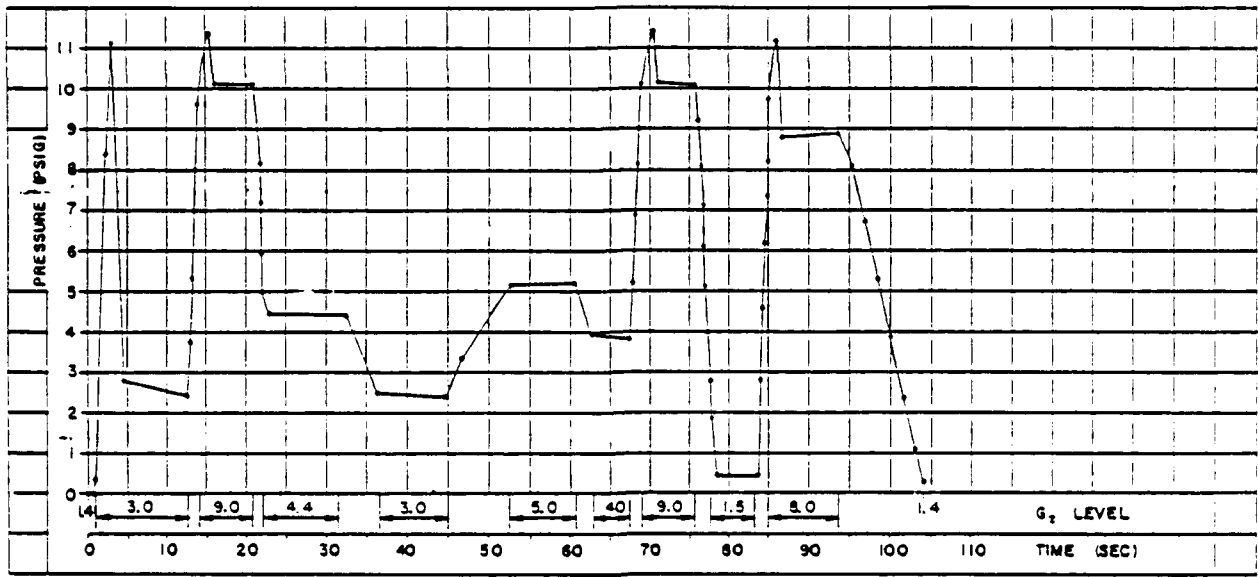


Figure 4.6-14. "Suit" pressures produced during SACM by AAMRL anti-G valve under conditions of: 150-psig source pressure; 10-liter volume; 0° angle.

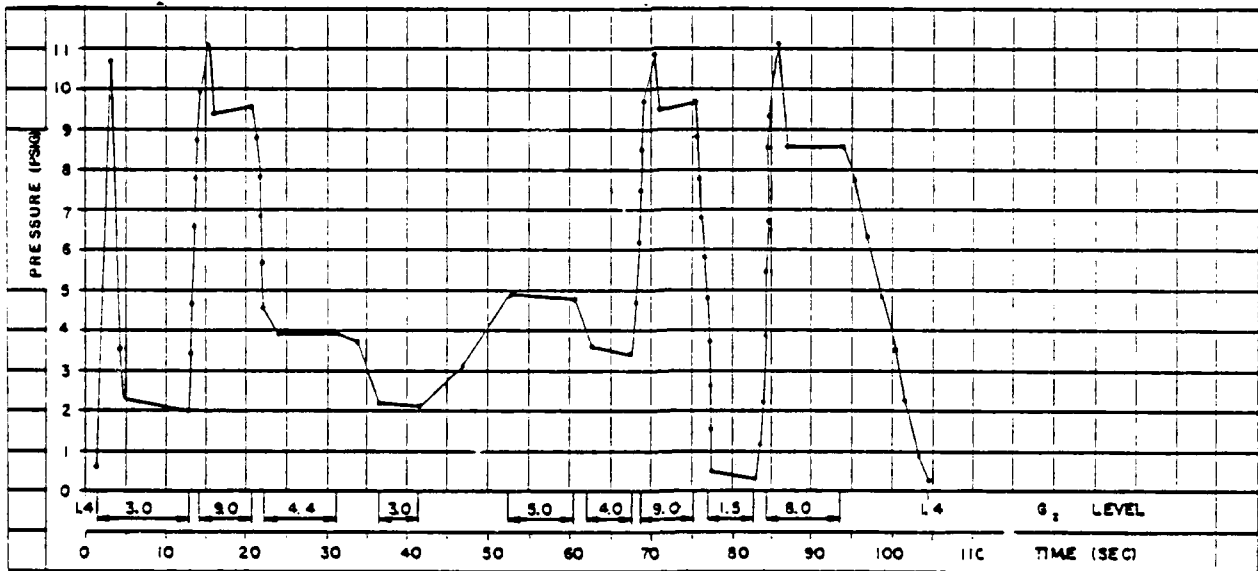


Figure 4.6-15. "Suit" pressures produced during SACM by AAMRL anti-G valve under conditions of: 150-psig source pressure; 10-liter volume; 15° angle.

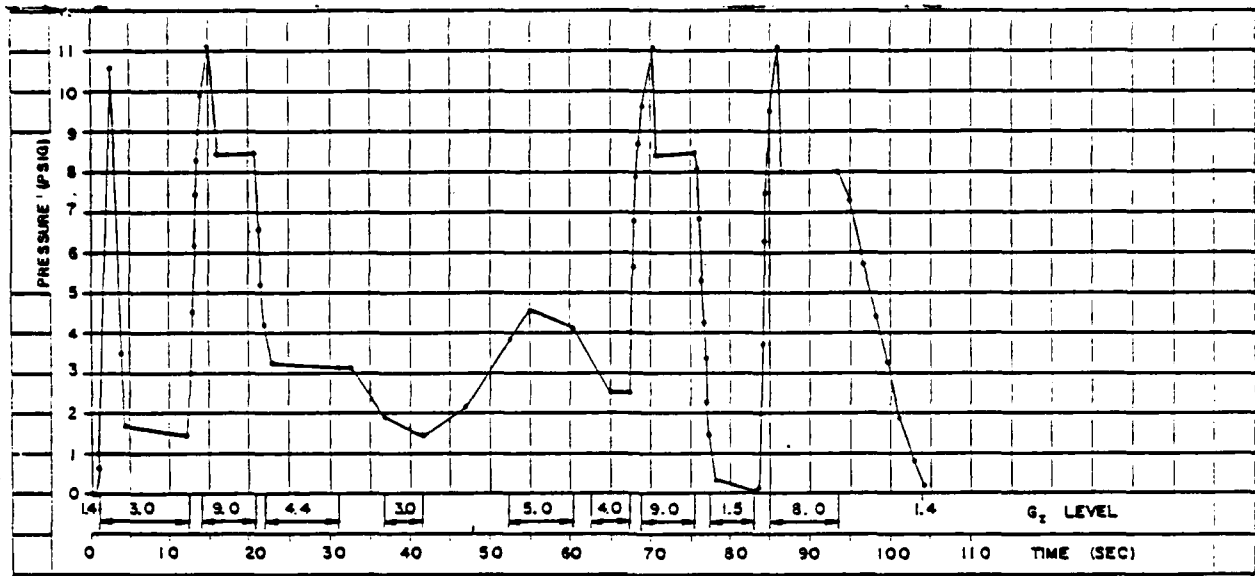


Figure 4.6-16. "Suit" pressures produced during SACM by AAMRL anti-G valve under conditions of: 150-psig source pressure; 10-liter volume; 30° angle.

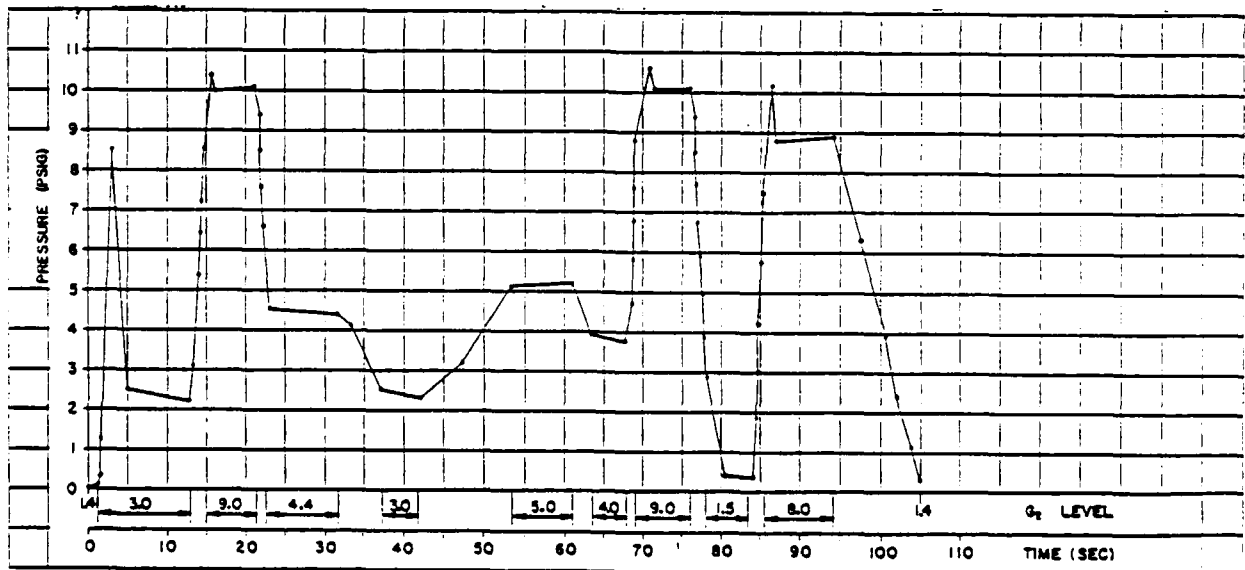


Figure 4.6-17. "Suit" pressures produced during SACM by AAMRL anti-G valve under conditions of: 30-psig source pressure; 14-liter volume; 0° angle.

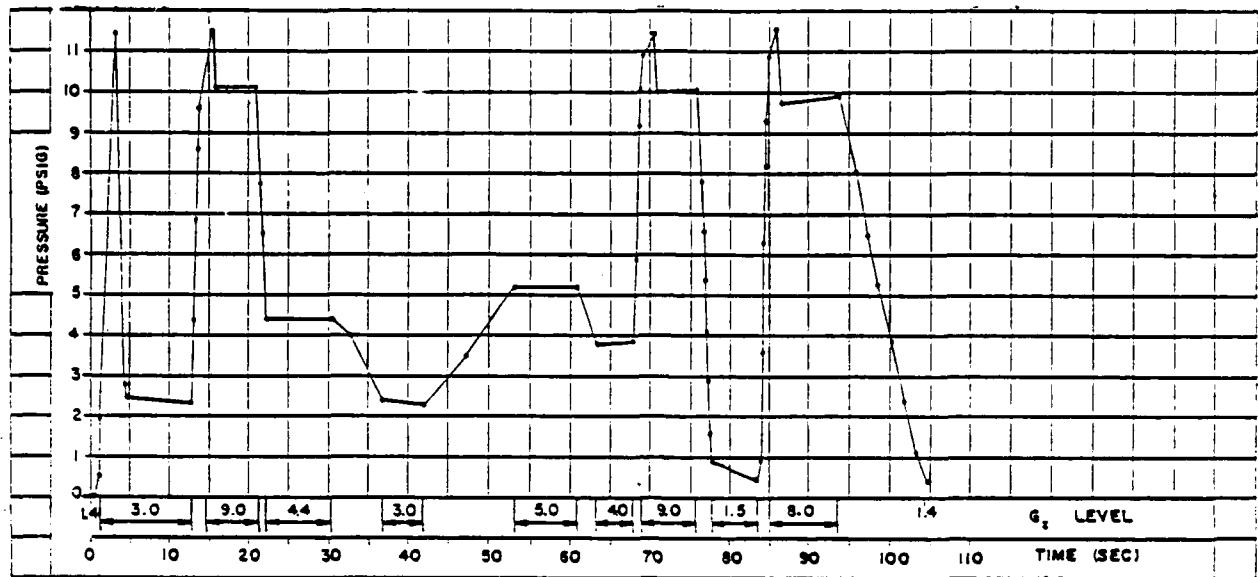


Figure 4.6-18. "Suit" pressures produced during SACM by AAMRL anti-G valve under conditions of: 300-psig source pressure; 6-liter volume; 0° angle.

5. DISCUSSION AND CONCLUSIONS

The prototype anti-G valves evaluated in this task were compared with the standard ALAR 8400A valve, and with each other, on the basis of both static and dynamic response characteristics.

Table 5.0-1 compares the maximum airflow capacity (in SCFM) under static test conditions (see Test Procedures, section 3.2.1) for the various valves. The G-onset rates were 0.5 G s⁻¹, and source pressures were the appropriate median values for each valve; these source pressures are specified in the Results section for each valve.

The ALAR 8400A produced a maximum airflow of 11.1 SCFM at 8 G and held this level without varying throughout the rest of the test. All of the five prototype valves were also producing maximum, or close to maximum, airflows at 8 G. The Garrett Electronic/Pneumatic (servo) valve reached a maximum of 27.8 SCFM at 5.5 G; it then dropped slightly but maintained 91-93% of maximum throughout the remainder of the test. The maximum airflows produced by the prototype valves were all considerably higher than that produced by the ALAR 8400A; they ranged from 18 SCFM to 28 SCFM (Table 5.0-1).

The dynamic response characteristics (measured as described in Testing Procedures, sections 3.2.2 and 3.2.3) of the valves are compared in Tables 5.0-2 through 5.0-4.

TABLE 5.0-1. MAXIMUM AIRFLOW CAPACITY (SCFM) AS A FUNCTION OF ACCELERATION (G_z) FOR ALL ANTI-G VALVES EVALUATED

(Conditions compared: $0.5 G s^{-1}$ onset rate, median source pressure*)

G_z Level	Valve					
	ALAR 8400A	ALAR HFRP	ALAR HF	Garrett Servo	Hymatic VAG-110	AAMRL "Bang Bang"
1.4	0.0	3.3	0.9	8.0	0.4	0.0
2.0	0.1	3.3	1.5	12.3	0.76	1.6
2.5	1.2	5.4	4.9	15.0	7.6	5.7
3.0	2.6	6.5	8.6	17.5	8.9	8.5
3.5	5.2	9.4	10.5	19.8	10.2	10.0
4.0	7.0	11.3	12.0	22.0	11.3	11.3
4.5	7.6	12.7	12.9	24.1	12.5	12.5
5.0	9.1	14.2	14.1	26.2	13.7	13.9
5.5	10.0	15.6	15.3	27.8	14.7	15.4
6.0	10.4	17.0	16.5	26.7	15.6	16.8
6.5	10.7	18.1	17.9	25.7	16.7	17.9
7.0	10.9	19.4	19.1	25.6	17.8	19.0
7.5	11.0	20.8	20.1	25.6	18.0	20.1
8.0	11.1	21.8	20.7	25.5	18.0	20.7
8.5	11.1	22.4	21.1	25.7	18.0	21.1
9.0	11.1	22.6	21.3	25.6	18.0	21.4
9.5	11.1	22.6	21.4	25.7	18.0	21.5
10.0	11.1	22.6	21.5	25.6	18.0	21.5
10.5	11.1	22.6	21.6	25.7	18.0	21.5
	At maximum G_z level					
<u>Initial</u>						
11.0	11.1	22.6	21.6	25.8	18.0	21.6
<u>Final</u>						
11.0	11.1	22.6	21.8	25.9	18.2	21.7

* Median source pressure varied with valve; see text.

The time in seconds required by each valve to produce a given suit pressure is shown in Table 5.0-2. All prototype valves produced any given suit pressure faster than the ALAR 8400A did. The ALAR 8400A required 3.60 s to produce a suit pressure of 9.0 psig; the "Bang-Bang" valve produced the same pressure in 41% of this time; the Garrett in 47%; the ALAR High Flow in 50%; the Hymatic in 51%; and the ALAR HFRP in 54%.

In comparing the performances of the ALAR HFRP and ALAR HF valves (Table 5.0-2), it will be noted that the ALAR HF pressurized the suit more quickly than the ALAR HFRP. This result appears to be in conflict with previous testing results, and with common sense, for two reasons. First, in the configurations tested, the HF valve opened (started the pressurization schedule) at 1.5 G_z , while the HFRP opened at 2.0 G_z ; this allowed the HF valve a 0.5 G_z lead on the HFRP. Second, the HFRP model tested was one of the later production versions, and had undergone several modifications to add damping in an effort to eliminate pressure oscillation ("chatter") during G_z onset and offset. These modifications limited the flow of this valve between 2-3 G_z (Fig. 4.2-3), and allowed the HF valve, which was not limited in this region, to lead the HFRP valve. This combination of factors negated the inherent advantage of the HFRP valve.

Under low-onset conditions (Table 5.0-3), the ALAR 8400A activated at 2.5 G, whereas two of the prototype valves activated at 1.4 G, two others at 2 G, and the remaining valve activated at 2.5 G also, but with a pressure considerably higher than the ALAR 8400A. The ALAR 8400A reached a maximum suit pressure of 7.0 psig at 7.5 G; this pressure would be equivalent to an inflation schedule of 0.93 psi G^{-1} . The Garrett valve also reached a maximum pressure of 10.3 psig at this same G level (7.5 G), approximating an inflation schedule of 1.37 psi G^{-1} . All other prototype valves did not reach their maximum pressures until the maximum G level (11 G) was attained, and their maximum pressure levels indicated inflation schedules less than 1 psi G^{-1} for all these valves.

Under high-onset conditions, all prototype valves activated earlier than the ALAR 8400A did (Table 5.0-4). The ALAR 8400A activated at 3 G (0.2 psig), whereas the prototype valves exhibited suit pressures of 0.6 - 4.0 psig at 3 G. The ALAR 8400A produced a maximum suit pressure of 9.6 psig at the end of the time at 11 G; at the start of the 11-G period, pressure was 6.0 psig, indicating an inflation schedule of 0.55 psi G^{-1} . All of the prototype valves tested also yielded maximum suit pressures at the end of the 11-G period; however, the pressures upon first attaining 11 G were all higher for these valves than for the ALAR 8400A, and the apparent inflation schedules varied from 0.84 to 1.05 psi G^{-1} . The ALAR 8400A valve at 8 G, yielded 35.5% of its maximum pressure of 9.6 psig (attained at end of 11-G time); as 11 G was initially attained, suit pressure was 64.5% of maximum. By contrast, the Garrett valve produced 91% of its maximum pressure of 9.3 psig at 8 G; 97% at 9.5 G; and 99% at 11 G initially, while the maximum pressure was again observed at the end of the 11-G period. The other prototype valves produced pressures equivalent to 54-79% of maximum values at 8 G; and 89-95% of maximum values upon reaching 11 G.

TABLE 5.0-2. SECONDS REQUIRED TO ATTAIN VARIOUS SUIT VOLUME PRESSURES UNDER HIGH-ONSET CONDITIONS

(Conditions compared: high G_z-onset rate, median source pressure*, median volume [10 liters])

Suit Pressure (psig)	Valve					
	ALAR 8400A	ALAR HFRP	ALAR HF	Garrett Servo	Hymatic VAG-110	AAMRL "Bang Bang"
0.0	0.00	-----	0.00	-----	0.00	0.00
0.2	-----	0.00	-----	-----	-----	-----
0.6	-----	-----	-----	0.00	-----	-----
1.0	0.89	0.63	0.72	0.25	0.73	0.28
2.0	1.14	0.85	0.91	0.50	0.88	0.41
3.0	1.42	1.03	1.05	0.67	1.02	0.53
4.0	1.66	1.20	1.19	0.80	1.16	0.66
5.0	1.87	1.36	1.31	0.92	1.30	0.77
6.0	2.13	1.49	1.43	1.04	1.44	0.90
7.0	2.39	1.62	1.55	1.17	1.56	1.03
8.0	2.74	1.75	1.66	1.35	1.69	1.20
9.0	3.60	1.93	1.79	1.69	1.85	1.46
9.3	-----	-----	-----	2.48	-----	-----
9.4	5.12	-----	-----	-----	-----	-----
10.0	-----	2.22	1.93	-----	2.14	1.75
10.5	-----	-----	-----	-----	3.60	-----
11.0	-----	4.00	2.12	-----	-----	2.39
11.1	-----	4.8	-----	-----	-----	-----
11.3	-----	-----	-----	-----	-----	2.60
12.0	-----	-----	2.55	-----	-----	-----
12.4	-----	-----	4.50	-----	-----	-----

* Median source pressure varied with valve; see text.

TABLE 5.0-3. SUIT VOLUME PRESSURE (PSIG) PRODUCED UNDER LOW-ONSET CONDITIONS AS FUNCTION OF ACCELERATION (G_z)

(Conditions compared: 0.5 G s⁻¹ onset rate, median source pressure*, median volume [10 liters])

G _z Level	Valve					
	ALAR 8400A	ALAR HFRP	ALAR HF	Garrett Servo	Hymatic VAG-110	AAMRL "Bang Bang"
1.4	0.	0.4	0.	0.8	0.	0.
2.0	0.	0.5	0.2	1.7	0.	0.3
2.5	0.2	1.2	0.8	2.4	1.9	1.1
3.0	0.7	2.0	1.7	3.3	2.5	2.0
3.5	1.6	2.6	2.4	4.1	3.1	2.8
4.0	2.3	3.3	3.1	4.9	3.6	3.6
4.5	3.0	4.0	3.8	5.7	4.2	4.4
5.0	3.7	4.6	4.6	6.5	4.7	5.2
5.5	4.4	5.4	5.3	7.3	5.3	6.0
6.0	5.1	6.0	6.0	8.1	5.9	6.8
6.5	5.8	6.8	6.7	8.9	6.4	7.5
7.0	6.4	7.4	7.3	9.6	7.0	8.1
7.5	7.0	8.0	8.0	10.3	7.5	8.5
8.0	7.1	8.5	8.5	10.3	8.0	9.2
8.5	7.1	9.0	8.9	10.3	8.7	9.6
9.0	7.1	9.4	8.4	10.3	9.2	10.0
9.5	7.1	9.8	9.7	10.3	9.8	10.3
10.0	7.1	10.2	10.0	10.3	9.9	10.5
10.5	7.1	10.4	10.3	10.3	10.2	10.5
At maximum G _z level						
<u>Initial</u>						
11.0	7.1	10.8	10.6	10.3	10.4	10.7
<u>Final</u>						
11.0	7.1	10.9	10.7	10.3	10.5	10.8

* Median source pressure varied with valve; see text.

TABLE 5.0-4. SUIT VOLUME PRESSURE (PSIG) PRODUCED UNDER HIGH-ONSET CONDITIONS AS FUNCTION OF ACCELERATION (G_z)

(Conditions compared: high G_z -onset rate, median source pressure*, median volume [10 liters])

G_z Level	Valve					
	ALAR 8400A	ALAR HFRP	ALAR HF	Garrett Servo	Hymatic VAG-110	AAMRL "Bang Bang"
1.4	0.	0.2	0.	0.6	0.	0.
2.0	0.	0.3	0.2	1.3	0.	1.7
2.5	0.	0.6	0.4	2.1	0.1	2.9
3.0	0.2	1.1	0.8	2.8	0.6	4.0
3.5	0.5	1.5	1.3	3.6	1.2	5.0
4.0	0.9	2.0	1.8	4.4	1.9	5.8
4.5	1.3	2.5	2.4	5.1	2.5	6.6
5.0	1.7	3.0	3.0	5.8	3.0	7.2
5.5	1.9	3.5	3.6	6.5	3.7	7.8
6.0	2.3	4.0	4.3	7.1	4.2	8.2
6.5	2.5	4.5	4.9	7.6	4.8	8.5
7.0	2.8	5.0	5.6	8.0	5.3	8.8
7.5	3.0	5.5	6.1	8.3	5.9	9.0
8.0	3.3	6.0	6.9	8.5	6.5	9.2
8.5	3.6	6.6	7.5	8.7	7.1	9.5
9.0	4.0	7.2	8.1	8.9	7.7	9.7
9.5	4.4	7.8	8.8	9.0	8.3	10.0
10.0	4.8	8.4	9.4	9.1	8.9	10.3
10.5	5.3	9.0	10.2	9.2	9.4	10.6
At maximum G_z level						
<u>Initial</u>						
11.0	6.0	9.9	11.5	9.2	10.0	10.8
<u>Final</u>						
11.0	9.6	11.1	12.4	9.3	10.5	11.6

* Median source pressure varied with valve; see text.

6. REFERENCES

1. Thompson, R. W., C. E. Galvan, P. E. Love, and A. G. Krueger, Procedural tests for anti-G valves. SAM-TR-79-30, Vol. I, Dec 1979.
2. Thompson, R. W., C. E. Galvan, P. E. Love, and A. G. Krueger, Procedural tests for anti-G valves. SAM-TR-79-31, Vol. II, Dec 1979.

ABBREVIATIONS, ACRONYMS, AND SYMBOLS

AAMRL	Armstrong Aerospace Medical Research Laboratory
ACM	Aerial Combat Maneuver
AWG	American wire gauge
DC	direct current
F _v	airflow
G	units of G _z
G _z	acceleration along the Z axis (head-to-foot)
Hz	Hertz (cycles per second)
kHz	kilohertz (1000 cycles per second)
LSE	Life-support equipment
p-p	peak-to-peak
P _r	final pressure of known volume in psig
P _s	source pressure
P _o	valve output pressure (psig)
psi	pounds per square inch
psid	pounds per square inch differential
psig	pounds per square inch gauge
P _v	suit pressure (psig)
RDT&E	Research, Development, Test, and Evaluation
SACM	Simulated Aerial Combat Maneuver
SCF	Standard cubic feet
SCFM	Standard cubic feet per minute
T&E	Test and Evaluation
USAFSAM	U.S. Air Force School of Aerospace Medicine
V _o	known volume in cubic inches (or liters)
VAC	volts alternating current
V _s	unknown suit volume in cubic inches (or liters)
VDC	volts direct current
XDCR	transducer

[How to order Appendixes A-F]

RE: The USAF School of Aerospace Medicine's Technical Report Series on
Research and Development of Anti-G Life Support Systems:
Part 4. Engineering Test and Evaluation of Six Anti-G Valves.
(USAFSAM-TR-86-36-PT-4)

APPENDIX A: ALAR 8400A Anti-G Valve Experimental Data
APPENDIX B: ALAR High-Flow Ready-Pressure Anti-G Valve
Experimental Data
APPENDIX C: ALAR High-Flow Anti-G Valve Experimental Data
APPENDIX D: Garrett Electronic/Pneumatic Anti-G Valve
Experimental Data
APPENDIX E: Hymatic VAG-110-022 Anti-G Valve Experimental Data
APPENDIX F: AAMRL ("Bang Bang") Anti-G Valve Experimental Data

In order for experimental data on this research to be readily accessible, microfiche have been made of these Appendixes. The microfiche are available through:

The Strughold Aeromedical Library
USAFSAM STINFO Office (USAFSAM/TSKS)
USAF School of Aerospace Medicine
Brooks AFB, Texas 78235-5301